The origin and development of cerebellar macroglia

DISSERTATION

zur Erlangung des akademischen Grades

doctor rerum naturalium

(Dr. rer. nat.)

vorgelegt von

Nora Mecklenburg

aus Berlin

eingereicht im Fachbereich Biologie, Chemie, Pharmazie
der Freien Universität Berlin

Alicante/ Berlin Dezember 2011

Diese Arbeit wurde von September 2007 bis Dezember 2011 am Instituto de Neurociencias in Alicante (Spanien) unter der Leitung von Prof. Dr. Constance Scharff und Prof. Dr. Salvador Martínez erstellt.

1. Gutachter: *Prof. Dr. Constance Scharff*
                    (Freie Universität Berlin)

2. Gutachter: *Prof. Dr. Salvador Martínez*
                    (Universidad Miguel Hernandez, San Juan de Alicante)

Disputation am 17.04.2012

Für meine Eltern

und meinen Großvater

needs to improve their systems. To Ana and Raquel for teaching me all the necessary things about "pollornizes", to Jon for revising my manuscripts, to Arancha, Almu, Carlos, Diego P., Elena, Jesus J., Maria, Olga, Paqui, and Valentina.

Thanks to Bristol and Manuel. Even though I have to leave now I´ll be back. We´ve made it all the way and I hope I can come to Alicante for your theses. I love you guys, and I´ll miss you a lot.

I want to say thanks to Ari and Iván for lazy, crazy, mind opening, educative, philosophic, posttraumatic evenings, for pool nights, Wii evenings and all the other special events I´d rather not write about here :-D

Thanks to Regine, Kai and Julie for great holidays whenever I was back in Berlin. Thanks for the calls, the emails, the visits and all your support.

Thanks to Gela, for countless calls, for not giving up on me, for being as supportive as someone could be, for making me feel less homesick and for all the little but no less important things during the past 4 years.

And last but not least I want to thank my family: Martin, the best brother in the world. My father and Katja for supporting me all the years. And special thanks to my mother and Peter for all the mental support, for calling and listening, for advises and for vey special weekends in Nerja.

Zusammenfassung

Projekt 1: Herkunft von Oligodendrogliazellen des Kleinhirns

Die Herkunft von Oligodendrogliazellen des Vorderhirns und Rückenmarks wurde in den letzten Jahren intensiv studiert und analysiert. Die Herkunft von Oligodendrogliazellen des Kleinhirns ist hingegen weitgehend unbekannt. Um den Ursprung und den entsprechenden Migrationsweg genauer zu bestimmen, wurde *in ovo* das Mittelhirn von Wachtelembryonen entlang der rostro- caudalen und dorso- ventralen Achse in Hühnerembryos transplantiert. Im Anschluss wurden die Chimären bis zum Alter von 19 Tagen inkubiert (Hamburger Hamilton- Stadium 45/ HH45). Sowohl der Ursprung des Transplantats als auch die Wanderung wurden kartiert und der Phänotyp immunhistologisch analysiert. Es konnte gezeigt werden, dass homotopische und homochrone Transplantate des Mittelhirns Zellen generieren, die vom Transplantat über das Marksegel (velum medullare) in das ventrale Kleinhirnmark wandern. Die Spenderzellen wanderten durch das Kleinhirnmark in alle Schichten des Kleinhirns, mit Ausnahme der externen Körnerschicht. In der Purkinjezellschicht exprimierten diese Zellen Vimentin mit der typischen Struktur von Bergmann Glia. In den anderen Schichten und insbesondere im Kleinhirnmark konnten PLP und Olig2 als Marker für Oligodendrozytenschicksal nachgewiesen werden. Die eingehende Analyse einer Vielzahl von Transplantaten erlaubte es, den Ursprung dieser Zellen zu kartieren und auf die parabasale Platte des Mittelhirns einzugrenzen.

Projekt 2: Expressions- und Funktionsanalyse des Wachstums- und Differenzierungsfaktors *Gdf10* im Kleinhirn

Gdf10/ Bmp3b gehört zur TGF-ß- Familie und ist in Bergmann Gliazellen exprimiert. Dies wurde mittels „single- cell transcriptional profiling" herausgefunden (Koirala and Corfas 2010). Um eine Basis für weiterführende Studien zur Funktion von *Gdf10* zu entwickeln, wurde die Expression im Kleinhirn genauer charakterisiert. Hierzu wurden *in situ* Hybridisierungen in Mäusen von E14,5 bis zum adulten Stadium durchgeführt. Es konnte gezeigt werden, dass *Gdf10* sowohl im embryonalen als auch im adulten Stadium exprimiert ist. Embryonal variierte die Expression entlang der rostro- caudalen Achse zwischen lateralem und medialem Kleinhirn. Im rostralen Kleinhirn wurde *Gdf10* vor allem

in der sich entwickelnden Vermis detektiert, in der lateralen Ventrikulärzone, die unmittelbar an die intraventrikuläre Rautenlippe grenzt, sowie in der interventrikulären Rautenlippe selbst. Im caudalen Kleinhirn hingegen, wurde *Gdf10* in allen Zonen des Kleinhirns exprimiert, welches die intraventrikuläre Rautenlippe, die Ventrikulärzone und die Intermediärzone einschließt. Die Expression im medialen Kleinhirn dehnte sich radiär aus, während im lateralen Kleinhirn nur tangential eine Ausweitung unterhalb der externen Körnerschicht beobachtet wurde. Postnatal wurde *Gdf10* vorranging in der Purkinjezellschicht lokalisiert. Diese Expression war stabil bis ins adulte Stadium. Aus der detaillierten Charakterisierung von *Gdf10+* Zellen mit Gliazellmarkern und der Analyse des Expressionsmusters kann geschlussfolgert werden, dass *Gdf10* ab dem Übergang vom Stadium der radialen Gliazellen in Bergmann Gliazellen bis ins adulte Stadium in diesem Zelltyp vorhanden ist. *Gdf10* ist daher ein spezifischer Marker zur Verfolgung der Genese, Migration und terminalen Differenzierung von Bergmann Glia. Weiterhin wurden bei der Untersuchung der Expression von *Gdf10* und Nestin zwei Migrationsmodi entdeckt. Zum einen eine bereits langjährig bekannte radiäre Migration, ausgehend von der Ventrikulärzone, und zum anderen eine primär radiäre Migration, die in der finalen Phase in einer 90° Biegung in Richtung der externen Körnerschicht endet. Diese Art der Migration wurde ausschließlich im caudalen Kleinhirn beobachtet und erklärt die vermeintlich tangentiale Ausweitung der *Gdf10* Expression. Des Weiteren wurde untersucht, ob Gdf10 von sonic hedgehog (Shh) reguliert wird, welches in Purkinjezellen des Kleinhirns exprimiert ist. Dazu wurde die *Gdf10-* Expression in Kleinhirnen von konditionellen *Shh-* defizienten Mäusen geprüft. Die persistierende *Gdf10* Expression in diesen Mäusen schließt eine direkte Regulierung durch Shh aus. Eine *in silico* Analyse von *Gdf10* auf Konsensussequenzen für Transkriptionsfaktoren, zeigte eine Reihe weiterer möglicher Gene, die in die Regulation der *Gdf10* Expression involviert sein könnten.

Abstract

1st project: The origin of cerebellar oligodendroglia

While the origin of oligodendroglia in the prosencephalon and the spinal cord has been extensively studied and accurately described, the origin of this cell type in the cerebellum is largely unknown. In order to investigate the site where cerebellar oligodendrocytes originate and what migratory pathways they follow to reach their final destination in the adult, *in ovo* transplants were performed using the quail/ chick chimeric system. The chimeric embryos were developed up to HH43-49 (17-19 days of incubation) to map the location of donor cells and analyze their phenotype by immunohistochemistry. As a result, mesencephalic homotopic and homochronic transplants generated cellular migratory streams moving from the grafted epithelium into the host cerebellum, crossing the isthmus mainly through the velum medullare and invading the central white matter. From here, these mesencephalic cells invaded all the layers of the cerebellar cortex except the external granule layer. The majority of the cells were detected in the central and folial white matter, as well as in superficial regions of the internal granule layer, surrounding the Purkinje cells. In the latter case, the donor cells presented a Bergmann glial morphology and were Vimentin positive, while in other areas they were PLP and Olig2-positive, indicating an oligodendroglial fate. The combinatory analysis of the different grafts allowed us to propose the fate map of chick cerebellar oligodendroglia at the neural tube stage. As a result, the majority of the cerebellar oligodendrocytes originate from the parabasal plate of the mesencephalon.

2nd project: Gdf10 in the development of cerebellar Bergmann glia

Growth differentiation factor 10 (*Gdf10*), also known as *Bmp3b*, is a member of the *transforming growth factor beta* (*TGF-ß)-* superfamily. *Gdf10* is expressed in Bergmann glial cells, which was investigated by single- cell transcriptional profiling (Koirala and Corfas 2010). In order to create a basis for further studies, the expression pattern of *Gdf10* mRNA was characterized between E14.5 and P28 in mice. At embryonic stages, the expression pattern varied along the antero-posterior axis of the cerebellum. Anteriorly *Gdf10+* cells were detected along the ventricular zone (VZ) of the developing vermis, following the dorsal cerebellar midline, whereas in the cerebellar hemispheres *Gdf10* was expressed

both in the rhombic lip and the neighboring ventricular epithelium. Posteriorly, *Gdf10* expression labeled the entire cerebellar rhombic lip and ventricular zone of the 4th ventricle. Furthermore, *Gdf10* expression was detected in the intermediate zone and close to the developing external granule cell layer (EGL). A detailed coexpression analysis of *Gdf10* with prominent glial markers such as GFAP, Nestin, GLAST and Vimentin was performed to investigate the expression at different time points. From these results and the analysis of the expression pattern we concluded that *Gdf10* most likely induces the transition from radial glia to Bergmann glia development and is a promising marker to follow Bergmann glial cell development. The analysis of *Gdf10* and Nestin expression revealed two modes of migration. First, a well characterized radial migration from the medial ventricular zone, as well as a primarily radial migration, which finally undergoes a perpendicular turn towards the EGL. The latter was only observed in the posterior cerebellum. To investigate a possible mechanism regulating *Gdf10* in cerebellar development, *Gdf10* expression was analyzed in conditional mutants of Shh. We found that *Gdf10*, even though differentially expressed, is not regulated by Shh. The screening for transcription factor binding sites revealed possible regulators of *Gdf10*.

Table of contents

1 Introduction

1.1 Segmentation of the brain

The central nervous system (CNS) arises from the neural plate, a homogenous sheet of epithelial cells. As the neural plate precedes its differentiation, its lateral edges thicken and roll up on the antero- posterior axis, to close dorsally and form the neural tube (neurulation).

1.1.1 Antero- posterior segmentation

In the vertebrate embryos, most of the neural tube gives rise to the spinal cord, while the rostral end enlarges to form the three primary brain vesicles; the prosencephalon (forebrain), the mesencephalon (midbrain) and the rhombencephalon (hindbrain); (Sanes et al. 2006). The prosencephalon gives rise to the telencephalon and the diencephalon. The mesencephalon gives rise to the midbrain, whereas the rhombencephalon gives rise to the brainstem and the cerebellum (Figure 1).

Copyright © 2006 Elsevier, Inc.
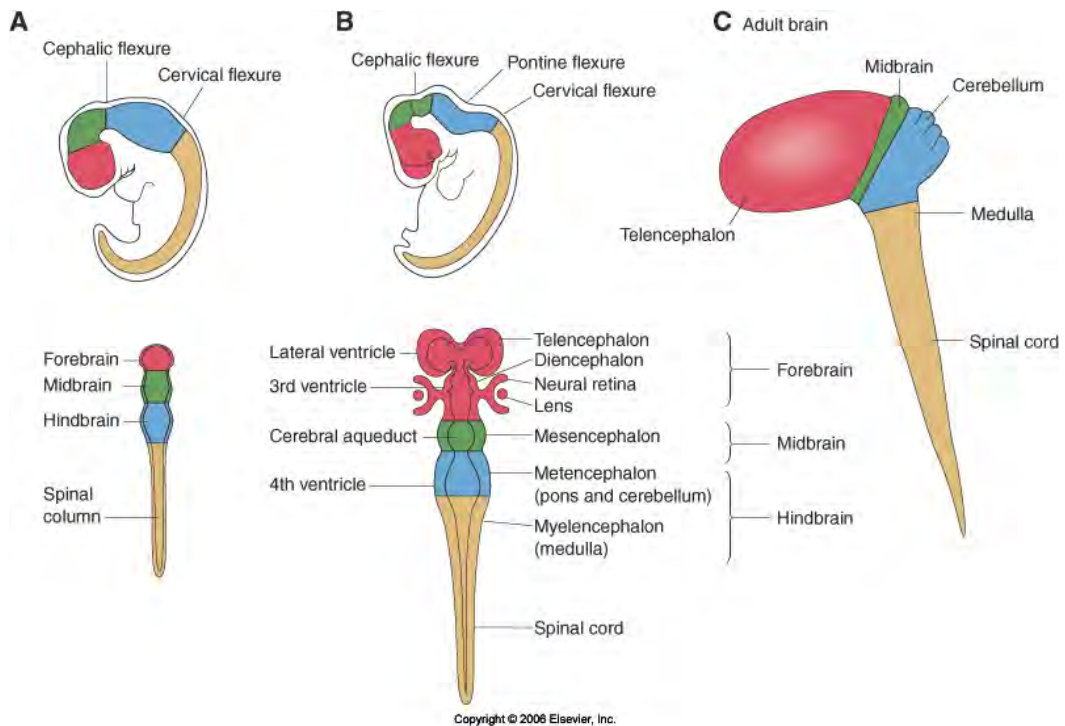
Figure 1: Early brain segmentation in the vertebrate embryo. The vertebrate brain and spinal cord develop from the neural tube. A-C (upper panels) illustrate lateral views of human embryos at successively older stages of development, whereas A, B lower panels illustrate a dorsal view. The three primary subdivisions of the brain; the prosencephalon (red), mesencephalon (green) and the rhombencephalon (blue), occur as three brain vesicles (A). The next stage of brain development (B) results in further subdivisions, with the forebrain vesicle becoming subdivided into the paired telencephalic vesicles and the diencephalon, and the rhombencephalon becoming subdivided into the brainstem and cerebellum. These basic divisions can be related to the overall anatomical organization of the mature brain (C). (Adapted from Sanes *et al.* 2006)

1.1.2 Dorso- ventral subdivision (Longitudinal domains)

The longitudinal domains of the neural tube are a direct result of the initial processes of the medio- lateral regionalization of the neural plate, which during neurulation is converted into a dorso-ventral regionalization of the neural tube. The fundamental idea behind this concept is, that certain longitudinal bands of the neural tube's wall divide the tube into different histogenetic areas, that influence the dorso- ventral regionalization. The specification of the longitudinal territories within the neural epithelium is based on the gradual distribution of directing molecules involved in histogenetic processes (Puelles et al. 2008).

The formation of the floor plate (FP) and the basal plate (BP) depends on the accurate vertical induction by the axial mesoderm. The entire process depends on the expression and secretion of sonic hedgehog (Shh). In contrast, the alar

plate (AP) as well as the roof plate (RP) are the result of dorsalizing events from the extraneural epithelium; and once the neural tube closes, also from the roof plate itself (Figure 2 A). A large variety of genes is necessary for the precise formation of the dorsal tube, this involves *noggin*, *bone morphogenetic proteins* (*Bmp´s*), *dorsalin* and members of the *wingless-type MMTV integration site* family *(Wnt-* family); (Puelles et al. 2008).

Once the longitudinal division is completed, the four plates are present along the antero- posterior axis (Figure 2 B, C). Certain genes expressed along the antero-posterior axis can identify each of the domains. *Wnt1* is a classical roof plate marker, its expression is induced by *fibroblast growth factor 8* (*Fgf8);* (Alexandre et al. 2006). The limit between the alar and basal domain (ABL) is the result of the equilibrium between ventralizing and dorsalizing molecules. The alar plate of the midbrain for example expresses *paired box protein 7* (*Pax7);* (Aroca et al. 2006; Shin et al. 2003). The basal plate is characterized by the expression of *Shh*, which is produced in the notochord and floor plate, and is implicated in the induction of ventral cell types in CNS (Tanabe and Jessell 1996; Watanabe and Nakamura 2000).

The alar and basal plates themselves can be divided into longitudinal subdomains. For example, the parabasal plate, which is located at the dorsal limit of the basal plate, is part of the basal plate and can be identified by the expression of the bHLH transcription factors *Mash1* and *Megane (Mgn),* and *Sulfatase 1 (Sulf1);* (García-Lopez et al. 2009; Gimeno and Martinez 2007).

There are a large variety of markers additionally useful to distinguish between the different longitudinal domains. The expression of these markers changes during development, therefore depending on the developmental stage, different markers must be taken into closer consideration.
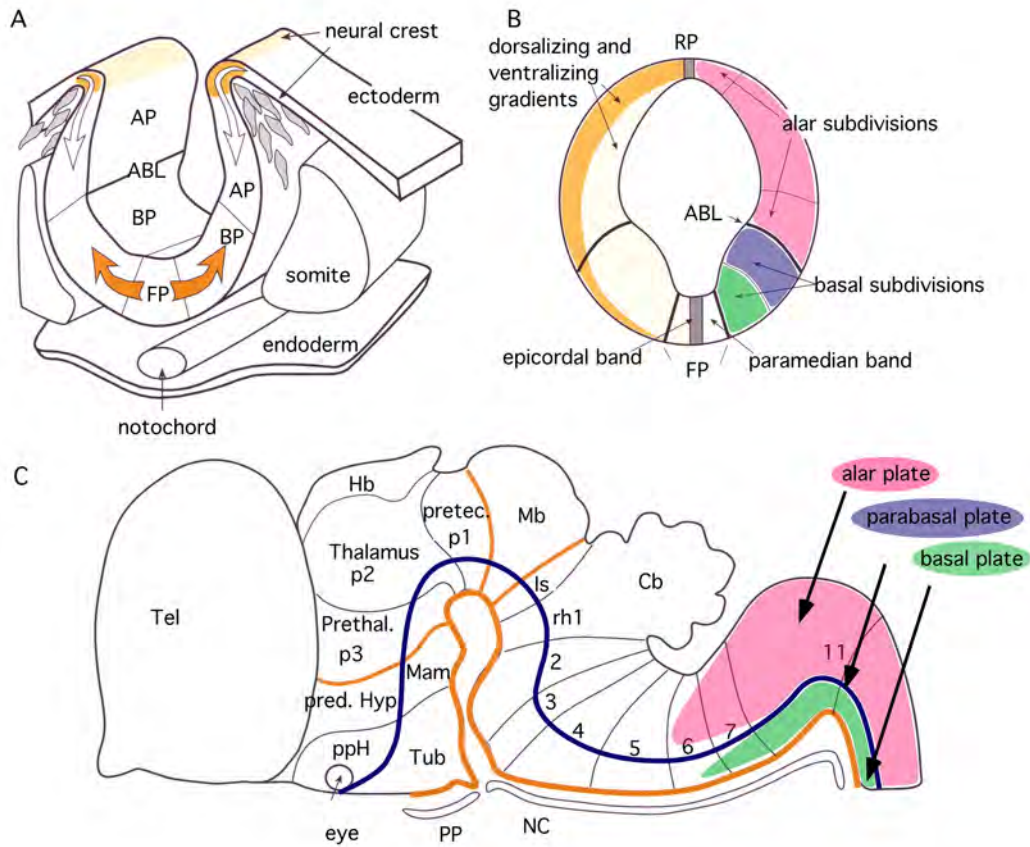
Figure 2: Dorso- ventral segmentation of the embryonic brain. The longitudinal domains of the neural tube during development are a direct result of the initial processes of the medio- lateral regionalization of the neural plate (A), which during neurulation is converted into a dorso- ventral regionalization of the neural tube (B, C). The formation of the floor plate (FP) and the basal plate (BP) depends on the accurate vertical induction by the axial mesoderm. In contrast, the alar plate (AP) as well as the roof plate (RP) is the result of dorsalizing events from the extraneural epithelium; and once the neural tube closes also by the roof plate itself. The alar and basal plates themselves can be divided into longitudinal subdomains. For example, the parabasal plate (B, C), which is located at the dorsal limit of the basal plate, can be identified by the expression of *Sulf1*. (Modified from Puelles et. al 2008)

1.2 The cerebellum

The cerebellum, especially the cerebellar cortex, is one of the central regions in which organizational structural patterns are most obvious. Its apparent simplicity and geometrical disposition have attracted many investigators for its potential in providing an understanding of the mechanisms involved in the development of the nervous system (Sotelo 2004). The cerebellum is involved in the coordination of voluntary motor movement, balance and equilibrium and muscle tone. Its function is to facilitate the performance of movements by coordinating the action of the various participating muscle groups. This is often spoken of simply as "smoothing out" motor acts. Damage to the cerebellum leads to dramatic alterations in ordinary movements. Lesions of the cerebellum result in the decomposition of the activity, or fractionation of movement, so that the action is no longer smooth and coordinated. Certain cerebellar lesions also produce a tremor, which is seen when performing voluntary acts, better known as an intention tremor (Hendelmann 2000).

1.2.1 Origin of the cerebellum

The three primordial brain subdivisions, the prosencephalic, mesencephalic and rhombencephalic vesicles, are already individualized by the 10–12 somites stage (Colas and Schoenwolf 2001; Sadler 2005). Chicken embryos reach that stage after 33 to 40 hours of incubation referring to Hamburger Hamilton HH10 (Hamburger and Hamilton 1992).

To investigate how a cell or tissue moves and what is their fate during normal development, different fate mapping techniques were developed. Nicole Le Douarin in 1969 introduced the chick/quail chimeric system, studying the migration and differentiation of progenitor cells in developing embryos (Le Douarin and Barg 1969). The method is based upon the occurrence of condensed heterochromatin associated with the nucleoli of all quail cells. Because such a condensation does not exist in chick cells, the histochemical visualization of DNA has been for years the best approach to distinguish quail cells from chick cells in the chimeric embryos (Le Douarin et al. 1996).

The chimeric approach has been extremely useful in determining the location and extent of the cerebellar primordium in the 2-day-old (E2, HH10-HH12) avian neural tube (Hallonet et al. 1990; Martínez and Alvarado-Mallart 1989). The results of this approach were rather unexpected: the alar plate of the metencephalon is not the origin of the entire cerebellum. The two laterals parts of cerebellar tissue arise from a triangular mass of the alar plate of the caudal mesencephalic vesicle (Alvarez Otero et al. 1993; Hallonet and Alvarado-Mallart 1997; Hallonet et al. 1990; Martínez and Alvarado-Mallart 1989).

Therefore, the constriction, that at the stage of grafting separated the mesencephalic from the rhombencephalic vesicle, the midbrain- hindbrain-boundary (MHB), is not the boundary between collicular (mesencephalic) and cerebellar tissues, as classically accepted. In conclusion, the cerebellum arises from both, mesencephalic and rhombencephalic vesicles, in contrast to the classical view of its exclusive rhombencephalic origin. The chimeric approach has also determined that the cerebellar primordium extends from the caudal third of the mesencephalic vesicle to the anterior part of rhombomere 2 (rh2), as the entire rhombomere 1 (rh1) and the most anterior part of rh2 provides cells for the medial and most lateral parts of the cerebellum, respectively (Alvarado-Mallart

2000; Alvarez Otero et al. 1993; Hallonet and Alvarado-Mallart 1997; Hallonet et al. 1990; Hidalgo-Sánchez et al. 2005; Martínez and Alvarado-Mallart 1989).

Molecularly, the anterior and posterior neural tube is separated by two main transcription factors. In mouse and chick embryos, *Gbx2* (*gastrulation brain homeobox-2)* expression is observed in the entire posteriormost portion of the embryo. At stage HH4, *orthodenticle homeobox 2* (*Otx2)* and *Gbx2* expressions are observed in the rostral and caudal portion of the chick embryo, respectively. In chick embryos, while at stage HH8, the *Otx2* and *Gbx2* territories are not contiguous, at stage HH9 they slightly overlap. At stage HH10, *Otx2* transcripts are detected in the entire prosencephalic vesicle, and in the mesencephalic vesicle except for its caudal fifth, which is *Otx2* negative (Figure 3 B). This *Otx2*-negative area expresses the *Gbx2* gene (Figure 3 A). Double labeling experiments with *Otx2* and *Gbx2* probes show, that at stage HH10, the two genes are expressed in contiguous and exclusive territories, although a few doubly labeled cells might occur at the interface. Thus, at stage HH10, the *Otx2/Gbx2* common border is far from the MHB constriction and marks the anterior limit of the cerebellar presumptive territory (Martinez and Alvarado-Mallart 1989).

The caudal *Otx2*-negative (*Gbx2*-positive) area shrinks between stages HH12 and 15 until it finally disappears from stages HH17–18 onwards. At this stage of development the rostral limit of *Gbx2*, coincides with the MHB constriction (Figure 3 C- E); (Hidalgo-Sánchez et al. 2005).
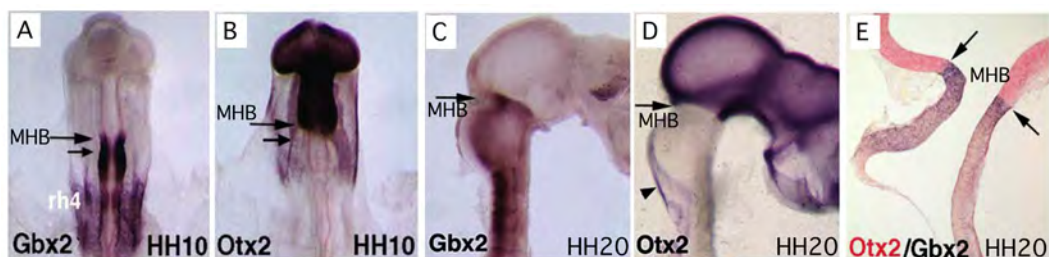
Figure 3: Expression pattern of *Otx2/ Gbx2* mRNA during embryonic development in chicken. *Otx2* and *Gbx2* are complementary expressed during development. Whereas *Gbx2* is expressed in the caudal part of the neural tube (A and C), *Otx2* marks the rostral neural tube (B and D). The border between both genes represents the midbrain- hindbrain- boundary (MHB) ; (arrow bars in the figures) and moves caudally during development. (Modified from Hidalgo-Sánchez 2005)

1.2.2 The cerebellar cortex

The trilayered cerebellar cortex is composed of the molecular layer (ML), the Purkinje cell layer (PCL) and the granule cell layer (GCL); (Figure 4). Each layer hosts specific cell types. The molecular layer hosts inhibitory interneurons such as basket and stellate cells. Purkinje neurons, candelabrum cells (Laine and Axelrad 1994) as well as Bergmann glia are localized in the Purkinje cell layer, a monolayer situated below the molecular layer (Voogd and Glickstein 1998). The granule cell layer hosts granule cells, Golgi and Lugaro interneurons and the recently discovered unipolar brush cells, (Mugnaini et al. 1997). These layers overly an inner core composed of white matter and three pairs of symmetrical clusters of deep cerebellar nuclei (DCN); (Sillitoe and Joyner 2007). The cortex receives three kinds of extra cerebellar afferents: the mossy fibers, the climbing fibers, both of which are excitatory, and the diffusely organized mono-aminergic and cholinergic afferents (Voogd and Glickstein 1998).
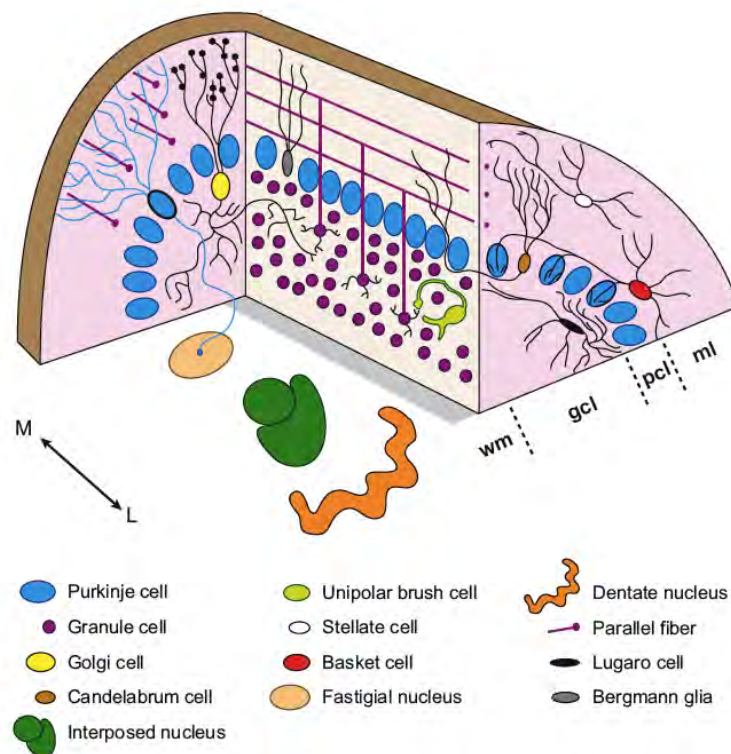
Figure 4: Structure of the cerebellum. The trilayered cerebellar cortex is composed of the molecular layer, the Purkinje cell layer and the granule cell layer. The ML hosts inhibitory interneurons. Purkinje neurons, candelabrum cells as well as Bergmann glia are localized in the PCL. The GCL hosts granule cells, Golgi and Lugaro interneurons and unipolar brush cells. These layers overly an inner core composed of white matter and three pairs of symmetrical clusters of deep cerebellar nuclei (DCN). (Adapted from Silitoe and Joyner 2007)

1.2.3 Origin of cerebellar neurons

So far it is postulated that cerebellar progenitors derive from two distinct germinative centers, the ventricular zone (VZ) of the 4th ventricle and the rhombic lip (RL). Recent studies show that cerebellar neurogenesis is strictly compartmentalized, with VZ progenitors giving rise to GABAergic neurons and RL precursors giving rise to glutamatergic cells (Figure 5); (Englund et al. 2006; Fink et al. 2006; Grimaldi et al. 2009; Machold et al. 2007). Thus, precursors coming from the rhombic lip are *atonal homolog 1* (*Math1)* positive and later differentiate into granule cells, unipolar brush cells and deep nuclear projection neurons. Precursors of the ventricular zone of the 4th ventricle at early stages express *pancreas transcription factor 1a (Pft1a)*. A subpopulation of these cells differentiate into deep nucleo-olivary neurons and Purkinje cells, whereas others will start expressing *paired box 2 (Pax2)* and differentiate into molecular layer basket and stellate cells, Golgi and Lugaro cells of the granule cell layer and deep nuclear interneurons.

Apart from having a different origin following a spatial segregation, the cerebellar neurons are generated according to a well-defined time sequence. Birth dating studies (Altman and Bayer 1997; Sotelo 2004) show, that different neurotransmitter categories are generated according to a characteristic time schedule.
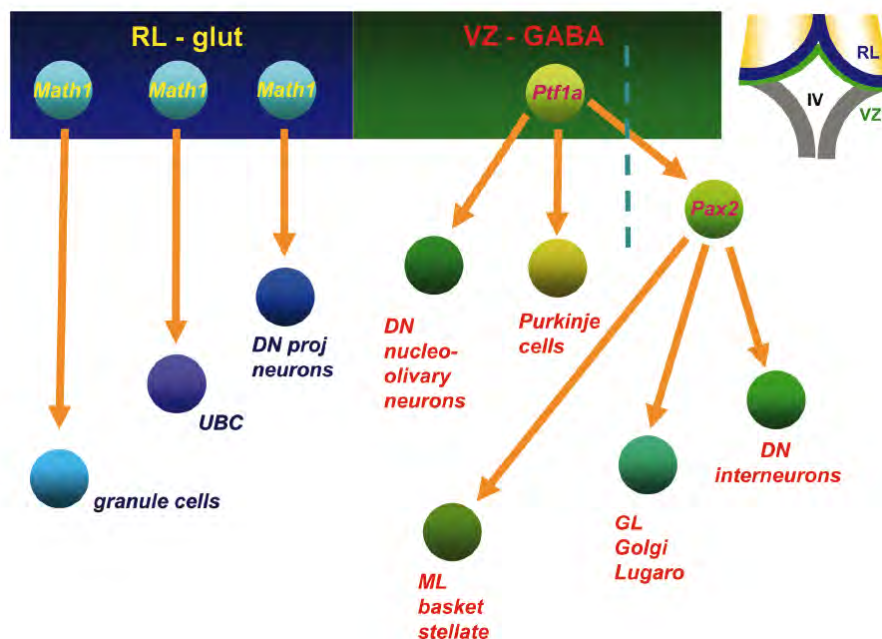
Figure 5: Spatial segregation of glutamatergic and GABAergic lineages in the developing cerebellum. All cerebellar phenotypes derive from two germinative neuroepithelia: the ventricular zone (VZ, green) and the rostral half of the rhombic lip (RL, blue; the position of the germinal zones is also highlighted in the cartoon on the *right* side of the figure; IV, fourth ventricle). The Math1-expressing progenitor cells of the RL give rise to all types of glutamatergic neurons of the cerebellum (deep nuclear [DN] projection neurons, unipolar brush cells [UBC] and granule cells). The VZ contains progenitor cells expressing the transcription factor *Ptf1a*, which are the source of all GABAergic neurons, including nucleo-olivary projection neurons, Purkinje cells, and inhibitory interneurons. The latter derive from a subset of precursor cells characterized by the expression of *Pax2*. (Adapted from Calretti and Rossi 2008)

First, projection neurons of the deep nuclei, such as glutamatergic deep nuclear neurons (blue) derived from the rhombic lip and GABAergic (green) nucleo-olivary projection neurons as well as Purkinje cells derived from the ventricular zone, are originate at mid-embryonic stages, between E12-16 (Figure 6). Local interneurons are born during late embryonic and early postnatal life (Figure 6). Importantly, not the order but the time points at which these neurons are born varies between different species. In chicken these neurons are born earlier in development, since the chicken cerebellum develops faster than the ones of mice or rats. From the point of view of Dahmane and collegues a E10 cerebellum is equivalent to that of an ~E18 mouse embryo comparing the development of foliation patterns (Dahmane and Ruiz i Altaba 1999). For example, by E5 the cerebellar anlage is already made up of an epithelium about 15 cell bodies thick. By E8 the cerebellar anlage is already covered by the external granule layer and by E10 the external granule layer is fully developed, with a thickness of about 10 cell bodies and Purkinje cells can be observed from E8 onwards (Hallonet et al. 1990).
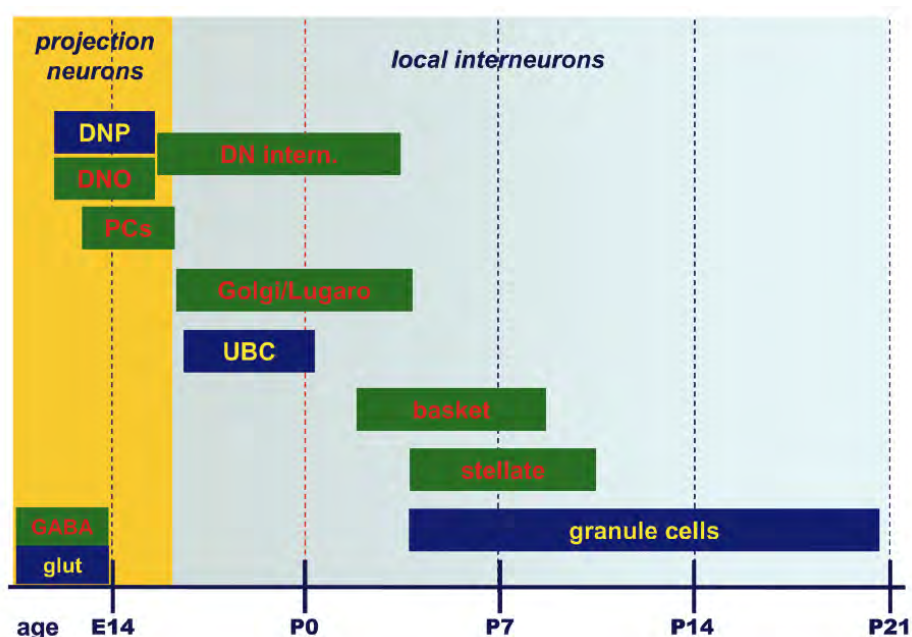
Figure 6: Time sequence of cerebellar neuron generation in mouse embryos. The different types of neurons that populate the adult cerebellum are generated according to a precise time schedule. Projection neurons of the deep nuclei and cortex are the first to be born at the outset of cerebellar neurogenesis. These include glutamatergic deep nuclear neurons (blue) derived from the rhombic lip and GABAergic (green) nucleo-olivary projection neurons and Purkinje cells derived from the ventricular zone. Local interneurons (of both neurotransmitter phenotypes) are born during late embryonic and early postnatal development. GABAergic interneurons are generated according to an inside-out sequence, starting from the deep nuclei and proceeding to the granular and molecular layer. DNP: deep nuclear projection neurons; DNO: nucleo-olivary projection neurons; PC: Purkinje cell; UBC: unipolar brush cell. (Adapted from Calretti and Rossi 2008)

1.2.4 Origin of oligodendrocytes

Oligodendrocytes are subgroup of macroglial cells. Their main function is the myelin formation to insulate the axons in the CNS of vertebrates. Like other glial cells the oligodendrocytes have also a supporting role towards neuronal function, intimately involved in signal propagation (Baumann and Pham-Dinh 2001).

In the mammalian forebrain, oligodendrocyte precursors (OPCs) are generated in a temporal ventral-to-dorsal gradient in most of the parts of the telencephalic ventricular zone including the medial ganglionic eminence (MGE) – the anterior entopeduncular area (AEP), the lateral ganglionic eminence (LGE) – the caudal ganglionic eminence (CGE) and the cortex (Kessaris et al. 2006). The existence of both ventral and dorsal sources of OPCs in the telencephalon mirrors the situations in the spinal cord. The majority of OPCs in the spinal cord is produced in the motor neuron precursor (pMN) domain of the ventral ventricular zone around E12.5 in mice (Lu et al. 2002; Sun et al. 1998; Takebayashi et al. 2002; Zhou and Anderson 2002). However, a minority of 10-15% of OPCs is generated from more dorsal territories around E16.5 (Cai et al. 2005; Fogarty et al. 2005; Vallstedt et al. 2005). Dorsally and ventrally derived OPCs compete for space in the spinal cord as well as in the forebrain. In the spinal cord the ventrally derived population predominates, whereas is the forebrain the dorsally derived populations prevail (Kessaris et al. 2006; Vallstedt et al. 2005). These compensatory effects may serve as a fail-safe myelination of the mammalian brain as a fast and flexible response to demyelinating damage and/or disease.

The ventricular origin and the migratory pathways followed by OPCs during embryonic development were analyzed in homotopic and homochronic quail and chicken chimeras (García-Lopez and Martínez 2010; Le Bras et al. 2005; Olivier et al. 2001). Telencephalic OPCs originate from the anterior alar plate of the

entopeduncular area (Le Bras et al. 2005; Pérez-Villegas et al. 1999), enter and colonize the entire telencephalon following a tangential mode of migration (Figure 7). Diencephalic OPCs originate from the parabasal pretectum and alar diencephalon following axonal pathways (Delaunay et al. 2009; García-Lopez and Martínez 2010) whereas, the rhombencephalic OPCs originate from the basal plate and colonize only their rhombomere of origin with a radially restricted rostrocaudal migration (Figure 7). Therefore, these earlier investigations have strongly suggested that the foci of oligodendrogenesis were localized in the parabasal band of the basal plate of the hind-, mid- and caudal forebrain; while in the rostral forebrain the oligodendrocytes emerged from alar plate territories (Le Bras et al. 2005).
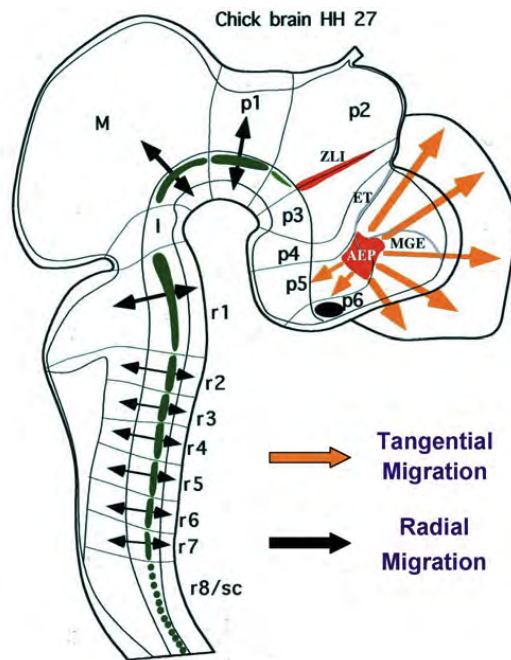
Figure 7: Model of spatial development of oligodendrocytes in the avian developing brain. Sagittal representation of the brain at stage HH27 (E5-6). In the ventricular layer, the basoventral territories of emergence are colored in green, the alar domains in red. Arrows indicate the migratory pathways. Note that oligodendrocyte progenitors emerging from the basoventral foci, in the epicordal domain of the brain, migrate radially (black arrows), while those arising from the alar plate, in the precordal domain of the brain, follow extensive tangential migratory pathways (orange arrows). AEP: anterior entopeduncular area; ET: eminentia thalami; I: Isthmus; M: mesencephalon; MGE: medial ganglionic eminence; p: prosomere (p1 to p6); rh: rhombomere (rh1 to rh7), sc: spinal cord; ZLI: zona limitans intrathalamica. (Adapted from Perez-Villegas et al. 1999 and Le Bras et al. 2005)

Concerning the cerebellar OPCs, they were first considered to be originated from the metencephalic vesicle (Ono et al. 1997). However, more recent evidence obtained from transgenic mouse embryos with *achaete- scute complex homolog 1 (Ascl1)* knockout indicates that this transcription factor is required for OPC maturation, because in the mutant cerebellum they are greatly reduced in number (Grimaldi et al. 2009). Moreover, transplantation and electroporation experiments in these mice have provided indirect data indicating that while all GABAergic interneurons, that also require *Ascl*1 for their maturation, originate from the cerebellar VZ, most, if not all, of the cerebellar OPCs were produced in extracerebellar locations. These latter OPCs reached the cerebellar anlage

during embryonic life, and by E14.5 they were already present in the cerebellum (Grimaldi et al. 2009). Nevertheless, the precise routes of migration and the location of their ventricular epithelium of origin remain unknown.

1.3 The oligodendritic lineage development

Oligodendrocytes originate from migratory and mitotic precursors and mature progressively into postmitotic myelin-producing cells. The sequential expression of developmental markers divides the lineage into distinct phenotypic stages. Some of them are characteristic myelin components. Myelination requires a number of sequential steps in the maturation of the oligodendroglial cell lineage accompanied by a coordinated change in the expression of cell surface antigens often recognized by monoclonal antibodies. Differentiation involves the loss of certain surface or intracellular antigens and the acquisition of new ones (Baumann and Pham-Dinh 2001). Some of the most prominent markers are described above and summarized in figure 8.

1.3.1 Oligodendrocyte transcription factor 2 (Olig2)

Olig2 belongs to the family of *basic helix-loop-helix* (*bHLH*) transcription factors and is one of the earliest markers for OPCs (Figure 8). It is expressed in both, the developing and mature vertebrate central nervous system (Ligon et al. 2006; Ono et al. 2009; Woodruff et al. 2001). *Olig* function is necessary for embryonic and fetal-born oligodendrocytes. Complete failure of oligodendrocyte development is

observed in *Olig1/2* null embryos (Lu et al. 2002; Zhou and Anderson 2002). In explants of *Olig2⁻ᐟ⁻* embryos a failure in the production of OPCs, expressing oligodendrocyte surface antigen 4 (O4), was observed as late as the equivalent of P7 (Lu et al. 2002), ruling out a mere delay in development. Moreover, *Olig1/2⁻ᐟ⁻* neurospheres are incapable of OPC production *in vitro* (Zhou and Anderson 2002). Thus, while the sites of oligodendrocyte production may change from the early embryo to postnatal stages, the requirement for Olig function remains a consistent feature (Ligon et al. 2006).

1.3.2 Paleted- derived growth factor receptor alpha (PDGFRα)

Another prominent early marker for OPCs is *PDGFRα*. In the spinal cord, *PDGFRα*+ oligodendrocyte progenitor cells first appear in a highly restricted region of the ventral neuroepithelium around E14 in the rat (E12.5 in mouse, E7 in chick); (Pringle and Richardson 1993; Pringle et al. 1996; Woodruff et al. 2001). In the forebrain, there is a discrete ventral focus of *PDGFRα*+ cells spanning the boundary between the anterior hypothalamus and the medial ganglionic eminence (MGE), that first appears around E13 in the rat (E11 mouse); (Pringle and Richardson 1993; Spassky et al. 1998; Woodruff et al. 2001). In the chick forebrain at E5, there is a corresponding focus of *PDGFRα*+ cells in the entopeduncular area (Pérez Villegas et al. 1999) and also a separate focus at the base of the 4th ventricle around E7 (Woodruff et al. 2001). The latter focus, which is not found in rodents, presumably corresponds to the ventral source of O4+ oligodendrocyte progenitors described in the chick by Ono et al. (1997). *PDGFRα* expression is maintained in immature oligodendrocytes but disappears during the transition to remyelinating oligodendrocytes (Figure 8); (Nishiyama et al. 2009).
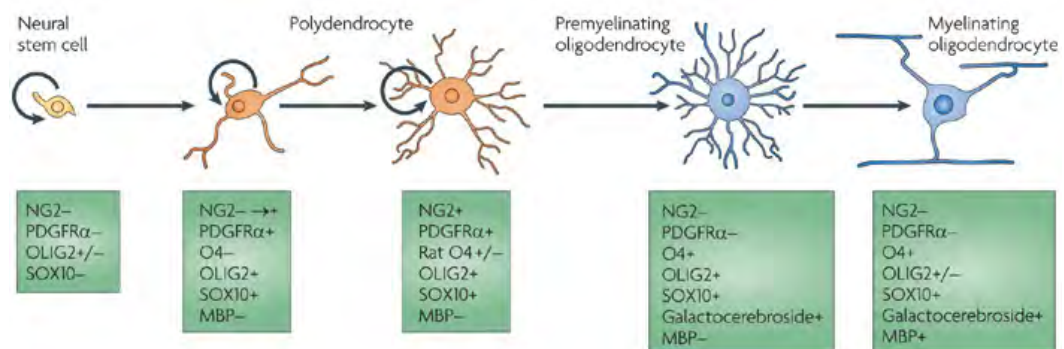
Figure 8: A scheme showing the oligodendrocyte lineage. The two markers for polydendrocytes, *chondroitin sulfate proteoglycan NG2* and platelet-derived growth factor receptor- α (*PDGFRα*), are not expressed by neural stem cells but are expressed by proliferating progenitor cells (proliferation is indicated by the semicircular arrows) of the oligodendrocyte lineage. As polydendrocytes undergo terminal differentiation into mature oligodendrocytes they lose the expression of *NG2* and *PDGFRα* and begin to express the immature *oligodendrocyte surface antigen O4*, followed by galactocerebroside and subsequently myelin basic protein (MBP). *SOX10* is expressed throughout development, whereas *Olig2* seems to be downregulated in the mature oligodendrocytes. (Nishiyama et al. 2009)

1.3.3 SRY (sex determining region Y)-box 10 (Sox10)

Sox10 is a HMG-domain transcription factor, that is expressed throughout oligodendrocyte development and is an important component of the transcriptional regulatory network in these myelin-forming CNS glia (Kuspert et al. 2010). *Sox9* and *Sox10* influence the survival and the migration of oligodendrocyte precursors in the spinal cord by regulating *PDGFRα* expression (Finzsch et al. 2008). Additionally, it has been shown recently that *Sox10* is also required for oligodendrocyte differentiation as well as for oligodendrocyte survival following axon wrapping (Takada et al. 2010). Furthermore *Olig1* and *Sox10* have been demonstrated to interact synergistically to drive *myelin basic protein* (*MBP*) transcription in oligodendrocytes (Li et al. 2007).

1.3.4 Oligodendrocyte surface antigen 4 (O4)

Oligodendrocyte precursors express *chondroitin sulfate proteoglycan NG2* (Nishiyama et al. 2009) and proliferate in response to platelet-derived growth factor (*PDGF*); (Noble et al. 1988; Richardson et al. 1988). Later in development, labeling with the cell surface antigen *O4* identifies OPCs and immature oligodendrocytes (Bansal et al. 1989; Yang et al. 2011) Recent data show that oligodendrocyte precursors expressing *O4*, cell surface ganglioside epitope *A2B5* and oligodendrocyte cell surface antigen *O1* are controlling the onset of CNS myelination (Yang et al. 2011).

1.3.5 Proteolipid binding protein (PLP)

PLP has been first identified and characterized in mice (Yan et al. 1993; Yan et al. 1996) and is a marker for mature oligodendrocytes. In chicken the expression of *PLP* starts around HH10 (E2) in migrating cephalic neural crest cells (Pérez Villegas et al. 1999). In the CNS, *plp/dm-20*-expressing cells were first observed

at stage HH18 (E2.5) and were localized exclusively in the brain. They formed four discrete foci in the ventricular layer, with a segmental distribution along the rostro-caudal axis. The more rostral site of *plp/dm-20* expression was detected medially at the rostral pole of the prosencephalon in the chiasmatic area. In the diencephalic prosomere 1 (p1) and in the mesencephalon, two other foci were localized bilaterally in the basal plate. In the hindbrain, the *plp/dm-20* cells formed two paramedian columns, on either side of the floor plate, interrupted at the interrhombomeric boundaries. In the spinal cord, caudal to r7, no *plp/dm-20-* expressing cells were detected (Pérez Villegas et al. 1999). *PLP* expression in the ventricular domains corresponds to the foci that give rise to oligodendrocytes in the chick developing brain. *PLP* expression starts remarkably early in the ventricular layer of the brain anlage and is closely associated to the domain of expression of *Shh* (Pérez Villegas et al. 1999).

1.3.6 Myelin basic protein (MBP)

MBP, the second most abundant protein in central nervous system, is responsible for adhesion of the cytosolic surfaces of multilayered compact myelin (Boggs 2006). After Schwann cell and oligodendroglial processes have attached to the axon and initiated polarization of their secretory pathways for transport of membrane towards the axon, specific sorting mechanisms ensure vectorial delivery of myelin-membrane components to the glial-axon contact site. One major myelin component, which does not reach myelin by vesicular transport, is myelin-basic protein (MBP); (Simons and Trotter 2007). Targeting of MBP to myelin relies on transport of *MBP* mRNAs in the form of granules that are assembled in the cell perikaryon and transported along processes to the myelin membrane where in response to a stimulus local translation occurs (Simons and Trotter 2007). A number of studies have shown that the highly positively charged MBP interacts with the negatively charged cytoplasmic membrane surface and this binding is likely to be crucial for the assembly of myelin (Simons and Trotter 2007).

1.4 Bergmann glia in cerebellar development

Bergmann glial cells create their own subclass within the group of astrocytes in the cerebellar cortex. They are unipolar astrocytes located around the soma of Purkinje cells with Bergmann fibers extending through the molecular layer terminating at the pial surface. Historically Bergmann glial cells are also called "epithelial cells with Bergmann fibers" and "Golgi epithelial cells" (Yamada and Watanabe 2002). There are approximately 8 Bergmann glial cells for each Purkinje cell (Reichenbach et al. 1995). The whole dendritic arbors of Purkinje cells are covered with Bergmann glial fibers, but they are not only in close contact to Purkinje cells but also known to associate with migrating granule cells from which the concept of glia guided neuronal migration has been proposed (Rakic 1971; Yamada and Watanabe 2002).

1.4.1 Bergmann glia development

The development of Bergmann glia is divided into four main stages. First of all is the stage of radial glia until E14 in mouse embryos. At this developmental stage most, if not all, glial precursors in the cerebellum take the form of radial glia, expressing *glutamate- aspartate transporter* (*GLAST)* and *tenascin-C*. At E13 the

expression is restricted to the ventricular zone, whereas at E14 a few cells express *GLAST* in the mantle zone near the ventricular zone (Yamada and Watanabe 2002). This stage of development coincides with the birthdate of Purkinje cells, which are produced between E11-13 in mice (Miale and Sidman 1961). During Purkinje cell migration, radial- glial fibers are apposed and are in contact with calbindin- positive Purkinje cells at E14 and E15 (Yuasa et al. 1996; Yuasa et al. 1991). Whether or not Bergmann glial fibers thereby guide Purkinje cell migration has not been proven yet (Yamada and Watanabe 2002).

The second stage of Bergmann glia development is referred to as migration and takes place between E14 and P7. This stage is characterized by an increase in *GLAST* and tenascin expressing cells in the mantle zone at E15, that is, on the next day of active Purkinje cell migration. At E15 *GLAST* expressing glial cells are evenly distributed among Purkinje cells, situated just beneath them. This indicates a strong correlation between glial and Purkinje cell migration. By E18 the expression of *GLAST* and *tenascin* further increases and locates beneath the multicellular layer of Purkinje cells. During the first postnatal week Bergmann glial cells form a compact epithelium- like lining in the Purkinje cell layer (Yamada and Watanabe 2002).

Transformation, as the third phase of development, is characterized by cytoarchitectonic changes during the second postnatal week (P7~ P21) and even up to the third week. During this time, thorn-like lateral expansions appear to protrude upwards from the proximal shaft of Bergmann fibers to the molecular layer (Altman 1975; Altman and Bayer 1997; Rakic 1971; Reichenbach et al. 1995). The second postnatal week is, when dentritogenesis and synaptogenesis are activated (Altman 1972c). It is the week of active production and migration of granule cells (Altman 1972a; Altman 1972b). Migrating cell bodies and their processes are directly attached to Bergmann fibers. In some cases, Bergmann fibers and trailing processes of granule cells form robust pillar- like bundles in the molecular layer. Thus the second postnatal week is characterized by dynamic expansions of the molecular layer as a result of active dendritogenesis and synaptogenesis of Purkinje cells as well as of the internal granule layer as a result of massive migration and granule cell production. Therefore active mitosis of Bergmann glia contributes to the supply of the glial framework and substrates to these newly expanding regions (Yamada and Watanabe 2002).

From P21 onwards Bergmann glial cells enter the stage of protoplastic astrocytes, which completely enwrap the spines and spiny branches of Purkinje cells by thin lamellate processes. The ascending portion of T-shaped granule cell axons is also bundled with Bergmann fibers. Therefore, it is clear that Bergmann fibers in the adult cerebellum maintain cellular affinities for the somato- dendritic domain of Purkinje cells and for the ascending axons of granule cells (Yamada and Watanabe 2002). The four stages of Bergmann glia development are summarized in table 1 as described in Yamada and Watanabe 2002.

Table 1: Four stages of Bergmann glia development in the rodent cerebellum: The birthday of cerebellar neurons in the mouse or rat is from Miale and Sidman (1961) and Altman and Bayer (1997), respectively. Developmental stages written in regular and italic fonts indicate those in the mouse or rat, respectively. BC: basket cell, CF: climbing fiber, DC: deep cerebellar nucleus neuron, EGL: external granular layer, Go: Golgi cell, Gr: granule cell, PF: parallel fiber, SC: stellate cell. (Adapted from Yamada and Watanabe (2002)

Bergmann glia	Purkinje cell	Other cerebellar neurons
Radial glia (~E14/~E17)	Production (E11-13/ E13- 16)	DC production (E11-E13/ E13-14)
Migration (E15~P7/E17~P8)	Monolayer alignment CF synaptogenesis	EGL formation Go production (E12-15/ E18-P3) BC production (P4-11)
Transformation P7-21/P8-25)	Dendritogenesis PF synaptogenesis CF translocation/ elimination	SC production (P7-12) Gr production (~P15/~P21)
Protoplasmic astrocyte (P21~/P25~)	Synaptic transmission Long- term depression Motor coordination	

1.4.2 The Bergmann glia lineage development

During development Bergmann glial cells express a wide range of markers of which most are commercially available. Some prominent markers, also used in this study are listed below.

1.4.2.1 Glutamate- aspartate transporter (GLAST)

GLAST is presumed to be an astroglial protein, which is expressed in cerebellar primordium at early developmental stages such as E14.5 and E16.5. Its expression increases during postnatal development and is restricted to the Purkinje cell layer in adult stages (Furuta et al. 1997; Regan et al. 2007). In the Purkinje cell layer *GLAST* is expressed abundantly in Bergmann glia and plays a major role in glutamate uptake at the excitatory synapses in cerebellar Purkinje cells preventing glutamate spillover (Takayasu et al. 2006).

1.4.2.2 Intermediate filament proteins

Furthermore the intermediate filament proteins II (*Vimentin* and *GFAP*) and VI (*Nestin*) are expressed in Bergmann glia (Yamada and Watanabe 2002).
Nestin is regarded as one of the classical neural stem cell markers (Gilyarov 2008; Wei et al. 2002) and is expressed in neurons (Fukuda et al. 2003) as well as glial cells (Matsumura et al. 2010). In Bergmann glia, *Nestin* was expressed predominantly between postnatal stages P1 to P21 (Hockfield and McKay 1985; Sotelo et al. 1994).
Glial fibrillary acid protein (*GFAP*) is an astrocytic marker expressed in mature astrocytes (Fuchs and Weber 1994) and in Bergmann glial cells from P4 until adulthood (Gimenez et al. 2000).
Vimentin is expressed by immature astroglia and present in Bergmann glia from embryonic stage E15 until adulthood (Bovolenta et al. 1984; Colucci-Guyon et al. 1999).

Bergmann glia express a large variety of proteins during development. Based on the publication of Yamada and Watanabe (2002) they can be classified into cytoskeletal proteins, metabolic enzymes, neurotransmitter receptors, extracellular matrix proteins/ cell adhesion molecules and transcription factors/ regulators. They have been summarized according to their subgroup and their stage of expression in figure 9.
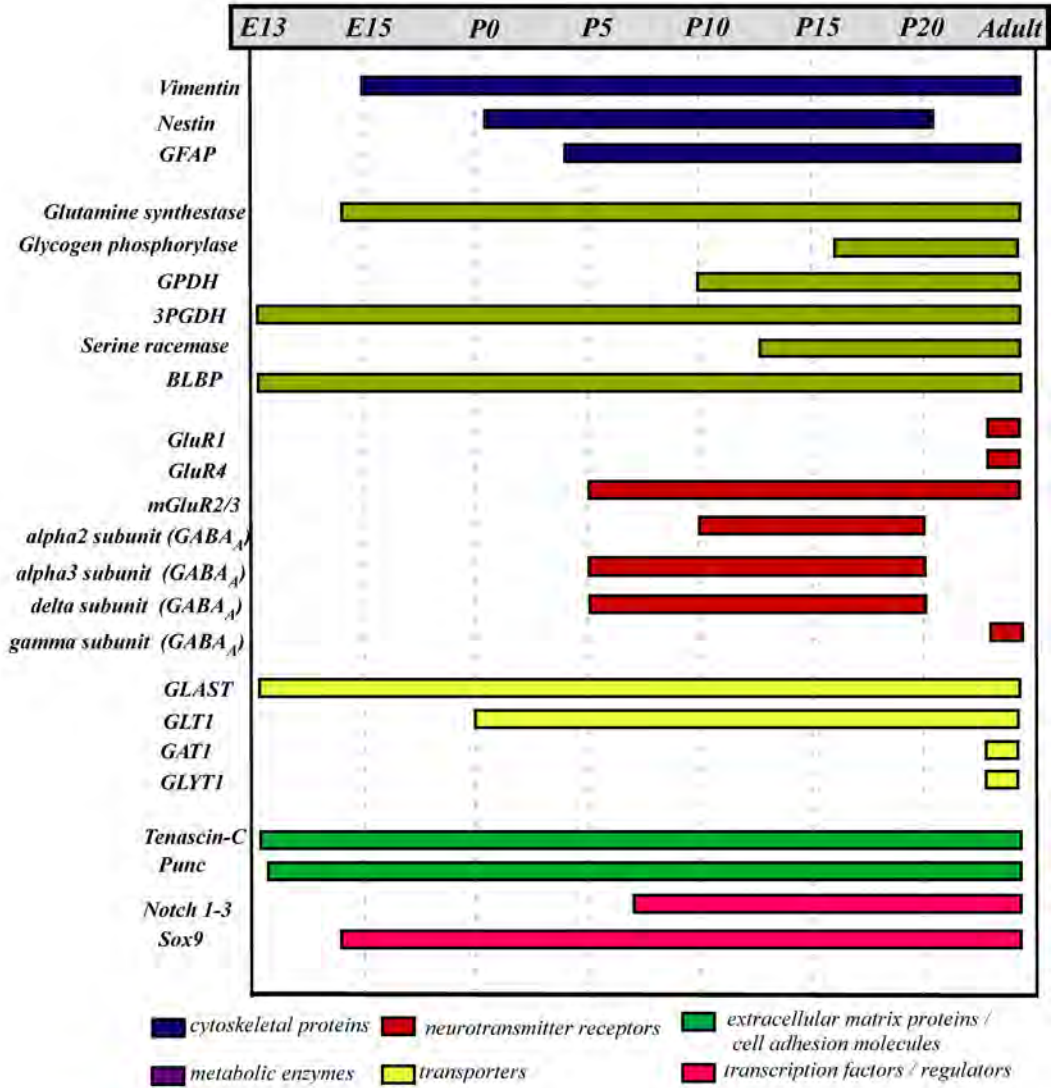
Figure 9: Molecules expressed in Bergmann glial cells. Figure based on table 1 in Yamada and Watanabe 2002

1.5 Growth differentiation factor 10 (*Gdf10 / Bmp3b*)

Growth differentiation factor 10 (*Gdf10*), also known as *Bmp3b*, is a member of the *transforming growth factor beta* (*TGF-ß)-* superfamily. *TGF-ß* family members are structurally related polypeptide growth factors regulating cellular processes such as cell proliferation, lineage determination, differentiation, motility, adhesion and death (Massagué 1998). *TGF-ß* and related factors regulate gene expression by receptor serine/threonine protein kinases. These receptors phosphorylate each other, which in turn phosphorylates SMAD proteins. The SMAD proteins move into the nucleus and generate transcriptional complexes of specific DNA-binding ability (Susumu et al. 2000). There are type I and type II receptor families. Gdf10, as a member of the Bmp3 subfamily, binds to type II receptors. In vertebrates, the type II receptor subfamily includes TGFß-II, BMPR II and AMHR, which selectively bind TGF-ß, Bmps and MIS (Massagué 1998).

Phylogenetic analysis revealed that *Gdf10* and *Bmp3* are paralogs. *Gdf10* and *Bmp3* homologs are well conserved, especially within the C-terminal TGF-ß-like domain (Katoh and Katoh 2006). The Human *BMP3b* gene is located on chromosome 10, which is correlates with its location in the mice genome, where

it is located in the proximal region if chromosome 14. That corresponds to the human chromosome 10 (Cunningham et al. 1995; Hino et al. 1996).

It was shown that the coordination of *Bmp3b* and *cerberus* is required for head formation of *Xenopus* embryos (Hino et al. 2003). Comparative analysis of *Bmp3* and *Bmp3b* revealed that they function differentially to control axial patterning of Xenopus embryos (Hino et al. 2003). *Bmp3b* antagonizes ventralizing *Bmps* (*Bmp-2* and *ADMP*) and dorsal mesoderm inducers (*derrière* and *Xnr1*). *Bmp3* antagonizes only ventralizing *Bmps*. The precursor of *Bmp3b* is cleaved less than that of *Bmp3*, which might explain the difference in function compared to *Bmp3* (Hino et al. 2003).

In mice Gdf10 was identified as a marker expressed in the Purkinje cell layer of the cerebellum (Zhao et al. 1999). Based on a publication by Zhao and colleagues *Gdf10* is neither expressed in Bergmann glia nor in Purkinje and granule cells. However, Koirala and Gold et. al. (Gold et al. 2003; Koirala and Corfas 2010) demonstrated that *Gdf10* is expressed in Bergmann glia. The second part of this work focuses on a detailed characterization of *Gdf10* during embryonic and postnatal development and will address this question.

Little is known about the role *Gdf10* holds in the brain. The following paragraphs give a short summary of indications for the function of *Gdf10* in the CNS. Some of them were investigated in more detail and are part of this work.

In Purkinje cell degeneration mice (*pcd*[3J]) of 4 month *Gdf10* is reduced to 15 % of the wild type signal obtained from wildtype littermates of the same age (Rong et al. 2004). This reduction of *Gdf10* to 15 %, due to the degeneration of Purkinje cells, indicates a strong relation between *Gdf10*, Bergmann glia and Purkinje cell development, which needs to be investigated.

Another study shows, that *Gdf10* is downregulated by factor 1.94 in *Pax6* -/- mice (Holm et al. 2007). *Pax6* is a transcription factor of the *Pax* gene family, which plays an important role in the development of the nervous system (Schmahl et al. 1993; Stoykova et al. 1997; Warren and Price 1997). The absence of *Pax6* influences proliferation, cell fate and patterning in the brain and spinal cord (Ericson et al. 1997; Hack et al. 2004; Haubst et al. 2004; Osumi et al. 1997; Schmahl et al. 1993; Stoykova et al. 1997; Takahashi and Osumi 2002). *Gdf10* is

downregulated in *Pax6* deficient mice suggesting that *Pax6* also affects Bergmann glia development.

Further studies demonstrate that mutations in the orphan nuclear receptor $ROR\alpha$ block Purkinje cell differentiation with secondary loss off afferent granule cells. They also show that $ROR\alpha$ via Sonic hedgehog negatively regulates the expression of *Gdf10* which might suggest this gene as a canditate mitogene for granule cell precursors (Gold et al. 2003).

Another candidate gene, which might be a regulator of *Gdf10* is *Sox9* (Lafont et al. 2008). It was shown to be expressed in glial cells of the developing cerebellum and is involved in the modulation of glial specification and differentiation in the nervous system (Kordes et al. 2005; Stolt et al. 2003). The depletion of *Sox9* greatly reduces *Gdf10,* indicating that *Gdf10* is directly or indirectly regulated by *Sox9* (Lafont et al. 2008).

The most recent data obtained from studies with *Gdf10* revealed an important role as a tumor suppressor interacting with *soybean Ca(2+)- ATPase 1* (*Sca1*). *Sca1* is necessary for maintaining tumorigenicity of mammary tumors by inhibiting the expression of *Gdf10* and thereby inhibiting Tgf-ß signaling (Upadhyay et al. 2011). Upadhyay and colleagues were able to characterize the signaling pathway the Gdf10 protein acts through, which is illustrated in figure 10. *Sca1* is depicted as interacting with Tgfß-RI to interfere with Tgfß-RI- Tgfß-RII complex formation and subsequently activate the Smad3 signaling cascade. When *Sca1* expression is reduced, *Gdf10* expression is increased, leading to stabilization of the receptor complex and Smad3 activation (Upadhyay et al. 2011).
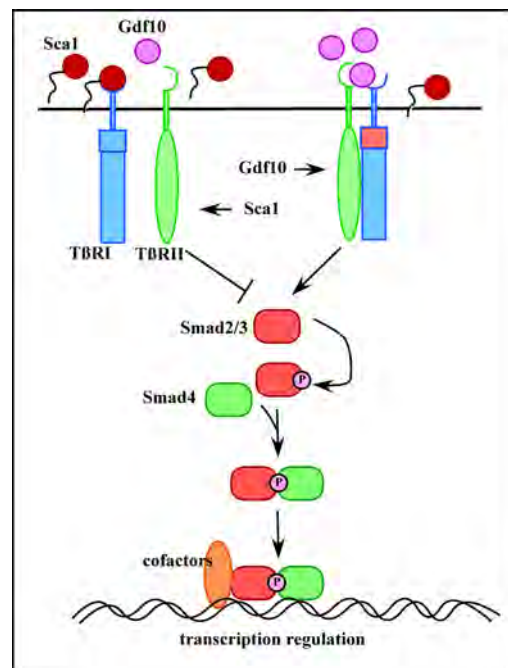
Figure 10: Gdf10 signaling cascade: *Sca1* is depicted as interacting with Tgfß-RI to interfere with Tgfß-RI- Tgfß-RII complex formation and subsequent activation of *Smad3*. When *Sca1* expression is reduced, *Gdf10* expression is increased, leading to stabilization of the receptor complex and Smad3 activation. (Adapted from Upadhyay *et al.,* 2011)

1.6 Sonic hedgehog (*Shh*) in cerebellar development

The Shh pathway acts on gene expression through the activity of the glioma-associated oncogene (Gli) transcription factor family, which comprises the genes Gli1, Gli2, and Gli3 as illustrated in figure 11. In the absence of Shh, its transmembrane receptor Patched 1 (Ptch1) inhibits by default the transmembrane protein G coupled receptor Smoothened (Smo). This prevents the translocation of Smo to the primary cilia. Consequently, Gli3 becomes constitutively cleaved and converted into its transcriptional repressor form. Upon the binding of Shh to Ptch1, the inhibition exerted on Smo is released, and this allows its accumulation in the cilia (Vaillant and Monard 2009). Smo activates an inhibitory G protein Gαi that stops cAMP production (Huangfu and Anderson 2006). The full-length Gli3, no longer cleaved, becomes transcriptionally active together with Gli2, and both initiate a downstream activation of Gli1 (Fuccillo et al. 2006; Sillitoe and Joyner 2007). The target genes of the Gli factors are only partly identified. They belong to the cell cycle regulators and to the Shh pathway itself (Vaillant and Monard 2009).
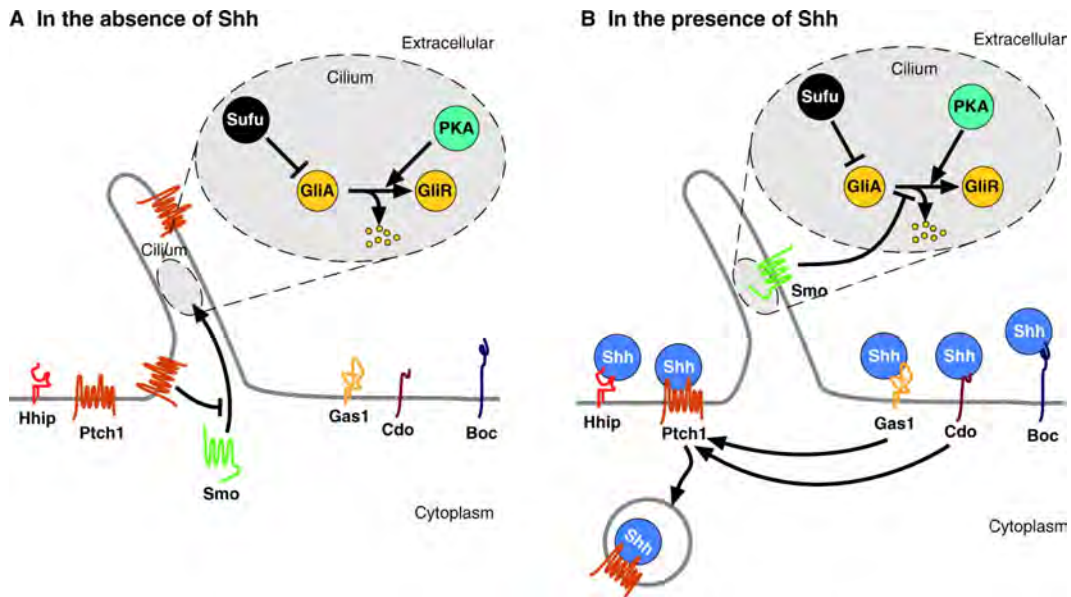
Figure 11: Vertebrate Shh signal transduction. A summary of Shh signal transduction in vertebrates in (**A**) the absence and (**B**) the presence of Shh. (A) Patched 1 (Ptch1), a twelve-pass transmembrane protein that binds Shh and represses the activity of a seven-pass transmembrane protein, smoothened (Smo), in the absence of ligand. (B) When bound by Shh, Ptch1 relieves its inhibition of Smo, allowing Smo to transduce Shh signaling intracellularly. (A) In the absence of Shh, Ptch1 localizes to cilia, and Smo is not present in cilia. (B) Upon Shh exposure, Ptch1 leaves the cilia, leading to an accumulation of Smo and to the activation of signaling. Downstream of Smo, several proteins, including suppressor of fused (Sufu), protein kinase A (PKA) and possibly costal 2 (Cos2), are implicated in signal transduction. Three Gli transcriptional regulators (Gli1, 2 and 3) are present and expressed in the neural tube, where *Gli3* expression is repressed at high Shh signaling levels. Gli3 is a bifunctional transcriptional repressor and activator. In the absence of Shh signaling, Gli3 is proteolytically processed to generate a transcriptional repressor (GliR). Similarly, Gli2 also undergoes proteolytic processing in the absence of Shh signaling, but in contrast to Gli3, Gli2 is mostly completely degraded (yellow spots). Finally, *Gli1* expression is completely dependent on Gli2/3 activator (GliA) function. Gli1 is also trafficked from the nucleus in the absence of active signaling. Therefore, Shh signaling not only induces *Gli1* expression, but also regulates its nuclear accumulation and thereby its function. (Dessaud et al. 2008)

Shh was discovered as the master player triggering the expansion of cerebellar granular neuronal precursors. Indeed, a putative involvement of Shh in the cerebellum was first suspected from studies on the inhibition of cholesterol synthesis. As Shh needs to be cholesterol-modified to be active, this inhibition led to a defective Shh signaling causing abnormal cerebellar development (Dehart et al. 1997; Lanoue et al. 1997; Repetto et al. 1990). From E17.5, Shh was shown to be continuously secreted from the Purkinje cells and to diffuse up to the external granular layer (EGL) (Dahmane and Ruiz i Altaba 1999). The outer EGL, composed of proliferative granule cell precursors, shows the highest expression of *Gli1*, read-out of the Shh pathway. Studies demonstrated the potent proliferative role of Shh on these progenitors using diverse combinations of *in vitro* and *in vivo* assays based on granule cell precursor cultures, slices, and/or explants and injection of inhibitory anti-Shh antibodies (Dahmane and Ruiz i

Altaba 1999; Dessaud et al. 2008; Wallace 1999; Wechsler-Reya and Scott 1999).

Among the already identified mitogens in the cerebellum (*Fgf-2*, *insulin- like growth factor 1* (*IGF-1)*, epidermal growth factor (*EGF*)), *Shh* turned out to clearly be the most potent mitogenic factor, as it is solely able to trigger up to a 100-fold increase of granule cell precursor proliferation *in vitro* (Wechsler-Reya and Scott 1999). Shh addition to cultured cerebellar explants promotes Bergmann glia differentiation (Dahmane and Ruiz i Altaba 1999). In addition, the fibers of the Bergmann glia are malformed and irregular upon conditional mutation of *Gli2* (Corrales et al. 2004). The exact role of *Shh* in Bergmann glia maturation and function remains presently unclear. These observations, however, indicate that Shh does not only contribute to the final number of mature granule cells by promoting their initial expansion but also by inducing the maturation of their migration support. Shh overall expression profile in early postnatal stages is directly responsible for the final size and shape of the cerebellum (Dessaud et al. 2008).

Finally, Shh was shown to determine the differential growth of the EGL ending in a defined size of folium. Absence of foliation was first demonstrated after conditional deletion of *Shh* or injection of blocking anti- Shh antibodies (Dahmane and Ruiz i Altaba 1999; Lewis et al. 2004). *Shh*-P1 mutants, in which *Shh* was overexpressed in Purkinje cells, presented a larger cerebellum. An extralobule could even be formed upon further increase of Shh activity in the *Shh*-P1; Ptch1+/− mouse (Corrales et al. 2004). In conclusion, *Shh*, although dispensable for determination of folium position, is required for full lobe extent (Dessaud et al. 2008). A schematic view of the importance Shh holds in developing cerebellar cortex including cooperative and negative regulators of Shh pathway, is illustrated in figure 12.
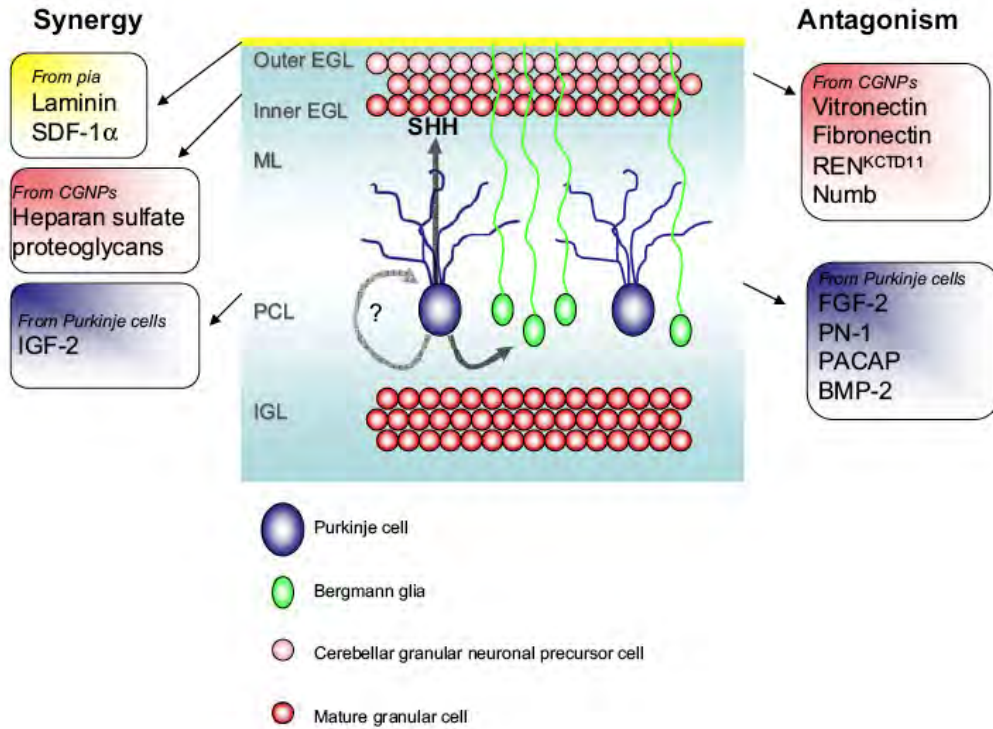
Figure 12: Schematic view of the developing cerebellar cortex including cooperative and negative regulators of the Shh pathway. Postnatally, Shh is constantly secreted by Purkinje cells and triggers granule cell precursor mitosis in the outer EGL, Bergmann glia differentiation and possibly Purkinje cell maturation in the PCL. Its promitogenic effect on granule cell precursors is synergized by cooperative modulators (left) or tuned down by negative modulators (right). Signals can originate from different compartments as specified. EGL: external granule layer, IGL: internal granule layer, ML: molecular layer, PCL: Purkinje cell layer. (Vaillant and Monard 2009)

1.7 Aim of the study

This study, focusing on the development of cerebellar oligodendroglia, has two goals. The main goal is to identify the origin of oligodendroglia in the chicken cerebellum. As described previously, the origin of cerebellar neurons is very well studied, but little is known about the origin of cerebellar oligodendroglia. The hypothesis is, that some cerebellar oligodendrocytes have an extracerebellar origin. In order to investigate this, *in ovo* homotopic and homochronic transplants of different neuroepithelial domains within the mesencephalic vesicle between quail and chick embryos at developmental stage Hamburger- Hamilton 10 (HH10) have to be performed. Therefore, grafts of one half of the mesencephalic vesicle have to be performed along the rostro- caudal axis as well as the dorso-ventral axis in order to create a fate map of the mesencephalic vesicle. Donor cells should be characterized with neuronal and oligodendroglial markers to identify their phenotype.

To confirm obtained results, specific grafts should be repeated by electroporating chicken embryos at HH10 and grafting electroporated chicken mesencephalon into untreated chicken embryos of the same age. Additionally DiI injections into the relevant area of interest should be performed to underline the hypothesis.

The second goal is to analyze the expression pattern of Gdf10 protein and mRNA during mouse development (E14.5 – adulthood). Furthermore the phenotype of *Gdf10* expressing cells and the time at which they co-localize with specific markers should be analyzed. This work should primarily focus on cerebellar development.

So far *Gdf10* has been mentioned only casually in a context independent of cerebellar development. In order to create a basis for further studies, the *Gdf10* gene should be analyzed for transcription factor binding sites using the Jasper database, which is an online database containing a curated, non-redundant set of profiles, derived from published collections of experimentally defined transcription factor binding sites for eukaryotes (http://jaspar.genereg.net/); (Stormo 2000; Wasserman and Sandelin 2004). The obtained data should be analyzed in the context of cerebellar development. Finally, a series of experiments using Gdf10 recombinant protein on brain slice cultures of mouse cerebellum at developmental stage E18.5/P0 should be performed. In addition to that, the expression of *Gdf10* mRNA in *Shh* conditional mutants has to be investigated to identify a possible upstream regulator of this protein.

2 Materials and Methods

2.1 Analysis of cerebellar oligodendroglia development in quail-chick chimeras

2.1.1 Experimental embryology

Quail (*Coturnix coturnix japonica*) and chick (*Gallus gallus)* fertilized eggs used for this study were obtained from commercial sources. In order to reach the adequate stages for the experiments, chick eggs were incubated at 37°C in a forcedair incubator for 36 hours, whereas quail eggs were incubated for 31 hours, as quail develops faster. Chick embryos were used at stage HH10 according to Hamburger and Hamilton (1951); (Hamburger and Hamilton 1992). The quail embryos used, showed equivalent morphological characteristics. Experiments were performed under relatively sterile conditions, and quail embryos were used as donors. A grid with concentric circles was inserted in one ocular of the operating microscope in order to normalize graft dimensions and establish relative distances between recognizable structures and presumptive territories. At the working magnification used during microsurgery (40x), the difference in radial distance between any two adjacent concentric circles in the grid was 40 µm. For surgery, the grid center was positioned in the center of the midbrain, while the vertical axis of the grid was superposed to the ventral midline (Figure 13A).
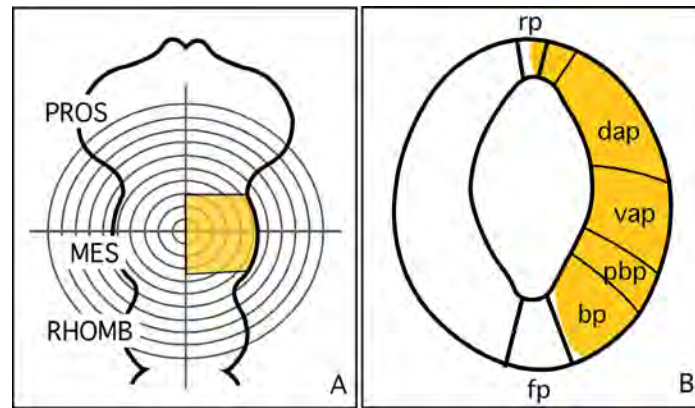
Figure 13: Area of transplantations. A) For transplantation a grid with concentric circles was inserted into one of the oculars of the microscope in order to normalize graft dimensions. Grafts were performed in the region marked in orange (A and B). (bp: basal plate, dap: dorsal alar plate, fp: floor plate, MES: mesencephalon, pbp: parabasal plate, RHOMB: rhombencephalon rp: PROS: prosencephalon, roof plate, vap: ventral alar plate)

2.1.2 Microsurgery

The egg shell was opened using tape to fixate it and then by cutting a small window with scissors. First, embryos were counterstained *in ovo* with Indian ink (Pelikan, Germany), diluted 1:5 in Tyrode's solution (0.2 M NaCl, 4.5 mM KCl, 4 mM $CaCl_2$, 0.4 mM $MgCl_2$, 0.8 mM NaH_2PO_4) supplemented with Penicillin (10000 U/ml - Gibco, USA) / Streptomycin (10000 µg/µl – Gibco, USA), 28 mM Glucose and 59 mM $NaHCO_3$. which was injected under the blastoderm using a glass micropipette. Afterwards, the vitelline membrane was slit open over the anterior pole of the embryo with a tungsten needle and the selected neuroepithelial segment was excised from the host. An equivalent piece of tissue from the quail donor was cut using the same tungsten needle and the same procedure as in the chick. The graft was transferred to the host using a glass micropipette, and grafted into the chick embryo. The piece of donor tissue was inserted into the space prepared previously in the host, maintaining the original rostro- caudal and dorso- ventral orientation. Emplacement with respect to the ocular frame was annotated for each homotopic and tissue isochronic transplant. After the procedure, the eggs were sealed with a piece of tape and incubated without tilting until they reached the stages chosen for histological analysis. Utmost care was taken to minimize distortion of the chimeric neural tube. Chimeric embryos with morphological alterations were rejected. This method was described in detail by Nicole Le Dourain (Le Douarin et al. 2008).

Grafts were performed along the rostro- caudal axis of the mesencephalic vesicle. To distinguish the exact origin of cells migrating into the cerebellum,

small grafts confined to only one side of the neural tube of the mesencephalic vesicle, were performed transplanting the alar, parabasal and basal plate of the vesicle (Figure 13 B).

2.1.3 GFP- electroporated donor chick/ chick embryo transplants

Chicken embryos at developmental stage HH10 were electroporated with 300ng/µl enhanced green fluorescent protein (EGFP) in 0.04% (w/v) fast green (Sigma, USA) /PBS (phosphate-buffered saline solution; 0.1M, pH 7.4). The EGFP is under a chicken ß-actin promoter. To electoporate the chicken embryos the egg was prepared as described above. After the vitelline membrane was slit open over the anterior pole of the embryo a small slit was cut into the dorsal neural tube along the midline. Afterwards the EGFP/ fast green/ PBS solution was injected into the neural tube with a small glass capillary until the rostral part of the tube was filled with the solution indicated by the green color (Figure 14). Then, about 250 µl Tyrodes solution was poured over the embryo with a sterile plastic pipette and the electrodes were placed on both sides of the neural tube as indicated in figure 15. The following electroporation parameters were used: 25mV, 5 pulses, Pon: 5ms, Poff: 900ms (Electroporator EDIT Type CUY21, Bex Co., LTD - Japan).

After electroporation another 250 µl of Tyrodes solution were pipetted on top of the embryo and the eggshell was sealed. Always following that protocol ensured to constantly electroporate the right half of the neural tube. The electroporated side of mesencephalic vesicle was then transplanted into chicken embryos of the same stage as described above. After additional 3 to 16 days of incubation, the transplanted embryos were fixed over night with 4% (w/v) paraformaldehyde.
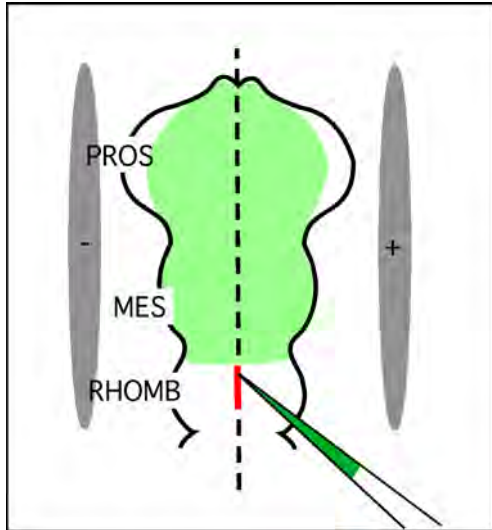
Figure 14: Electroporation of chicken embryos at HH10. In order to electroporate chicken embryos, the vitelline membrane covering the embryo was removed and a small slit was cut into the dorsal neural tube along the midline. Afterwards the EGFP/ fast green/ PBS solution was injected into the neural tube with a small glass capillary until the rostral part of the tube was filled with the solution indicated by the green colour. The following electroporation parameters were used: 25mV, 5 pulses, Pon: 5ms, Poff: 900ms. Afterwards 250 µl of Tyrodes solution was pipetted on top of the embryo and the eggshell was sealed and incubated at 37°C. (PROS: prosencephalon, MES: mesencephalon, RHOMB: rhombencephalon.

2.1.4 Perfusion of chicken embryos

In order to preserve the integrity of organs like the brain, the tissue needs to be cleared of blood and fixed. Perfusions are the most efficient way of achieving this. Briefly, blood is flushed out of the body and exchanged with first PBS and later with 4% PFA to fix the organs. This was done as follows for all experiments with embryos older than HH40/ E14. First, the eggs containing the embryos were placed on ice for about 5 min. Afterwards, the tape covering the egg was removed in order to take out the embryo with forceps. The embryo was placed on its back on a rack. The limbs were spread and each paw was secured to the rack with a pin. Feathers were removed with forceps from the surgical area and a cut along the sternum, about 2 cm long, was made low enough to expose the sternum's end. The end of the sternum was grasped with forceps. Sharp scissors were used to cut the diaphragm laterally on both sides and then toward the head, across ribs and parallel to lungs. Once the heart was exposed in this way, a catheter needle was inserted into the protrusion of the left ventricle to an extend of approximately 5 mm. A small cut was made in the atrium with a sharp scissor. The heart serves as a pump to ensure the flow of the perfusion solution to the brain. Initially 70 ml of PBS was perfused at a steady flow. After the blood was cleared from the body and the draining fluid was clear, perfusion with 4% PFA solution (80 ml) commenced. Once the chicken embryo became rigid, fixation was completed. The embryo was removed from the rack, decapitated and the brain removed. To do this, an incision was made from the base of the head up to the eyes by the use of scissors. The skin was pulled away from the skull and the skull plates were removed to expose the brain. The remaining dura was cut with

small scissors and optical, cranial and olfactory nerves were cut. The brain was removed carefully with forceps, placed in a 50 ml Falcon tube with 4% PFA and stored at 4°C over night.

Afterwards, the brain was rinsed three times for 1 hour in PBS, dehydrated through a series of ascending ethanol concentrations, and stored in butanol for two hours at room temperature. Then, the brain was rinsed in liquid paraffin (GemCut^{TM} Emerald Paraffin, Polyscience, USA) for about 6 hours at 56°C and with at least three changes of paraffin. After 6 hours the brain was embedded in paraffin and 7-12 µm-thick sagittal/ coronal serial sections (Microtome, Leica Microsystems, Germany) were obtained and mounted in five parallel series.

2.1.5 Immuno- histochemical analysis of chimeras

In order to remove the paraffin from the brain sections, they were washed in Xylene for two hours and dehydrated through descending ethanol series. Depending on the antibody, sections were boiled by heating them in the microwave 4 times 4 min at 700 W in 0.01 M sodium citrate. This method was used especially for the detection of proteins expressed in the cellular nucleus. Afterwards sections were washed three times/ 10 min and treated for 30 min with 1% H_2O_2 / PBS-0.1% Triton. After additional three washing steps of 10 min with PBS-0.1% Triton a blocking step of one hour in 10% sheep serum/ PBS- 0.1% Triton was carried out. Brain sections were incubated with primary antibodies outlined in table 2 overnight at room temperature. The next day the sections were washed three times for 10 min with PBS before the appropriate secondary antibody was added. Light microscopy double immunostainings were achieved by incubating corresponding biotinylated secondary antibodies for one hour. This step was followed by an additional hour of incubation with "ABC" (Vector Labs, USA);(1:500 in PBS- 0.1% Triton). ABC stands for **A**vidin **B**iotinylated enzyme **C**omplex. Because avidin has such an extraordinarily high affinity for biotin, the binding of avidin to biotin is essentially irreversible. In addition, avidin has four binding sites for biotin, and most proteins including enzymes can be conjugated with several molecules of biotin (Hsu et al. 1981a; Hsu et al. 1981b).

This AB- complex was then developed with 1% 3,3'-Diaminobenzidine (DAB) (Applicam, Darmstadt, Germany) either in PBS containing 0.0005 g/ml nickel leading to a dark black staining (Nadkarini and Lindhardt 1997) or in 0.05 M Tris-buffer. DAB is a widely used to stain in immunohistochemistry. The substance

brown precipitate upon oxidation with 0.15 % of hydrogen peroxide and is insoluble in aqueous and organic solvents. This method therefore allows us to distinguish between two antibodies of same host, if one of them is a nuclear marker and the other a cytoplasmic marker. For example, nuclear mouse- anti- QCPN revealed with DAB/ nickel results in a black staining of the nucleus. Cytoplamic mouse – anti- Map2 revealed with DAB leads to a brown staining of the cytoplasm. Thus, this protocol gives us the possibility to detect double positive cells without false positive results.

 After immunostaining these slides were mounted in Eukitt (O. Kindler, Freiburg, Germany).

Corresponding fluorescent antibodies (Alexa Fluor (Molecular Probes, USA), 1:500) were applied directly after 5 washing steps of 10 min with PBS-0.1% Triton. In some cases we applied streptavidin- coupled- Cy3 (GE Healthcare, Great Britain); (1:700) to secondary biotinylated antibodies (Vector Labs, USA). DAPI (4',6-diamidino-2-phenylindole) was used to label cellular nuclei at 5mg/ml (Vectorlabs, USA). After fluorescent staining sections were mounted with Mowiol (Calbiochem, Darmstadt, Germany) and n- Propyl- Gallate (NPG, 1:10); (Sigma, St. Louis, USA).

 Selected sections revealed with DAB were photographed with a digital camera DC500 or DC350 (Leica, Wetzlar, Germany). Contrast and brightness of the photomicrographs were adjusted in Adobe PhotoShop, Macintosh or PC version, CS3 (Adobe Systems, San Jose, CA). Sections containing fluorescent antibodies were photographed either the same way as the DAB revealed sections or detailed, in series of planes, with confocal microscopy.

2.1.6 Used antibodies

One out of five parallel series was immunostained with a monoclonal **mouse anti- QCPN** (Hybridoma Bank, Iowa City, IA; 1:5) raised against quail wing bud ZPA (zone of polarizing activity). This antibody, developed by Bruce M. Carlson and Jean A. Carlson, stains the perinucleolar heterochromatin in all quail cells from stages HH20 through HH40 according to previous reports (Le Douarin et al. 1996). No staining was seen, when the antibody was used to stain tissue from control chicken embryos without quail tissue grafted. In some cases parallel serial sections were counterstained with cresyl violet to detect anatomical landmarks. To determine the phenotype of quail cells, a variety of different

antibodies was used. To visualize Purkinje cells we used monoclonal **rabbit anti-Calbindin** (D-28k), lyophilized antiserum produced against recombinant rat calbindin D-28k (Swant, Schwitzerland). Electroporated embryos were analyzed with a **rabbit anti- GFP** (IgG fraction, Molecular Probes, Eugene, USA). **Chicken anti-GFP** (IgY) is produced in chicken immunized with purified recombinant green fluorescent protein and IgY extraction from egg yolks (Aves Labs, Inc. USA). Radial glial cells were visualized using polyclonal **rabbit anti- Vimentin** (affinity purified, Acris Antibodies, Herford, Germany). Oligodendrocytes were visualized with **rat anti- PLP** was kindly provided by Bernard Zalc (Le Centre de Recherche de l'Institut du Cerveau et de la Moelle épinière (CRICM), Paris, France) and polyclonal **goat anti- Olig2** (Oligodendrocyte transcription factor 2) with a peptide mapping near the C-terminus of Olig2 of mouse origin (Santa Cruz Biotechnolgy). As astrocytic marker the polyclonal **rabbit anti- S100** (full length S100 protein purified from cow) was used (Abcam, Cambridge, MA, USA). As neuronal marker we used monoclonal **mouse anti- Map2** (Microtubule-associated protein 2) a rat brain microtuble-associated protein (Chemicon international). Interneurons were labeled with polyclonal **rabbit anti- Gad65/6**7 (glutamic acid decarboxylase 65/67) raised against Synthetic peptide K-DIDFLIEEIERLGQDL corresponding to the C-terminal region of Gad 67 of human origin (IgG fraction of antiserum, SIGMA, Saint Louis, Missouri, USA), polyclonal **rabbit anti- Pax2** (Paired box gene 2), which is a GST Pax2 fusion protein derived from the C-terminal domain (aa188-385) of murine Pax2 protein (Zymed Laboratories Inc, San Francisco, CA, USA) and polyclonal rabbit anti-Calbindin (recombinant rat calbindin D-28k, Swant, Bellinzona, Switzerland). To determine the border between alar and parabasal mesencephalic epithelium monoclonal mouse **anti- Pax7** (Hybridoma Bank, Iowa City, IA; 1:5) immunostainings were performed. In addition we used **mouse anti- Nkx2.2** (GST-fusion- E.coli expression) from Hybridoma (Hybridoma Bank, Iowa City, IA).

Table 2: Overview about used primary antibodies

Antibody	Dilution	Species	With/ without boiling (+/-)	Company
Calbindin	1:3000	rabbit	-	Swant
Gad 65/67	1:500	rabbit	-	Sigma
GFP	1:300	rabbit	-	Molecular Probes
GFP	1:500	chicken	-	Aves Labs
Map2	1:500	mouse	-	Chemicon
Nkx2.2	1:5	mouse	+	Hybridoma
Olig2	1:100	goat	+	Santa Cruz
Pax2	1:5	rabbit	+	Zymed Lab.
Pax7	1:4	mouse	+	Hybridoma
Plp	1:50	rat	-	Bernard Zalc (CRICM, Paris)
QCPN	1:3	mouse	+	Hybridoma
S100	pure	rabbit	-	Abcam
Vimentin	1:20	rabbit	-	Acris

2.1.7 Explants of chicken embryos at developmental stage HH35

To perform explants of chicken embryos at developmental stage HH35, eggs were incubated for 9 days. The eggshell was opened, using tape to fixate it, and then by cutting a small window with scissors. The embryo was taken out and washed in PBS. The head of the embryo was dissected in chilled PBS to expose the brain. The telencephalon was cut off and the remaining brain was cut along the midline. Each half was placed on a Millicell sterilized culture plate insert (0.4 µm, Millipore). DiI (Invitrogene), dissolved in Dimethylsulfoxid (DMSO), was injected with a glass micropipette into the mesencephalic end of the velum medullare. Then the explants were cultured in DMEM supplemented with 10 % FBS, 1% Penicillin (10000 U/ ml)/ Streptomycin (10000 µg/ µl) and 1% L-Glutamine (200 mM) at 37°C for two days. The medium was changed after 24 hours of incubation. Finally the explants were fixed over night in 4% PFA and analyzed under the fluorescence microscope.

2.1.8 Cell counts

Cell counts were performed as follows. In a mid-sagittal section of the cerebellum, three squares of the same size (at 400 magnifications) were counted in each cerebellar folia. Total cell number was calculated by cresyl violet staining and donor cell by QCPN staining. The three squares covered all layers of the folia including the granule cell layer (Figure 15 A), and the average of the three calculated (Figure 15 B, table 1). Similarly, cells of the folial and the central white matter were counted, choosing four squares of the same size. The calculation was performed on two medial sections of parabasal grafts. The average cell distribution between the two analyzed sections was calculated for each folia and each layer and subsequently the percentage of QCPN positive cells to the total cell number in each layer was calculated (Figure 15, B table 2). Finally, the average cell distribution for each layer was determined (Figure 15, B table 3). All calculations were performed with Microsoft Office Excel.
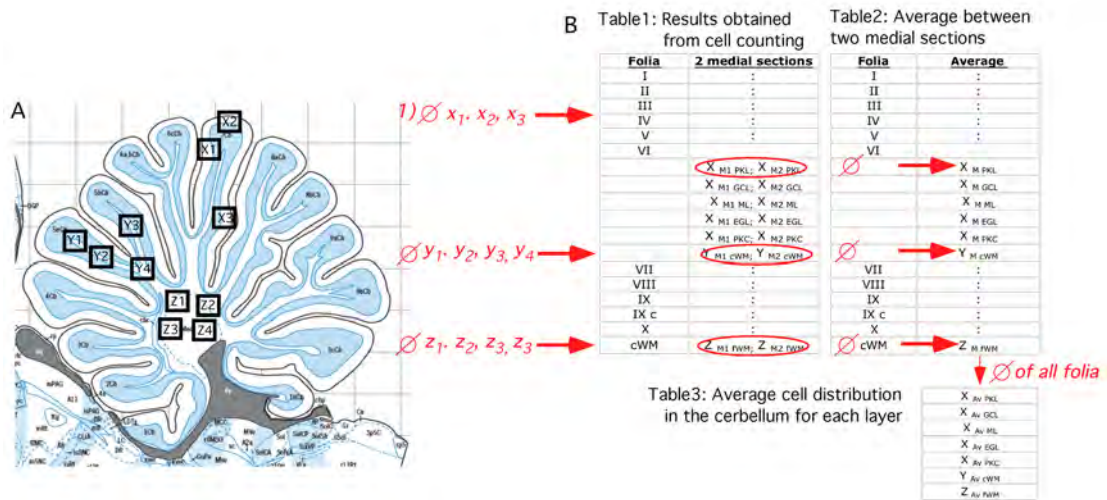
Figure 15: In each cerebellar folia three squares of the same size (40x) were counted for cells marked with cresyl violet to achieve a total cell number and for those marked with QCPN. The three squares were covering all layers of the folia including the granule cell layer (A, B Table 1). The means of these three squares were calculated for each folia of the cerebellum (B, Table 2). Similarly, cells of the folial and the central white matter were counted, choosing four squares of the same size. The calculation was performed on two medial sections of parabasal grafts. The average cell distribution between the 2 analyzed sections was calculated for each folia and each layer and subsequently the percentage of QCPN positive cells to the total cell number in each layer was calculated (B Table 2). Finally the mean cell distribution for each layer was worked out (B Table 3).

2.2 Analysis of Gdf10 expression and Bergmann glia development in mice

2.2.1 Mouse strains

The analysis of the expression of *Gdf10* mRNA was analyzed in wild type ICR mice. Embryos were collected from embryonic stages E14.5, E15.5 and E16.5 and from postnatal days (P) 0, 7, 10, 15, 22 and adults (>P28). The heads of the embryos were fixed over night in 4% PFA, processed to 20% sucrose, embedded in frozen section medium (NEG 50, Richard Allan Scientific), and sectioned in 12 µm cryostat (Microm HM525, Microm, UK) sections. Brains from postnatal mice were dissected after perfusion and fixed over night in 4% PFA. The perfusion was performed as described for chicken embryos except that mice were anesthetized in a glass box containing pads with isoflurane (2-chloro-2-(difluoromethoxy)-1,1,1-trifluoro-ethane). They were processed like the embryos and sectioned in 16 µm cryostat sections.

For further experiments a conditional knockout of Shh was generated with two different animal models. On one side a conditional *Shh^flox/flox* mouse line, which contains the Shhtm2AMC allele in homozygosis (loxP sequences flanking Shh exon2). This mouse line was generated in the laboratory of Andrew McMahon (Lewis et al. 2001). The second mouse line used was *En1^Cre/+*, which has the

endonuclease Cre under the promotor of the gen Engrailed 1 (En1). This mouse line was generated in the laboratory of Dr. Wolfgang Wurst (Kimmel et al. 2000). The Cre enzyme specifically recognizes loxP sites and eliminates the DNA located between both loxP sites. Thus, crossing the two mouse lines results in an elimination of Shh in cells expressing En1. To generate the mice heterozygous $En1^{Cre/+}$ males were crossed with homozygous $Shh^{flox/flox}$ females. From these crossings approximately 25 % conditional mutants ($En1^{Cre/+}$; $Shh^{flox/flox}$) were obtained.

2.2.2 Genotyping

To be able to select the conditional mutants $En1^{Cre/+}$; $Shh^{flox/flox}$, embryos were genotyped. Therefore the genomic DNA was extracted from a small part of the tail by placing the piece into tubes containing H_2O. This mixture was run in a PCR 9 min at 98°C. Afterwards 1 µg/µl Proteinase K was added and tubes were placed back into the PCR and run for 16 hours at 55°C, followed by an additional step of 10 min at 98°C to destroy the Proteinase K.

To genotype the embryos 1 µl of the DNA containing liquid was used for each of the PCRs as described below.

Genotyping of En1$^{Cre/+}$

Primers:	En1.11D:	5´- GTGCCTTCGCTGAGGCTTC -3´	
	CreB:	5´-ACCCTGATCCTGGCAATTTCGGC- 3´	
Conditions:	time	temperature	number of cycles
	4 min	94°C	1
	30 sec	94°C	35
	30 sec	54°C	
	1 min	72°C	
	10 min	72°C	1

In this PCR reaction a DNA fragment of 700 bp was amplified for the mutant allele. In the wildtype embryos no fragment was amplified.

Genotyping of Shh^{flox/flox}

| Primers: | ShhF: | 5´- ATGCTGGCTCGCCTGGCTGTGGAA -3´ |
| | ShhR: | 5´-GAAGAGATCAAGGCAAGCTCTGGC- 3´ |

Conditions:

time	temperature	number of cycles
1 min	94°C	1
1 sec	94°C	35
1 min	65°C	
30 sec	72°C	
10 min	72°C	1

In this PCR reaction a DNA fragment of 449 bp was amplified for the wildtype allele and a second fragment of 483 bp for allele containing the loxP sites.

2.2.3 Histological analysis of mouse brain sections

2.2.3.1 Immunohistochemistry

Immunohistological analyses were performed as described above for chicken embryo sections. The only difference was, that in comparison to paraffin sections, Xylene treatment was not necessary. Instead cryostat sections we dried in the oven at 37°C for 1 hour.

In addition to that, some brains were included in 4 % agarose in order to obtain gross sections, to follow cellular migration. These sections were treated for 1 hour with 6% H_2O_2 and washing steps were performed with PBS- 1% Triton. Afterwards they were mounted with glycerol jelly.

Used antibodies

Rabbit anti- Gdf10 affinity isolated antibody (Sigma/ Prestige Antibodies, USA). To determine the phenotype of Gdf10+ cells, a variety of different antibodies were used. Radial glial cells were visualized with a monoclonal **mouse anti-Vimentin** (H5) obtained from chick optic tectum (Joshua Sanes, Department of Anatomy, Washington University Medical School, St. Louis, USA / Hybridoma)

and revealed with DAB. Fluorescent colabelling of with Gdf10 and Vimentin was achieved by using polyclonal **rabbit anti- Vimentin** (as described in 2.1.6). **Gad65/67** and **Calbindin** were used as neuronal markers (as described in 2.1.6). As an astrocytic marker we used two different GFAP (Glial fibrillary acid protein) antibodies depending on the type of immunostaining performed. We either used **rat anti- GFAP IgG$_{2a}$** (Calbiochem, USA) or polyclonal **rabbit anti- GFAP** (Abcam, UK).

Table 3: Overview about used primary antibodies

Antibody	Dilution	Species	With/ without boiling (+/-)	Company
Calbindin	1:3000	rabbit	+	Swant
Gad 65/67	1:500	rabbit	-	Sigma
Gdf10	1:25	rabbit	-	Sigma/ Prestige
GFAP	1:200	rat	-	Calbiochem
GFAP	1:500	rabbit	-	Abcam
GLAST	1:100	rabbit	-	Novus
Ki67	1:200	rabbit	+	Thermo Scientific
Nestin	1:5	mouse	-	Hybridoma
Nestin	1:200	mouse	-	Chemicon
NeuN	1:50	mouse	+	Chemicon
Pax6	1:5	Mouse	+	Abcam
Vimentin	1:20	rabbit	-	Acris
Vimentin	1:100	mouse	+	Hybridoma

Rabbit anti- GLAST IgG (SLC1A3) is a 20 residue C- terminal synthetic peptide (rat) and reacts with Glutamate- aspartate transporter in the CNS (Novus Biologocals, UK). Nestin is a large intermediate filament protein (class Type VI) widely used as a marker for radial glia. We used monoclonal **mouse anti- Nestin** (Chemicon, USA) and **mouse anti- Nestin IgG1** (Rat-401) isolated form homogenized Sprague- Dawley rat spinal cord (Hybridoma, USA), Monoclonal

mouse anti- NeuN (neuronal nuclei) was used as a marker for newborn neurons (Chemicon, USA). Furthermore **mouse monoclonal Pax6** (Abcam, USA) was used to label granule neurons and **rabbit monoclonal Ki67** (Thermo Scientific, USA) was used as a proliferation marker. All used antibodies were summarized in table 3.

2.2.3.2 In- situ hybridization (ISH)

<u>*Gdf10- probe preparation*</u>

To prepare the probes for *in situ* hybridization lysogeny broth (LB) medium (LB, 50 µg/ml ampicillin (Sigma, USA)) was inoculated with Gdf10 cDNA containing bacteria*.* The cDNA was obtained from imaGenes, Germany (IRAVp968G04118D). The medium was incubated at 37°C overnight.

To isolate the plasmid-DNA from the cultured *E. coli,* the Qiagen Plasmid maxi kit (Qiagen, Germany) was used following the manufactures instructions. After the pellet was air-dried for 10 minutes it was redissolved in 50 µl Sigma- H_2O. The DNA concentration was determined with a Nanodrop spectrophotometer (Thermo Fisher Scientific, USA) and the quality of the DNA was analyzed by gel electrophoresis on a 1% agarose gel.

Plasmids were linearized using EcoRI restriction enzymes (Roche, Switzerland). Generally 5 µg DNA were digested with 5 U of EcoRI overnight at 37°C. Agarose gels for verifying DNA isolation, digestion and transcription contained 1% agarose in 0.5xTBE buffer with 0.0015 % ethidiumbromide. DNA- samples were run on the gel at 7.5 V/cm for about 30 minutes, RNA samples at 9 V/cm for 5 minutes and analyzed with a gel scanner and the appropriate software. As markers, a GeneRuler™ 1 kb DNA ladder (Fermentas, USA) was used. After digestion DNA was purified using the QIAquick PCR purification kit (250); (Qiagen, Germany) following the manufactures manual. DNA concentration was determined with a spectrophotometer (Nanodrop, Thermo Scientific, USA) and the quality of the DNA was checked on a 1% agarose gel.

To transcribe the cDNA inserted in the now linearized plasmid into mRNA, *in vitro* transcription was performed. The newly synthesized mRNA was labeled either by using a labeling mix containing Dig-AP-labeled UTP (Dig-UTP= digoxigenin-Omethylcarbonyl-ε- aminocaproyl-[5-(3-aminoallyl)-2'-uridine- 5'-triphosphate],

Na4); (Roche, Switzerland) or by using a labeling mix containing Biotin- 16- UTP (Roche, Switzerland). The labeling mix was prepared as follows:

ATP (100 Mm)	2 µl (10 mM)
CTP (100 Mm)	2 µl (10 mM)
GTP (100Mm)	2 µl (10 mM)
UTP (100Mm)	1,35 µl (6,5 mM)
UTP Dig/ Biotin(250 nmol)	7 µl (3,5 mM)

add 15 µl Sigma H_2O

All nucleotides were obtained from Roche, Switzerland.

The following mix was prepared for the *in vitro* transcription:

	1µg linearized DNA
+	2 µl dig-labelling mix
+	4 µl transcription buffer (Fermentas)
+	1 µl RNAse- inhibitor 40U/ µl (Roche)
+	1 µl T3 RNA- Polymerase (20 U/ µl); (Roche)

add 20 µl Sigma H_2O

The reaction was performed for 3 hours at 37°C. Following this, 2 µl of DNAse (10 U/ µl); (Roche, Switzerland) was added and the reaction was once again incubated for 30 min at 37°C to remove the template DNA. To precipitate the RNA, 80 µl TE- Buffer, 10 µl LiCl (8 mM) and 300 µl 100% ethanol were added and incubated overnight. The next day, the RNA was centrifuged for 20 min at 13000 rpm, 4°C. The supernatant was removed and the pellet washed in 200 µl 70% ethanol. Then another centrifugation step followed for 15 min, 13000 rpm, 4°C. Afterwards the pellet was air-dried, redissolved in 25 µl Sigma H_2O and 5 µl RNA was run on a gel to test that the transcription was successful.

RNA- ISH

In general, ISH can be used to detect both DNA and RNA using nucleic acid probes specific to intracellular complementary DNA/ RNA- sequences. Through the preservation of the tissue morphology ISH has become a very useful method for the precise localization of nucleic acids in the intact cell. RNA-ISH allows the detection of cell-specific mRNAs and thereby localizing the producer cell accurately, even though the translation into protein remains unknown.

At the 1st day the brain sections were rehydrated through a reverse ethanol series. Afterwards, sections were washed three times/ 10 min and treated for 30 min with 1% H_2O_2/ PBS-0.1% Tween20 (PBT). The sections were then treated with 10µg/ml proteinase K in PBS at RT for 30 min. This step is necessary to remove cross-links between target nucleic acids and cellular proteins to allow access of the probe to the target sequence. This step was only applied when sections were used exclusively for ISH, since the pretreatment with proteinase – K destroys some of the target proteins for antibodies. Afterwards, sections were washed twice for 8 minutes in PBT, post- fixed in 4% PFA for 20 min at RT and washed again 4 times, 8 min, each time in PBT with gentle shaking. Fixation with PFA was necessary to stabilize tissue structure following protease treatment. Following protease treatment and fixation, tissue was prehybridized with 500 µl/slide of ISH hybridization buffer (see table 4), incubated for 3 hours. Prehybridization is required to block non-specific targets. Prehybridization and hybridization buffer contain formamide, which destabilizes hydrogen bonds between probe and target sequences and decreases the melting temperature at which 50% of the probe/target is dissociated. Tween20 removes membrane lipids and 2xSSC (monovalent cation Na+ in SSC) at 70°C helps to unravel secondary structures in the target RNA and thereby enhances hybrid stability. Yeast tRNA and heparin block non-specific binding of RNA probes.

After prehybridization the buffer was replaced by 150 µl/ slide hybridization buffer (see table 4) containing 2 µl/ml labeled mRNA probe and covered with cover slips (Sigma, USA). The hybridization was performed overnight at 65°C. The following day, the sections were rinsed three times 45 min at 65°C in solution 1 (see table 4) and three times 45 min at 65°C in solution 2 (see table 4) to remove non-specifically bound and unbound components. Before the blocking step of 1 hour in 10% sheep serum in MABT (see table 4) was performed, additional three washing steps of 5 min each in MABT were realized. Initial high salt concentration washing steps with 4 x SCC remove unbound probes and the subsequent lower ionic strength washing steps with 2 x SSC remove mis-matched hybrids. For fluorescent *in situ* hybridizations the RNA-probe was detected with an streptavidin-Cy3 coupled antibody recognizing the biotin (Diamandis and Christopoulos 1991). To obtain a blue, non-fluorescent staining the anti-digoxygenin-AP antibody (1:5000, Roche, Switzerland) in 1% sheep serum/ MABT was incubated over night. Then the sections were rinsed in MABT at RT 5 times 30 min and kept overnight at 4°C in the coldroom. On the 3rd day a

color reaction catalyzed by alkaline-phosphatase was performed. To reveal the specifically bound probe, sections were rinsed 3 times 10 min in PBS. Revelation of alkaline-phosphatase activity was achieved with BM- purple at room temperature in the dark. BM- purple is a NBT/BCIP (nitro-blue tetrazolium chloride/ 5-Bromo-4-chloro-3'-indolyphosphate *p*-toluidine Salt) "ready-to-use" chromogenic substrate for alkaline phosphatase (Roche). After the staining the sections were washed 4 times 5 minutes in PBS and either processed for immunostaining or mounted with Eukit.

Table 4: Overview of composition of used solutions for ISH

Stock solutions	*Composition*
Prehybridization Buffer	50% Formamide, 5x SSC pH7, 50 µg/ml Heparin, 1mg/ml yeast tRNA, 0.1% Tween-20, 50µg/ml ssDNA
Hybridization Buffer	50% Formamide, 5x SSC pH7, 50 µg/ml Heparin, 0.1% Tween-20, 50ug/ml ssDNA
MAB 5x (500ml)	21,75 g NaCl, 29 g acido maleico, 19g NaOH
MABT	1x MAB, 0.1% Tween20
Solution 1	50% formamide, 4x SSC pH4.5, 1x SDS, add H_2O
Solution 2	50% formamide, 2x SSC pH4.5, 1% Tween20, add H_2O

2.2.4 Brain slice cultures of E18.5/P0 wild type mice

2.2.4.1 Treatment with Gdf10 recombinant protein

For brain slice cultures, E18.5/ P0 wildtype mouse embryos were dissected in chilled PBS, embedded in 4% low melting agarose and cut in chilled Krebs (1x) (see table 5) into 250 µm vibratome (VT1006, Leica, Germany) sections. Sections were transferred into a Petri dish containing enriched Krebs (see table 5). Afterwards brain slices were placed on a Millicell sterilized culture plate insert (0.4 µm, Millipore) and cultured for 1 hour at 37°C in DMEM (see table 5). The medium was changed to enriched neurobasal medium and brain slides were either treated with Gdf10 recombinant protein soaked beads or directly by applying Gdf10 protein by pipetting it on top of the cerebellum. Gdf10 recombinant protein was obtained from R&D Systems, reconstituted at 50 µg/ml in sterile 4 mM HCl containing 0.1% bovine serum albumin. In the case of the soaked beads Affi-Gel Blue Gel (BioRad, USA) beads of a diameter between 150

and 300 µm were used. They were washed with PBS and incubated over night in Gdf10 recombinant protein. Next day they were washed again three times in PBS and placed on the brain slices within. For the direct application of Gdf10 protein we used small glass capillaries to apply small quantities of protein to the cerebellum of the brain slides. Control beads soaked in 4 mM HCl/ 0.1% bovine serum albumin were used as controls or 4 mM HCl/ 0.1% bovine serum albumin was applied directly to the cerebellum. Both, beads and liquid protein were incubated for 48 hours at 37°C in a CO_2 incubator set to 5% CO_2 (Forma Scientific, Inc, USA). Medium was changed after 24 hours of incubation. The explants were fixed over night in 4% PFA.

Table 5: Overview of composition of used solutions for brain slice cultures

Stock solutions	*Composition*
Krebs 10x	1.26 M NaCl , 25 mM KCl , 250 mM $NaHCO_3$, 12 mM NaH_2PO_4 , 12 mM $MgCl_2$, 25 mM $CaCl_2$, ph7,2
Krebs 1x	450 ml H_2O, 0.99 g Glucose, 1.05 g $NaHCO_3$, 50 ml Krebs 10x
Krebs 1x enriched	49 ml Krebs 1x, 500 µl Hepes (1M), 500 µl Penicillin (10000 U/ ml)/ Streptomycin (10000 µg/ µl); (Gibco, USA), 100 µl Gentamicin (6 µg/ µl); (Sigma))
DMEM (Gibco, USA), enriched	44 ml DMEM, 500 µl L- glutamine (200 mM), 5 ml FBS (fetal bovine serum), 500 µl Penicillin (10000 U/ ml)/ Streptomycin (10000 µg/ µl); (Gibco, USA),
Neurobasal (Gibco, USA), enriched	47.5 Neurobasal, 1 ml B-27 (50x Gibco, USA), 500 µl glucose (50% w/v); (Gibco, USA), 500 µl Penicillin (10000 U/ ml)/ Streptomycin (10000 µg/ µl); (Gibco, USA), 500 µl glutamine (100x); (Gibco, USA),

2.2.4.2 Analysis of brain slice cultures

In order to detect differences between control and Gdf10 treated brain slices various immuno-histochemical stainings were performed as described above. Therefore, brain slices were dehydrated through ascending ethanol series, incubated in butanol for 1 hour and embedded in paraffin. Paraffin blocks were subsequently cut into 7 µm sections at the microtome. For further analysis paraffin sections were rehydrated as described above and additional immuno-stainings were performed.

3 Results

3.1 The origin of cerebellar oligodendroglia

3.1.1 Generation of a neural tube fate map

A fate map of the mesencephalic epithelium was constructed by examining grafts performed along the antero- posterior and dorso- ventral axis of the mesencephalic vesicle. In total 206 grafts were analyzed. Cases taken into consideration for a detailed analysis were summarized in table 5 at the end of section 3.1. The location of the grafts was determined by the distribution of quail cells in the host ventricular epithelium. The border between alar and parabasal/ basal plate was determined by the ventral limit of Pax7 expression in the alar plate (Aroca et al. 2006; Shin et al. 2003). At HH43 (17 incubation days), Pax7 was expressed in the ventricular epithelium of the alar mesencephalon: optic tectum (OT); (Figure 16 A, D, E), and the isthmic velum medullare (Figure 16 B, H). In mid-sagittal sections the expression of Pax7 was absent in the epithelium of the mesencephalic periaqueductal grey (mPAG); (Figure 16 G-I), which indicates the beginning of the parabasal plate (Figure 16 F).
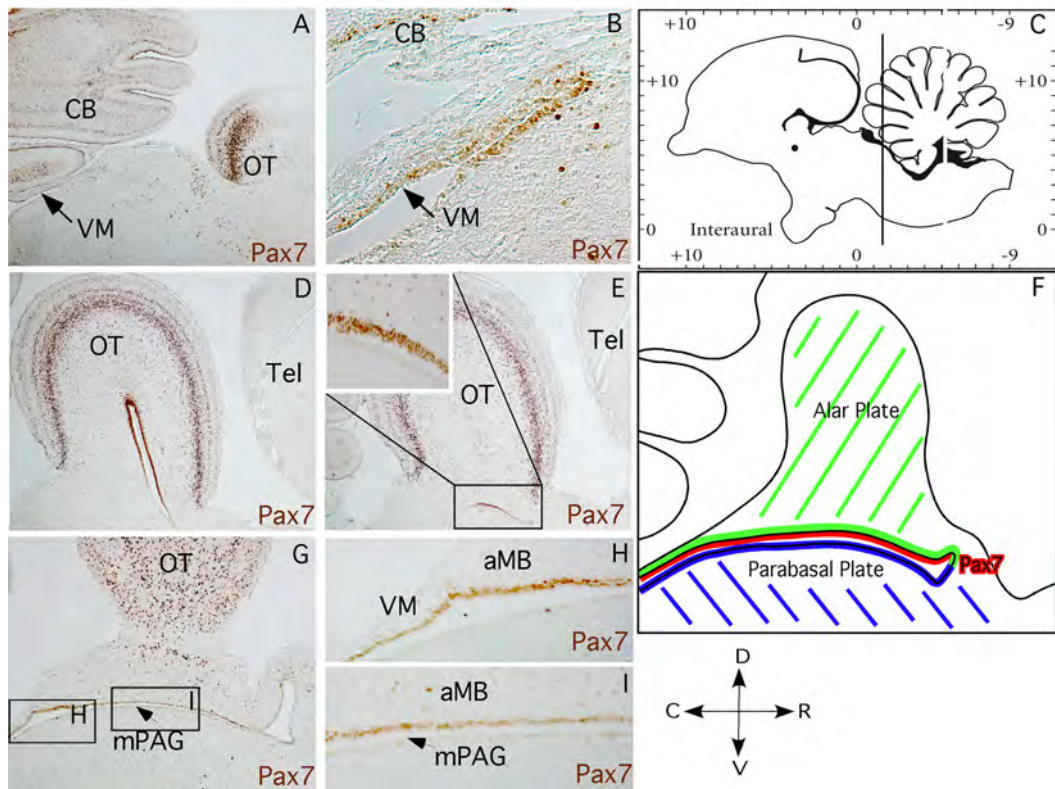
Figure 16: Pax7 expression in a 17-day-old chick embryo on sagittal and coronal sections. C indicates the location of the coronal sections illustrated in A and B. Pax7 can be detected in the ventricular epithelium of cerebellum (A), the optic tectum of the mesencephalon (A, D, E, G) and along the velum medullare (B, H). The border between alar and basal mesencephalon is shown in B (highlighted with arrow), E-I. The periaqueductal grey thereby is separating alar from basal neuroepithelium (arrows in G and I). Figure F summarizes the obtained results. Green marks the alar plate, blue the basal plate and red shows the expression of Pax7 at the border of the alar mesencephalon. Sections D – I are oriented as illustrated by arrows below Figure F. (C: caudal, CB: cerebellum, D: dorsal, aMB: alar midbrain, mPAG: mesencephalic periaqueductal grey, OT: optic tectum, R: rostral, Tel: telencephalon, V: ventral, VM: velum medullare); partially published in (Mecklenburg et al. 2011)

3.1.1.1 Fate map of the mesencephalic alar plate

To determine if alar mesencephalic cells migrated into the cerebellum grafts were performed including anterior or medial thirds of the experimental side of mesencephalic alar plate, whereas the contra- lateral half was used as control. Neither, caudal (Figure 17 A-E) nor rostral (Figure 17 F-J) grafts of alar mesencephalon showed significant cell migration towards the cerebellum as illustrated by the lack of quail cells in the cerebellum (Figure 17 J) and in the velum medullare (VM, Figure 17 E, I). More caudal grafts containing velum medullare and cerebellar neuroepithelium were not included in the present study.
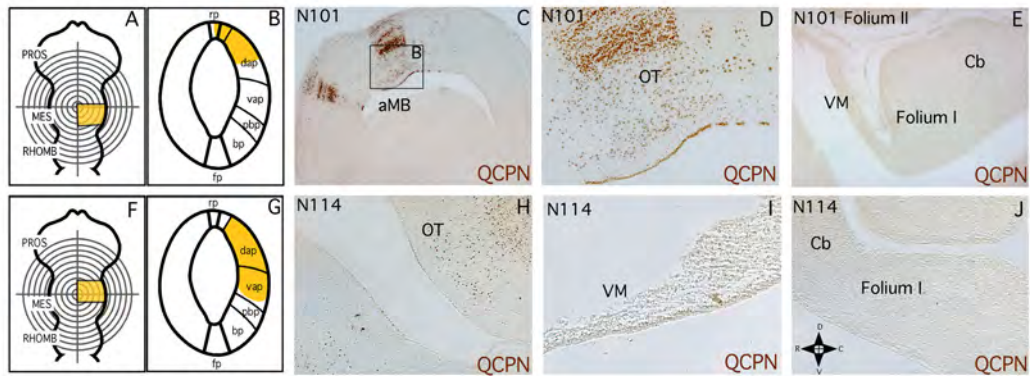
Figure 17: Transplantation of the mesencephalic alar plate. A-E illustrate caudal grafts of the vesicle, whereas in F - J more rostral grafts have been shown. None of the performed grafts lead to a migration towards or inside the cerebellum, which remains free of QCNP+ cells (E, I, J). Sections are oriented as illustrated by arrows in J. (aMB: alar midbrain, C: caudal, Cb: cerebellum, D: dorsal, OT = optic tectum, R: rostral, V: ventral, VM: velum medullare);(Mecklenburg et al. 2011)

As shown in table 6 a total of 11 alar graft cases were taken into closer analysis. In addition to the two already illustrated cases in figure 17, the obtained data from the other 9 transplants that were taken into closer analysis are summarized in figure 18. With these grafts the alar plate, along the antero- posterior axis as well as along the dorso- ventral axis, was covered. In none of the cases donor cell migration into the cerebellum was detected.
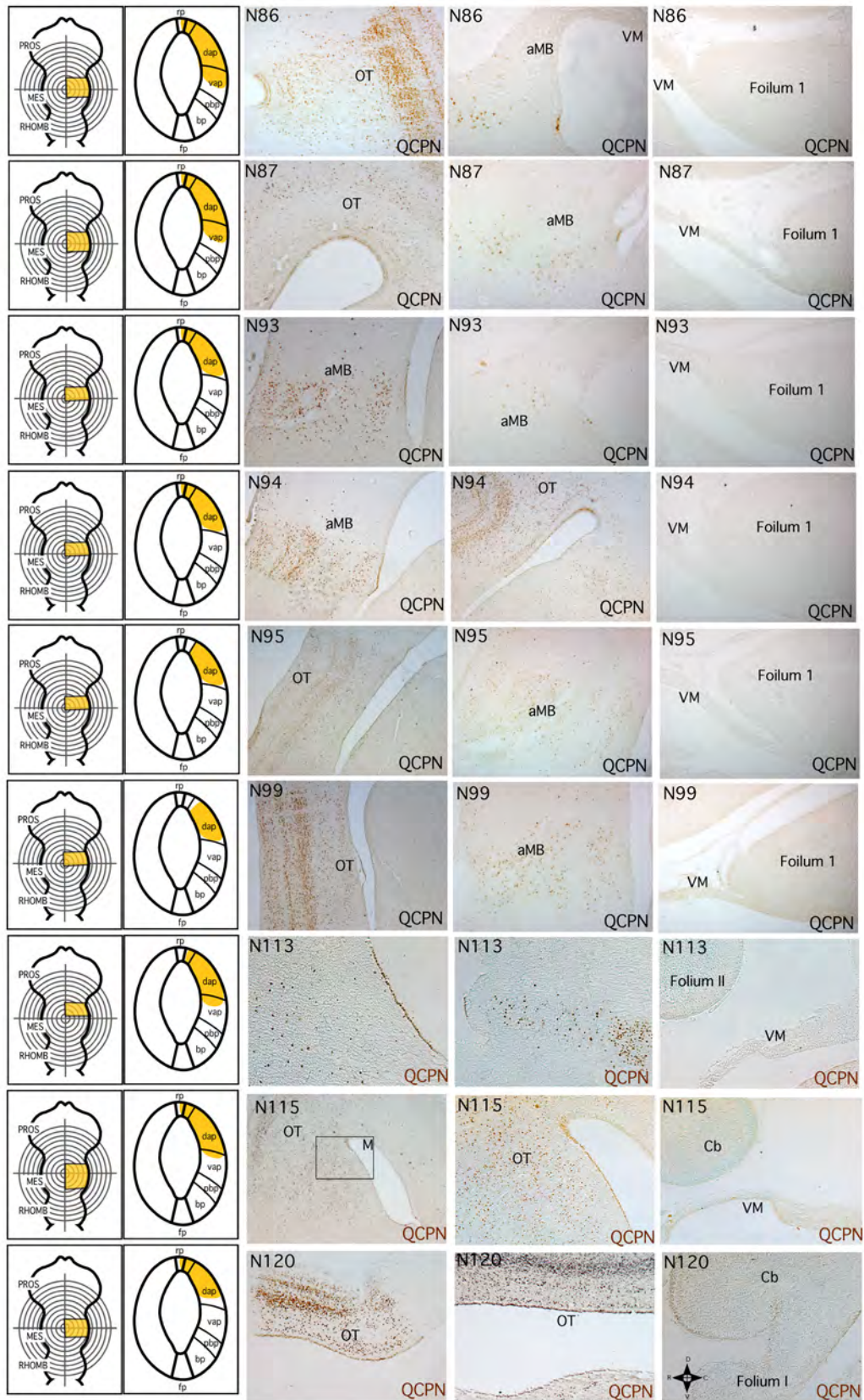
Figure 18: Transplantation of the mesencephalic alar plate. Grafts as illustrated cover the entire mesencephalic alar plate along the rosto- caudal as well as the dorso- ventral axis. None of the performed grafts lead to a migration towards or inside the cerebellum. Sections are oriented as illustrated by arrows in J. (aMB: alar midbrain, C: caudal, Cb: cerebellum, D: dorsal, OT: optic tectum, R: rostral, V: ventral, VM: velum medullare)

3.1.1.2 Fate map of the mesencephalic parabasal plate

The parabasal plate/ parabasal band is the longitudinal domain at the lateral edge of the basal plate, adjacent and ventral to the alar plate, which can be identified by *in situ* hybridization with *Sulf1* (García-Lopez et al. 2009; Gimeno and Martinez 2007). When the grafts included parabasal neuroepithelium a significant number of donor cells migrated from the grafted mesencephalon into the VM and the ipsilateral cerebellum. Grafts were performed covering different extents of the mesencephalic parabasal plate (Figure 19): anterior (n=4; Figure 19 A, B), central (n=5; Figure 19 F, G) or the entire parabasal plate (n=6; Figure 19 K, L).
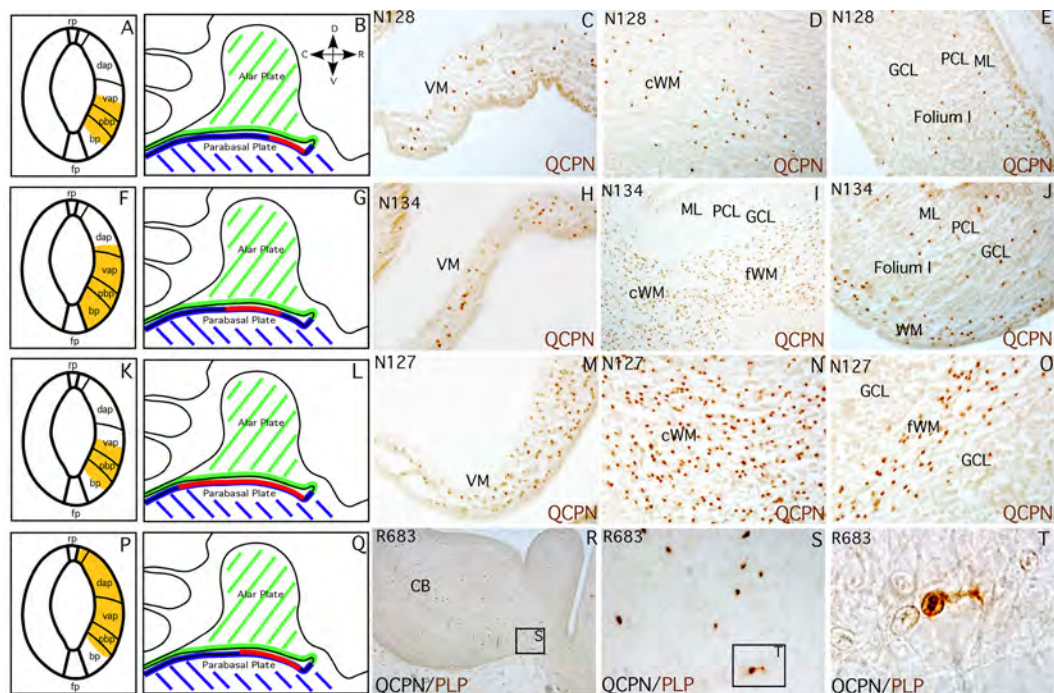
Figure 19: Transplantation of the mesencephalic parabasal plate. Grafts were performed covering the parabasal plate to a different extent. N128 is a rostral transplant of the mesencephalic parabasal plate (A, B) whereas N134 covers mainly the central parabasal plate (F, G). N127 covers almost the entire parabasal plate (K, L). In all of the analyzed cases we detect a strong migration of QCPN+ cells through the VM (C, H, M) into the cerebellum (D, E, I, J, N, O). In horizontal sections of R683 (E9/ HH35) the rostral mesencephalic alar and parabasal plate were grafted as indicated in P and Q. PLP at this stage of development just starts to be expressed, allowing us to detect the first QCPN+ cells in the cerebellum (S, T) expressing PLP (T). Sections are oriented as illustrated in B. (C: caudal, CB: cerebellum, cWM: central white matter, D: dorsal, fWM: folial white matter, GCL: granule cell layer, ML: molecular layer, PCL: Purkinje cell layer, R: rostral, V: ventral, VM: velum medullare); (Graft R683 was kindly provided by Raquel García- Lopez); (Mecklenburg et al. 2011)

In all of these cases, the VM appeared as the substrate for the migratory route of donor cells to enter into the cerebellum (Figure 19 C, H, M). Migrating quail cells transited through folium I (Figure 19 E, J), to reach the central white matter (Figure 19 D, I, N). The migration was restricted to the transplanted side, without contra-lateral migration.

To investigate the age at which donor cells started entering the cerebellum chimeric embryos were fixed at younger developmental stages (HH34-35/E8-9). The first mesencephalic quail cells in cerebellar regions were detected at HH35/ E9 (Figure 19 S, T). Graft R683 illustrates a transplant of the alar and parabasal plate of the rostral mesencephalon (Figure 19 P, Q). Horizontal sections of this case analyzed for the expression of QCPN and PLP showed that some QCPN+ cells in the cerebellum already expressed PLP (Figure 19 T).

In order to proof the obtained results more mesencephalic parabasal grafts were performed as illustrated in figure 21. In all of the grafts, a strong caudal migration into the cerebellum via the velum medullare was detected (Figure 20) as observed in the four cases shown in figure 20.

The histograms in figures 21- 26 illustrate the donor cell distribution in 6 different grafts taking into consideration all layers in each folium of the cerebellum. Within each layer of the cerebellum, the number of donor cells between antero-posterior folia did not vary significantly. The cell distribution of donor cells in the molecular, the Purkinje and the granule cell layer did not exceed 10 %. However, the difference between the white matter and the cortical layers was remarkable, with up to 52% of quail cells in the folial white matter.

In some of the cases a high amount of quail cells was present in folium 1 of the cerebellum. The most striking case was N65. This is due to the fact, that donor cells enter the cerebellum through folium 1 and therefore in some of the cases a higher number of donor cells was present in the first folium.
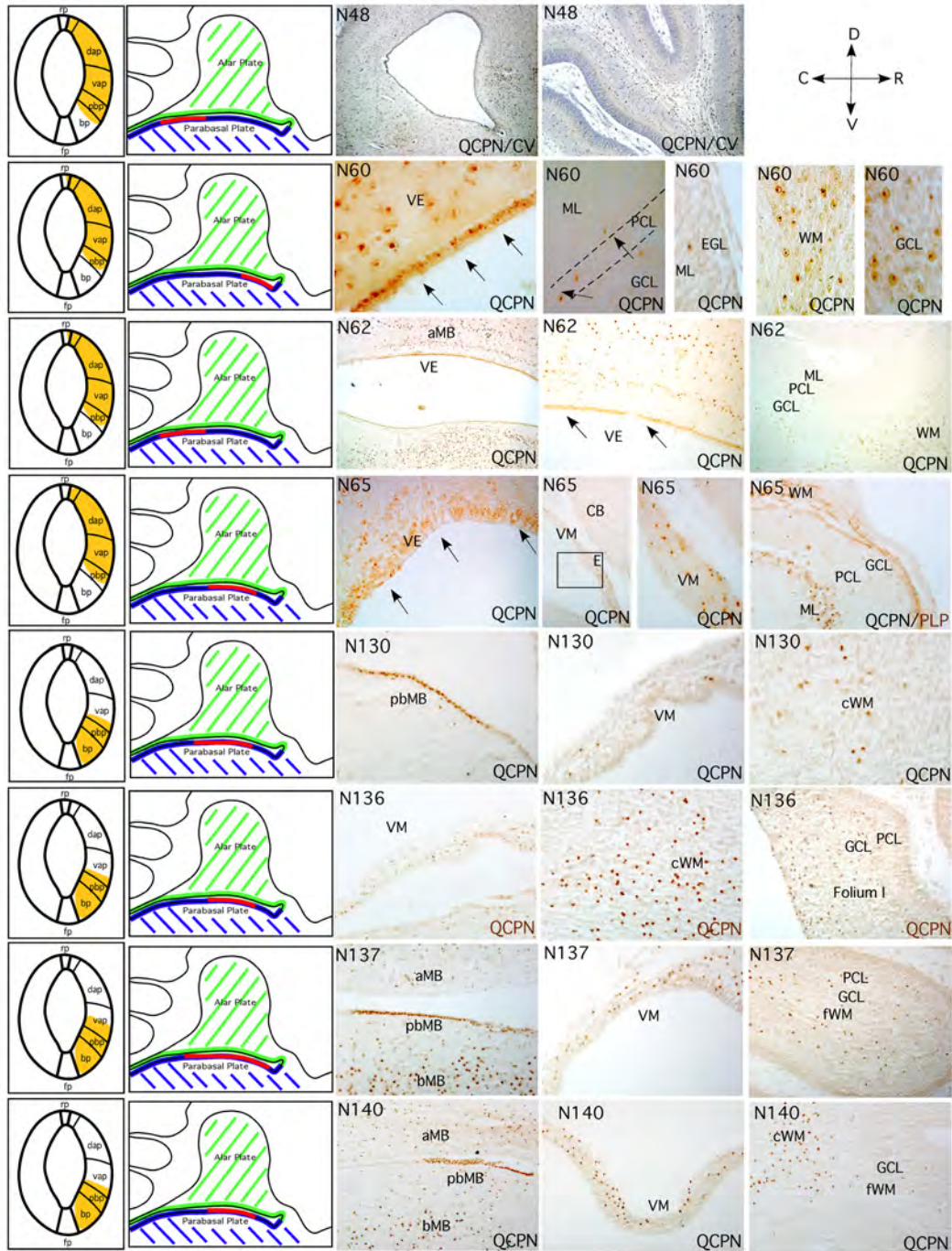
Figure 20: **Transplantation of the mesencephalic parabasal plate.** More parabasal grafts were analyzed and donor cell migration was detected to the same extent using the same migratory pathway, the velum medullare, to enter the cerebellum via folium 1. Sections are oriented as illustrated in the first row. (aMB: alar midbrain, bMB: basal midbrain, C: caudal, CB: cerebellum, cWM: central white matter, D: dorsal, EGL: external granule cell layer, fWM: folial white matter, GCL: granule cell layer, ML: molecular layer, pbMB: parabasal midbrain, PCL: Purkinje cell layer, R: rostral, V: ventral, VE: ventricular epithelium, VM: velum medullare, WM: white matter)
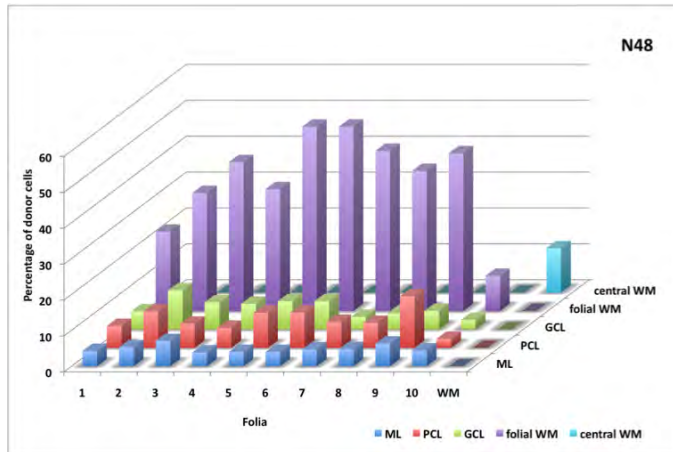
Figure 21: Donor cell distribution in graft N48. The histogram of graft N48 illustrates exemplary the cell distribution taking all folia and layers of the cerebellum into consideration. The external granule layer was not included since we did not detect a mentionable presence of donor cells there. (GCL: granule cell layer, ML: molecular layer, PCL: Purkinje cell layer, WM: white matter);(Mecklenburg et al. 2011)
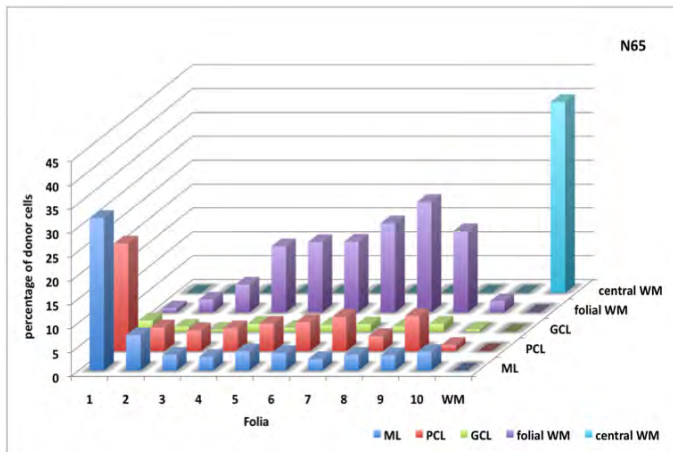
Figure 22: Donor cell distribution in graft N65. The histogram of graft N65 illustrates exemplary the cell distribution taking all folia and layers of the cerebellum into consideration. The external granule layer was not included since we did not detect a mentionable presence of donor cells there. (GCL: granule cell layer, ML: molecular layer, PCL: Purkinje cell layer, WM: white matter)
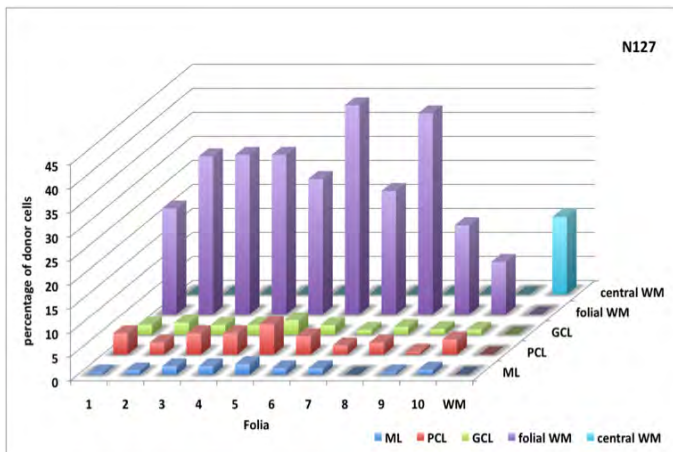
Figure 23: Donor cell distribution in graft N127. The histogram of graft N127 illustrates exemplary the cell distribution taking all folia and layers of the cerebellum into consideration. The external granule layer was not included since we did not detect a mentionable presence of donor cells there. (GCL: granule cell layer, ML: molecular layer, PCL: Purkinje cell layer, WM: white matter)

Figure 24: Donor cell distribution in graft N134. The histogram of graft N134 illustrates exemplary the cell distribution taking all folia and layers of the cerebellum into consideration. The external granule layer was not included since we did not detect a mentionable presence of donor cells there. (GCL: granule cell layer, ML: molecular layer, PCL: Purkinje cell layer, WM: white matter)

Figure 25: Donor cell distribution in graft N136. The histogram of graft N136 illustrates exemplary the cell distribution taking all folia and layers of the cerebellum into consideration. The external granule layer was not included since we did not detect a mentionable presence of donor cells there. (GCL: granule cell layer, ML: molecular layer, PCL: Purkinje cell layer, WM: white matter)

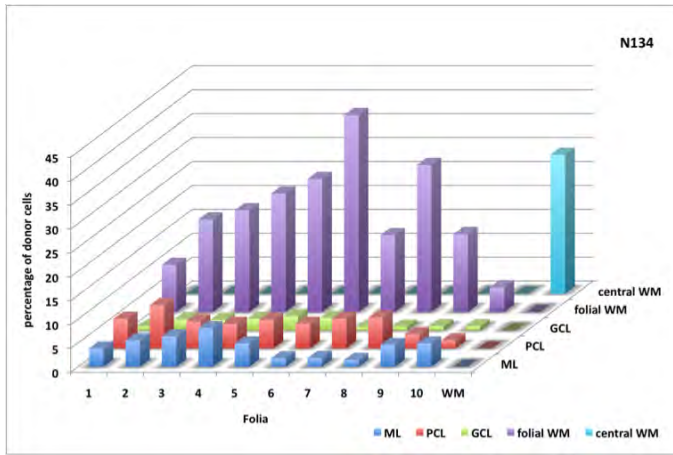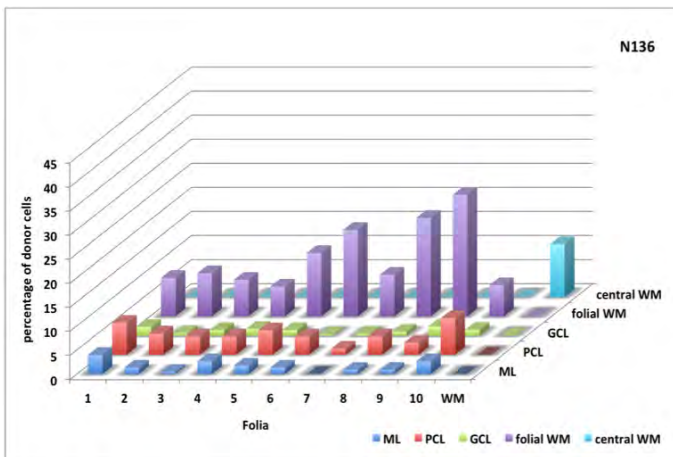

Figure 26: Donor cell distribution in graft N137. The histogram of graft N137 illustrates exemplary the cell distribution taking all folia and layers of the cerebellum into consideration. The external granule layer was not included since we did not detect a mentionable presence of donor cells there. (GCL: granule cell layer, ML: molecular layer, PCL: Purkinje cell layer, WM: white matter)
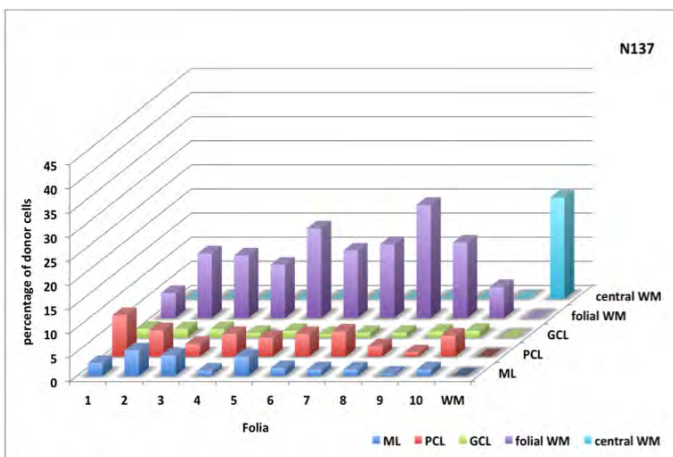
The mean of cell counts from 7 parabasal grafts, counting the different cerebellar layers (except the external granular layer, which did not reveal a mentionable presence of donor cells) showed the following percentages of donor cells: molecular layer 3.22 %; Purkinje cell layer 4.96 %; granule cell layer 2.25 %; folial white matter 18.41 % and the central white matter 19.88 % (Figure 28 W - AVG). The variation between the grafts is due to the fact, that in each of the cases the parabasal plate was grafted to a different extent.
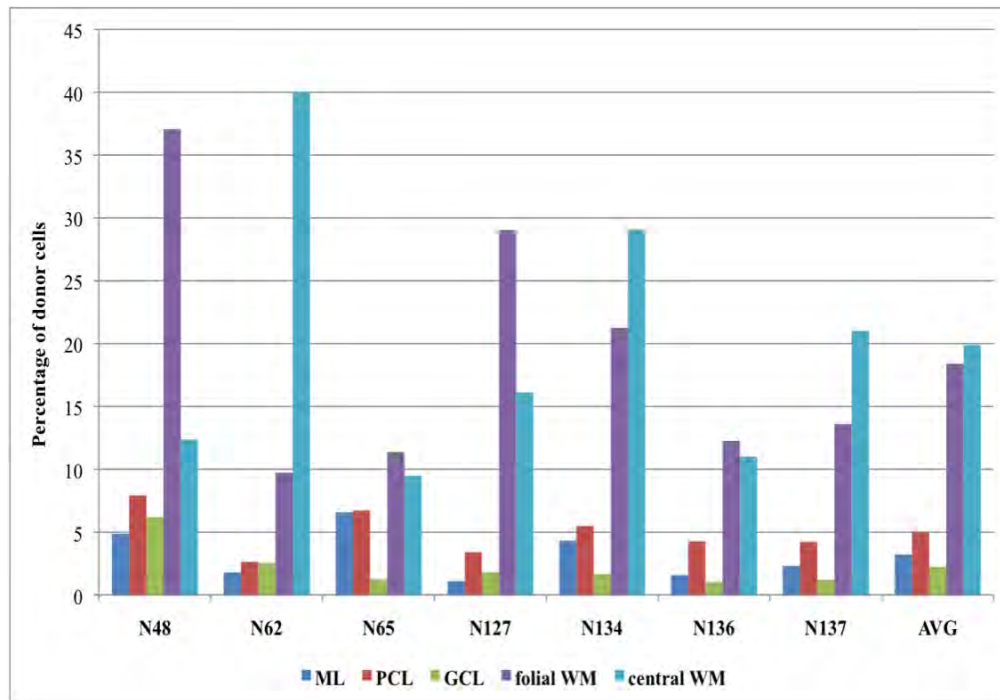
Figure 27: Average donor cell distribution of 7 parabasal grafts. The histogram summarizes the average cell counts for seven members of the group of parabasal transplants taking all different layers of the cerebellum into consideration. The external granule layer was not included since we did not detect a mentionable presence of donor cells there. In addition the average of these 7 grafts was calculated as illustrated in the last histogram named AVG. (GCL: granule cell layer, ML: molecular layer, PCL: Purkinje cell layer, WM: white matter); (Mecklenburg et al. 2011)

3.1.1.3 Fate map of the mesencephalic parabasal band neighboring epithelium

To accurately localize the origin of mesencephalic-cerebellar migrating cells in the parabasal plate, alar or basal epithelium bordering parabasal bands was grafted. The following section has therefore been divided into grafts that were performed either by transplanting mainly alar plate and a small portion of the parabasal plate or by transplanting mainly basal plate and a small portion of the parabasal plate.

In anterior grafts of the alar and little parabasal mesencephalic epithelium (N116; Figure 28 A, B), hardly any donor cells were detected in the VM or the cerebellum (Figure 28 C –E). Grafting the alar plate together with a small central part of the parabasal plate (N139; Figure 28 F – H) revealed a slight cell migration via the VM (Figure 28 I) into the cerebellum (Figure 28 J), although the number of these cells was very low.

Comparatively similar results produced the grafts of the basal plate with small portions of parabasal mesencephalic epithelium. The case of N132 (Figure 28 K – N) covered a small part of the rostral parabasal neuroepithelium leading to an insignificant presence of donor cells in the cerebellum (Figure 28 O). Grafting a more central part of the parabasal plate did not lead to any cell migration (Figure 28 P -T).
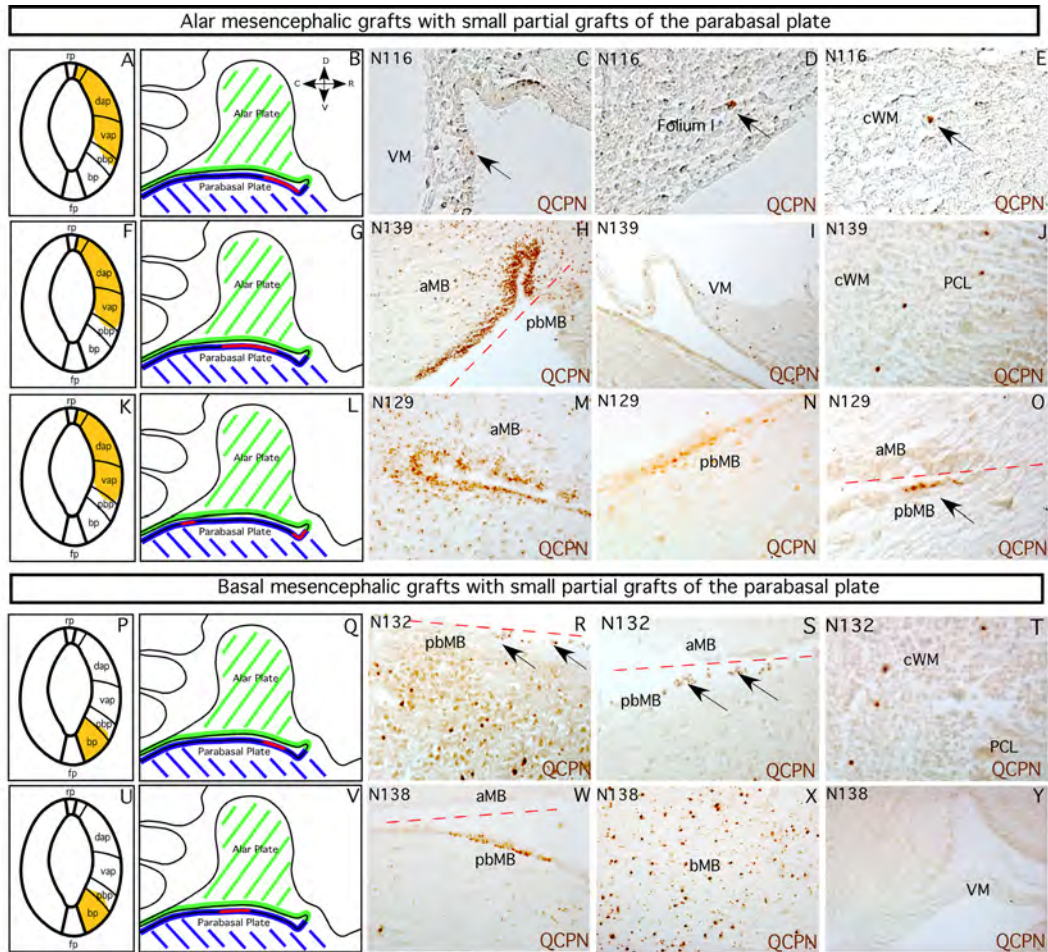
Figure 28: Alar and basal grafts with small partial grafts of the parabasal plate. When grafting alar plate and the very rostral part of the parabasal plate like in N116 (A, B), we hardly detected donor cells in the VM or the cerebellum (C –E). Whereas grafting the alar plate together with a small central part of the parabasal plate as in N139 (F – H) we observed a slight cell migration via the velum medullare (I) into the cerebellum (J). Although the number of observed cells is evanescently marginal. Sections are oriented as illustrated by arrows in B. (aMB: alar midbrain, bMB: basal midbrain, C: caudal, cWM: central white matter, D: dorsal, aMB: alar midbrain, PCL: Purkinje cell layer, pbMB: parabasal midbrain, R: rostral, V: ventral, VM: velum medullare); (Mecklenburg et al. 2011)

In figure 29 two more cases of alar grafts with partial parabasal grafts are attached. In none of these cases the graft resulted in a rostro- caudal cellular migration to the cerebellum, which is most likely due to the fact, that the parabasal plate, grafted in these cases is very small.
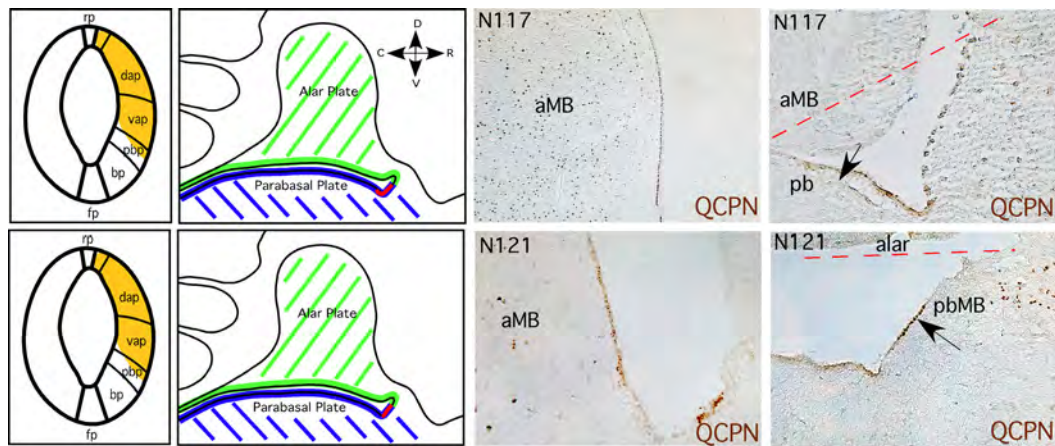
Figure 29: Partially grafted parabasal midbrain with mainly alar transplants. In these cases, due to the very small rostral transplant of the parabasal midbrain, we did not detect cell migration into the cerebellum. (aMB: alar midbrain, pb: parbasal plate, pbMB: parabasal midbrain)

All of the grafts mentioned in this chapter were summarized in the table on the next page. This table gives an overview about the developmental stages of the illustrated cases as well as the location of the grafts. Furthermore, the figures in which the different transplants are shown are mentioned in the last column.

Table 6: Summary of the performed transplants. (AP: alar plate, AP^PbP: alar plate with partial parabasal graft, BP: basal plate, BP^PbP: basal plate with partial parabasal graft, HH: Hamburger Hamilton, PbP: parabasal plate)

Name	Stage of Fixation (days/ stage HH)	Graft Location	Figure
GFP42	5/ HH26	PbP	*Figure 32*
GFP48	7/ HH31	PbP	*Figure 32*
GFP11	11/ HH37	PbP	*Figure 32, 34*
GFP12	12/ HH38	PbP	*Figure 32*
N48	14/ HH40	PbP	*Figure 20, 21, 27, 33*
N60	17/ HH43	PbP	*Figure 20*
N62	15/ HH41	PbP	*Figure 20, 27*
N65	17/ HH43	PbP	*Figure 20, 22, 27, 33*
N103	17/ HH43	PbP	*Figure 33, 34*
N127	16/ HH42	PbP	*Figure 19, 23, 27, 34*
N128	16/ HH42	PbP	*Figure 19*
N130	16/ HH42	PbP	*Figure 20*
N134	17/ HH43	PbP	*Figure 19, 24, 27, 34*
N136	16/ HH42	PbP	*Figure 20, 25, 27*
N137	16/ HH42	PbP	*Figure 20, 26, 27*
N140	16/ HH42	PbP	*Figure 20*
R683	9/ HH35	PbP	*Figure 19*
GFP 1	6/ HH29	AP	*Figure 30*
GFP8	10/ HH36	AP	*Figure 30*
N86	17/ HH43	AP	*Figure 18*
N87	17/ HH43	AP	*Figure 18*
N93	17/ HH43	AP	*Figure 18*
N94	17/ HH43	AP	*Figure 18*
N95	17/ HH43	AP	*Figure 18*
N99	16/ HH42	AP	*Figure 18*
N101	16/ HH42	AP	*Figure 17*
N113	17/ HH43	AP	*Figure 18*
N114	17/ HH43	AP	*Figure 17*
N115	17/ HH43	AP	*Figure 18*
N116	17/ HH43	AP^PbP	*Figure 28*
N117	17/ HH43	AP^PbP	*Figure 29*
N120	17/ HH43	AP	*Figure 18*
N121	17/ HH43	AP^PbP	*Figure 29*
N129	16/ HH42	AP^PbP	*Figure 28*
N139	16/ HH42	AP^PbP	*Figure 28*
GFP38	14/ HH40	BP	*Figure 31*
GFP39	10/ HH36	BP	*Figure 31*
GFP50	14/ HH40	BP	*Figure 31*
N132	17/ HH43	BP^PbP	*Figure 28*
N138	17/ HH43	BP^PbP	*Figure 28*

3.1.2 GFP electroporated chick/ chick transplants

To exclude, that the observed migration from the parabasal plate to the cerebellum in quail- chick transplants is due to difference in species, the mesencephalic vesicle of chicken embryos at stage HH10 was electroporated and transplanted into chicken embryos of the same age. In total 59 GFP electroporated chicken/ chicken transplants were analyzed. Some exemplary cases are described and illustrated in this section.

3.1.2.1 Transplants of the mesencephalic alar plate

GFP electroporated chicken mesencephalic vesicle was transplanted into isochronic chicken embryos at developmental stage HH10. The experimental embryos were analyzed from early developmental stage E5 until E16 to check the migration time of grafted mesencephalic cells to the cerebellum. At developmental stage E6, where the graft was located just at the border to the parabasal plate at the caudal half of the mesencephalic vesicle, none of the donor cells migrated towards the cerebellum (Figure 30 A, B, E –G). At older stages such as E10 rostral grafts also did not reveal migratory streams of donor cells moving towards, or as observed in parabasal quail- chick transplants, into the cerebellum. Performing exclusive alar plate grafts did not lead to a cell migration towards the cerebellum, nor a presence of donor cells in this area of the brain.
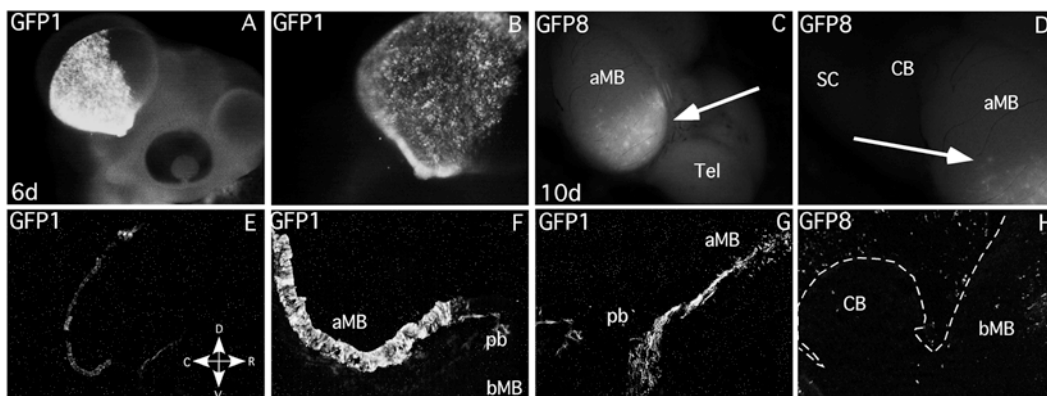
Figure 30: GFP electroporated chick/ chick transplants of the mesencephalic alar plate. Exclusively alar grafts (A- D) of the mesencephalic vesicle did not lead to a cell migration towards the cerebellum (E- H). (aMB: alar midbrain, C: caudal, CB: cerebellum, bMB: basal midbrain, CB: cerebellum, D: dorsal, pB: parabasal, R: rostral, SC: spinal cord, V: ventral)

3.1.2.2 Transplants of the mesencephalic basal plate

Similarly to the results obtained with the quail- chick- chimeras, basal plate grafts (Figure 31 A, B, E, F, J, K) of the mesencephalic vesicle did not lead to a cell migration towards the cerebellum. But basal grafts revealed a caudal migration of donor cells through the medial longitudinal fasciculus (MLF) towards and through the spinal cord (Figure 31 G- I, L – N).

Figure 31: GFP electroporated chick/ chick transplants of the mesencephalic basal plate. To be able to distinguish between alar and basal plate double immuohistochemical stainings were performed with Pax7, as a alar plate marker, and GFP to visualize grafted tissue. Exclusively basal grafts (A, B, E, F, J and K) of the mesencephalic vesicle did not lead to a cell migration towards the cerebellum. But basal grafts revealed a caudal migration of donor cells through the MLF towards (G- I and L- N) and through the spinal cord. (C: caudal, bMB: basal midbrain, CB: cerebellum, D: dorsal, MLF: medial longitudinal fasciculus, R: rostral, V: ventral, VM: velum medullare); partially published in (Mecklenburg et al. 2011)

3.1.2.3 Transplants of the mesencephalic parabasal plate

In order to support the obtained data, grafts including the parabasal plate were performed and analyzed at different developmental stages. At E5 (Figure 32 A-C) and E7 (Figure 32 D-F), although most of the cases were negative for cellular migration to the cerebellum, some isolate GFP-cells were entering the rostral cerebellum, when parabasal mesencephalon was transplanted. At E11 GFP+ cells entered the cerebellum via folium 1 (Figure 32 G, H), following a cellular migratory stream through the velum medullare, as was observed in quail/chick transplants, which allowed some cells to reach the cerebellum (Figure 32 G, I).

At E12 this migratory stream was observed from the grafted mesencephalon leading towards the velum medullare with many GFP+ cells present in the velum (Figure 32 J- L). As shown by immunohistological analysis, these cells expressed the glial marker Vimentin (Figure 34 M, N).
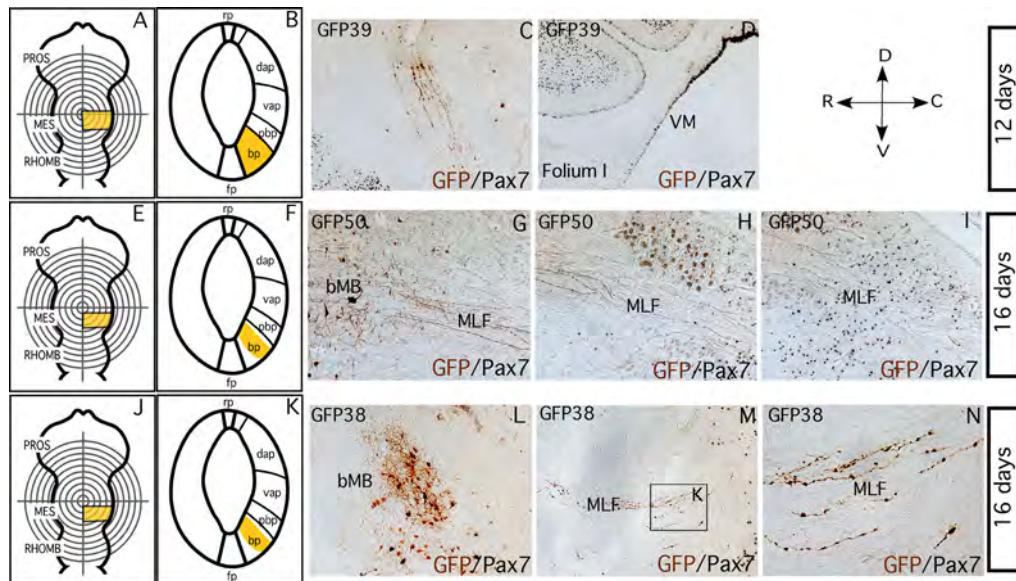

Figure 32: GFP electroporated chick/ chick transplants. GFP electroporated chicken mesencephalic vesicle was transplanted into isochronic chicken embryos at developmental stage HH10. In basal grafts a caudal migration of donor cells through the medial l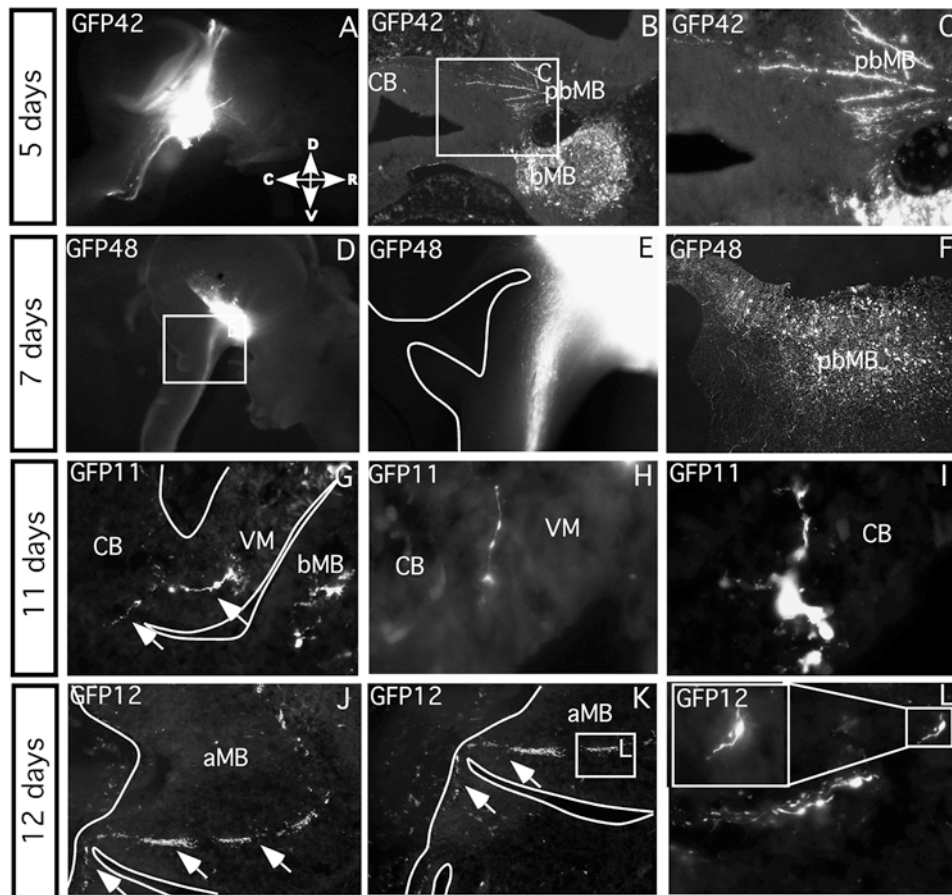ongitudinal fasciculus towards and through the spinal cord was observed (A, D, E). At E5 (A-C) some isolate GFP-cells migrated caudally towards the cerebellum (B, C). At E11 GFP+ cells entered the cerebellum via folium 1 (arrows in G). A few GFP+ cells were detected in the velum and in the cerebellum (H, I). At E12 a narrow migratory stream was observed from the grafted mesencephalon leading towards the cerebellum with GFP+ cells present in the velum (arrows in J, K), as shown in quail/chick transplants, which allowed some cells to reach the cerebellum (L). All sections are oriented as indicated in A. (aMB: alar midbrain, bMB: basal midbrain, C: caudal, CB: cerebellum, D: dorsal, pbMB: parabasal midbrain, R: rostral, V: ventral, VM: velum medullare); (Mecklenburg et al. 2011)

3.1.3 Cell fate analysis

To identify the fate of the migrating cells entering the cerebellum, immunohistological staining was performed with a variety of specific cell type antibodies. First, the possible neuronal character of these cells was explored using Map2 antibody. Although, QCPN positive cells never co-localized with

Map2 (Figure 33 A-C), suggesting that they were not neuronal in nature, this issue was analyzed more carefully with other markers specific for GABAergic interneurons (Gad65/67 and Pax2) to discard the presence of these cell types with extracerebellar origin (Figure 33 D-I). Moreover, calbindin, a marker for Purkinje cells, also did not show any co-localization with QCPN labeled nuclei (Figure 33 J-L).
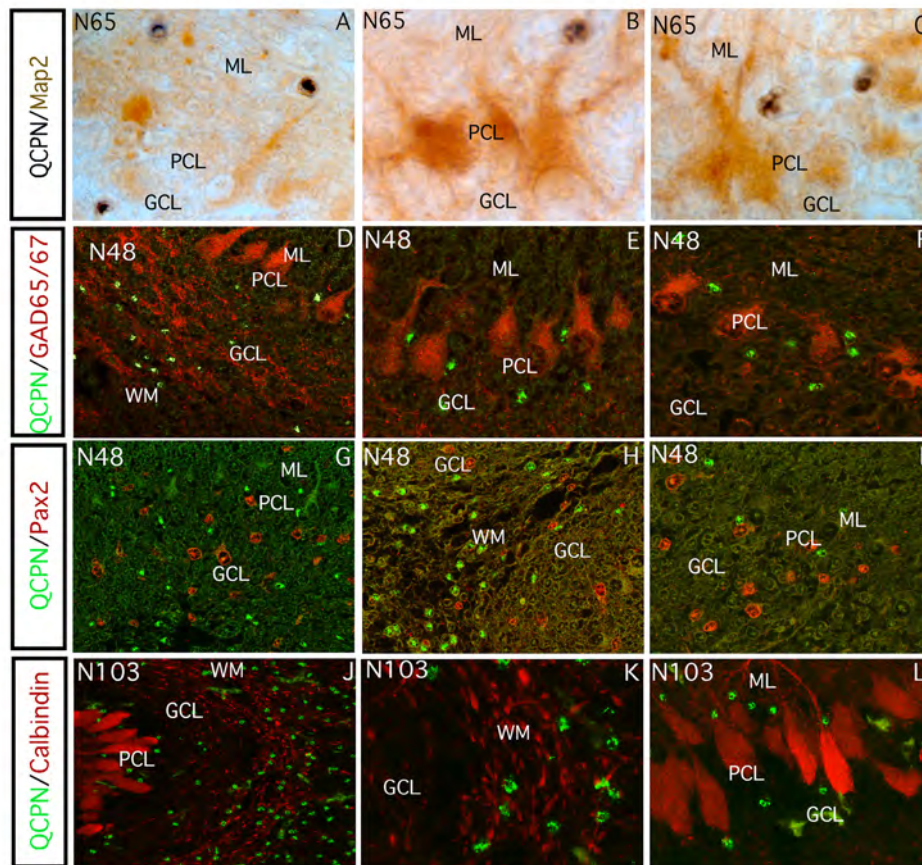
Figure 33: Immunohistochemical analysis of donor cells with neuronal markers. Donor cells did not generate cerebellar neurons since they could not be double labeled with neuronal markers such as Map2 (A-C), Gad 65/67 (D-F), Pax2 (G-I) or Calbindin (J-L). Therefore QCPN positive cells were not of neuronal nature, neither Purkinje cells nor interneurons. (GCL: granule cell layer, ML: molecular layer, PCL: Purkinje cell layer, WM: white matter); (Mecklenburg et al. 2011)

Then a glial phenotype was investigated, using Vimentin as a marker of radial and Bergmann glial cells, as well as of immature astrocytes (astrocyte progenitors) of the white matter (Milosevic and Goldman, 2002), and PLP (Figure 34 G-I) and Olig2 (Figure 34 J-L), as oligodendroglial lineage markers. Since the astroglial specific marker, GFAP, is weakly expressed in chicken embryonic brain until early postnatal stages (Kálmán et al. 1998) it has not been analyzed. Instead the astroglial marker S100 was used and found to be co-expressed with QCPN in 10% of the quail cells (Figure 34 D-F, O). Golgi epithelial cells in the

Purkinje cell layer and their Bergmann fibers, together with some embryonic astrocytes in the white matter were highly stained with Vimentin (Figure 34 A-C).
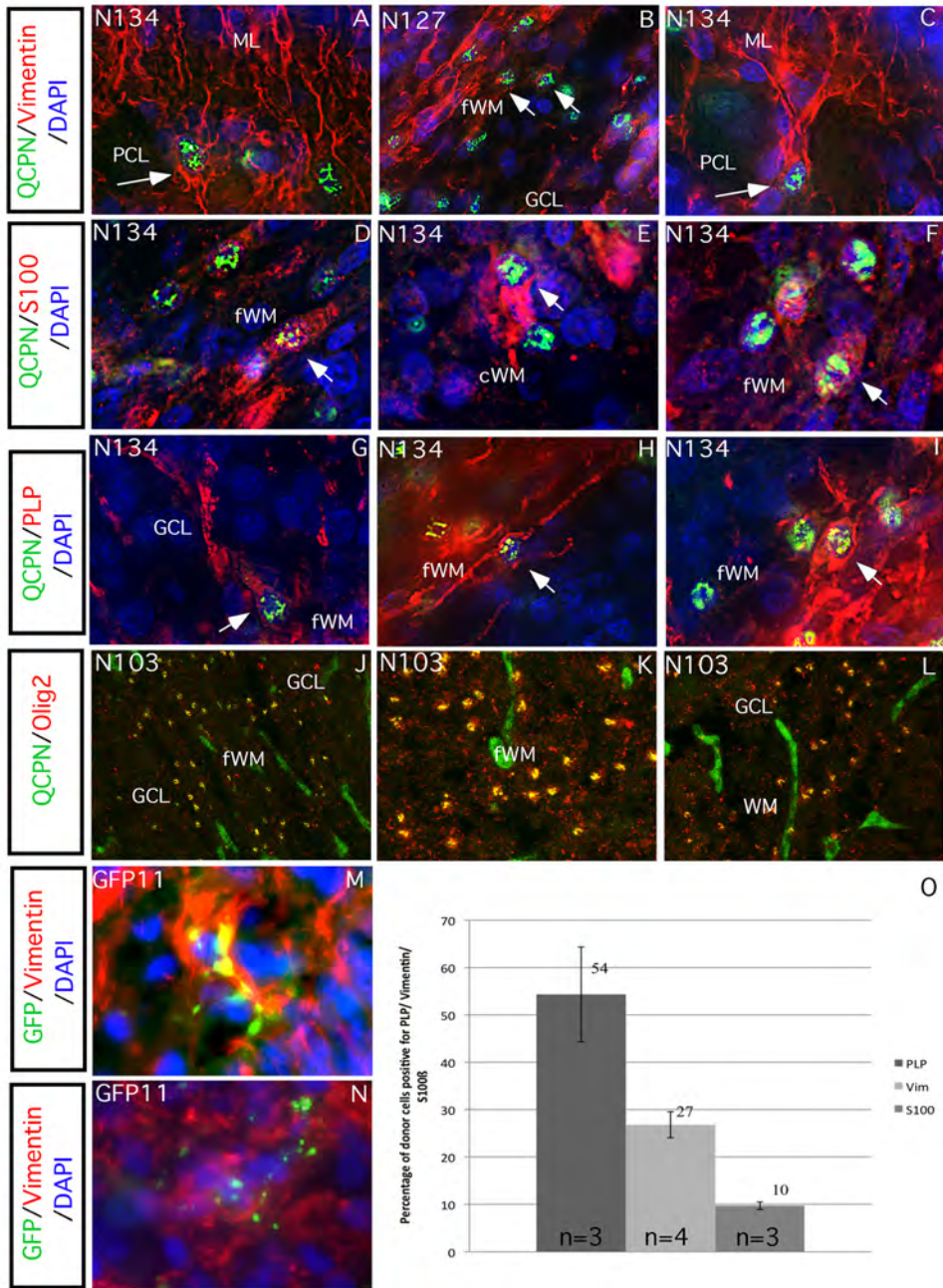
Figure 34: Immunohistochemical analysis of donor cells with glial markers. QCPN positive cells were double labeled with Vimentin (arrows in A-C), PLP (arrows in G- I) and Olig2 (J- L) indicating that these cells are respectively Bergmann glia, oligodendrocytes or astrocyte precursors in the white matter (B). Additionally co-localization with S100 an astrocytic marker was found (arrows in D-F). Furthermore, some of the GFP+ cells in the VM (M) and the cerebellum (N) expressed Vimentin. (O) Illustrates the histograms of the quantification of QCPN+ cells expressing PLP (first bar), Vimentin (second bar) and S100 (third bar). (cWM: central white matter, fWM: folial white matter, GCL: granule cell layer, ML: molecular layer, PCL: Purkinje cell layer, WM: white matter); (Mecklenburg et al. 2011)

Finally, PLP+ or Olig2+ oligodendrocytes in granule cell layer and particularly in the white matter, showed frequent co-localization with QCPN. Indeed, in the

white matter most QCPN+ cells not related with blood vessels were Olig2+ (Figure 34 G-L), indicating that the majority of the mesencephalic cells migrated into the cerebellum acquired oligodendroglial fate. Moreover, only between 25-30% of QCPN+ cells were Vimentin+ and around 50% expressed PLP (Figure 34 O). Since neural crest was also grafted with the mesencephalic neuroepithelium, some meningeal cells and blood vessels in the cerebellar territory showed QCPN immunoreactivity.

3.1.4 DiI injections into the velum medullare (VM)

DiI injections into the VM were performed to proof that the quail or GFP+ mesencephalic cells encountered within the cerebellum migrated through this structure. For this purpose, chicken embryos were incubated until developmental stage HH35, neural tube explants were made and DiI was injected into the velum medullare, at the border between the mesencephalon and the cerebellum. The aim was to label migratory cells in the VM moving from the mesencephalic parabasal plate to the cerebellum. Cells marked with DiI showed the appearance of migratory cells with bipolar shape and provided with a long single or bifurcated leading process oriented towards the cerebellum (Figure 35). The distal tips of these leading processes bore complex exploratory growth cones (Figure 35 D-F).
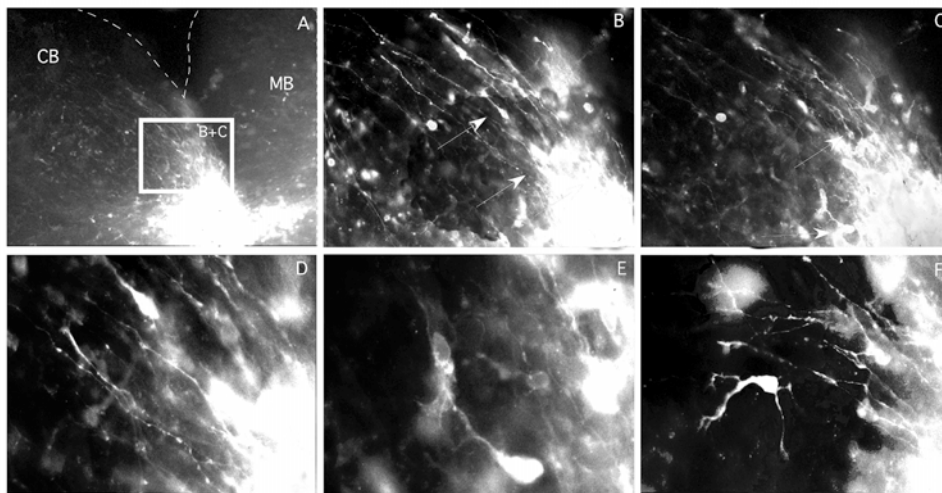
Figure 35: DiI injections into explants of chicken embryos at developmental stage HH35. The DiI was injected into the rostral end of the velum medullare in order to follow cellular migration towards the cerebellum (A-D). Cells marked with DiI showed the appearance of migratory cells with bipolar shape, provided with a long single or bifurcated leading process oriented towards the cerebellum, ending with large growth cones (D- F). (CB: cerebellum, MB: midbrain); (Mecklenburg et al. 2011)

3.1.5 Nkx2.2 expression in the developing midbrain and cerebellum

Nkx2.2 is a homeobox protein, which is expressed in oligodendrocytes of the spinal cord (Qi et al. 2001) and the midbrain (Fu et al. 2003). To investigate if Nkx2.2 might also play a role in oligodendrogenesis of the cerebellum, the expression pattern of this transcription factor during embryonic development in the chicken midbrain and cerebellum was analyzed. At E5/ HH26 a small band of Nkx2.2 expressing cells was present along the rostro- caudal axis of the parabasal plate of the entire neural tube including the mesencephalic vesicle (Figure 36 A, E). This band expanded continuously during development (Figure 36 B –D). In coronal sections of the mesencephalic vesicle of a 7.5-day-old/HH32 embryo two areas of *Nkx2.2+* cells were detected. These are the longitudinal parabasal plate of the mesencephalic vesicle (pbMes) and the pre-isthmic band (piB); (Hidalgo-Sánchez et al. 2005) of the alar mesencephalon (Figure 36 F, G). An equivalent location of the sections showed in (F) and (G) is illustrated by dotted lines in figure 36 C. At E9/HH35 *Nkx2.2* expression in pre-isthmic band, as well as the parabasal plate, further increased. The velum and the cerebellum were devoid of *Nkx2.2* expression at this stage (Figure 36 H-L). At embryonic day 14/ HH40 the parabasal band of *Nkx2.2+* cells further expanded to the neighboring alar and basal mesencephalon and did not serve any longer as a clear marker to distinguish between the different dorso-ventral plates of the midbrain (Figure 36 N-O). A strong expression of *Nkx2.2* was detected in the velum medullare and the cerebellum at this stage of development (Figure 36 P, Q). Double labeling using Nkx2.2 and oligodendrocytic marker PLP and the Bergmann glial marker Vimentin (Andrae et al. 2001) further allowed to identify these cells of respectively oligodendrocytic or Bergmann glia in nature (Figure 36 R-U). Figure 36 R shows the expression of Nkx2.2 in the mesencephalic ventricular epithelium of a HH28 chicken embryo. Vimentin, highly expressed at this stage of development, partially co-localized with Nkx2.2. From HH35 onwards, Nkx2.2+ cells were additionally found in the velum medullare (Figure 36 S) and the cerebellum (Figure 36 T), where they also partially co-localized with Vimentin (Figure 36 S, T). Later in development, Nkx2.2 expression was found in PLP+ oligodendrocytes of the cerebellum (Figure 36 U). The expression pattern of Nkx2.2, as well as its co-localization with oligodendrocytic markers, strongly indicates that this homeobox transcription factor is also involved in cerebellar oligodendrogenesis.
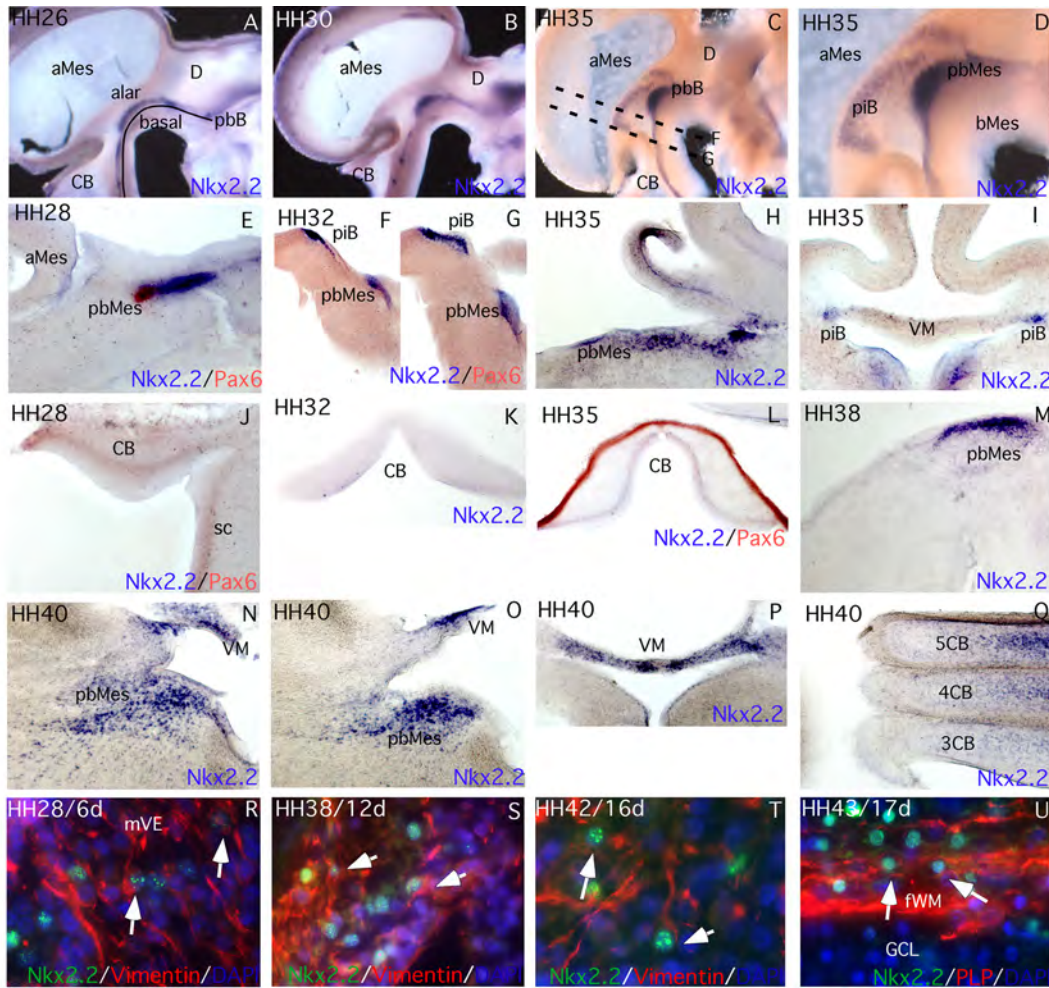
Figure 36: Expression pattern of Nkx2.2 in the developing embryonic chicken brain. Figures A – Q show *in situ* hybridizations of *Nkx2.2* in whole mount embryos (A-D) as well as on sagittal (E, J, M) and coronal sections (F- I, K, L, N-Q) at different stages of development as indicated in each figure. Nkx2.2 was expressed along the rostro- caudal axis of the parabasal plate (A, E). This band expands during development (B, D) and Nkx2.2 expression in the cerebellum was detected around E14 (P, Q). (*In situ* hybridizations were performed by Eduardo de Puelles) Figure R-U illustrate immuno staining on sagittal sections of E6, E12, E16 and E17 embryos with Nkx2.2 and the glial marker Vimentin (R-T) and the oligodendrocytic marker PLP (U). Both of them colocalize with Nkx2.2 expressing cells (arrow bars in R- U). (aMes: alar mesencephalon, CB: cerebellum, cWM: central white matter, GCL: granule cell layer, mPAG: mesencephalic periaqueductal grey, fWM: folial white matter, mVE: mesencephalic ventricular epithelium, pbB: parabasal plate, pbMes: parabasal mesencephalon, piB: pre-isthmic band, VM: velum medullare); partially published in (Mecklenburg et al. 2011)

3.2 *Gdf10* in the development of Bergmann glial cells

Since this work primarily focuses on cerebellar development, *Gdf10* was characterized in more detail in this area. In order to do that, the expression pattern, as well as the phenotype of *Gdf10+* cells, was analyzed at different developmental stages. In addition to that, the expression of *Gdf10* was characterized in Shh mutants to investigate a possible regulation by Shh. Finally, *Gdf10* was screened for transcription factors binding sites in order to identify potential regulators of this gene.

3.2.1 Expression pattern of Gdf10 mRNA and protein

The expression pattern of *Gdf10* mRNA was analyzed by *in situ* hybridization from E14.5 until adulthood (P28). Whole mount *in situ* hybridizations with *Gdf10* revealed an expression in the cerebellar upper rhombic lip at E14 (Figure 37 A-C). This expression was maintained between E14.5 and E16.5 (Figure 37 D- N). In addition to the expression in the cerebellar upper rhombic lip, *Gdf10* was also detected in the upper and the lower rhombencephalic rhombic lip (Figure 37 D, I, M). Furthermore, *Gdf10* labeled the ventricular zone of the cerebellar roof plate,

which gives rise to the cerebellar vermis (Figure 37 C, F, H, J, K, L, N). At E16.5 *Gdf10* expression, detected by ISH, appeared in two different colors, in dark blue and turquois. Tissue labeled in dark blue was located at the pial surface of the cerebellum, whereas the turquois-colored reaction was located more profoundly in the ventricular epithelium of the cerebellum.
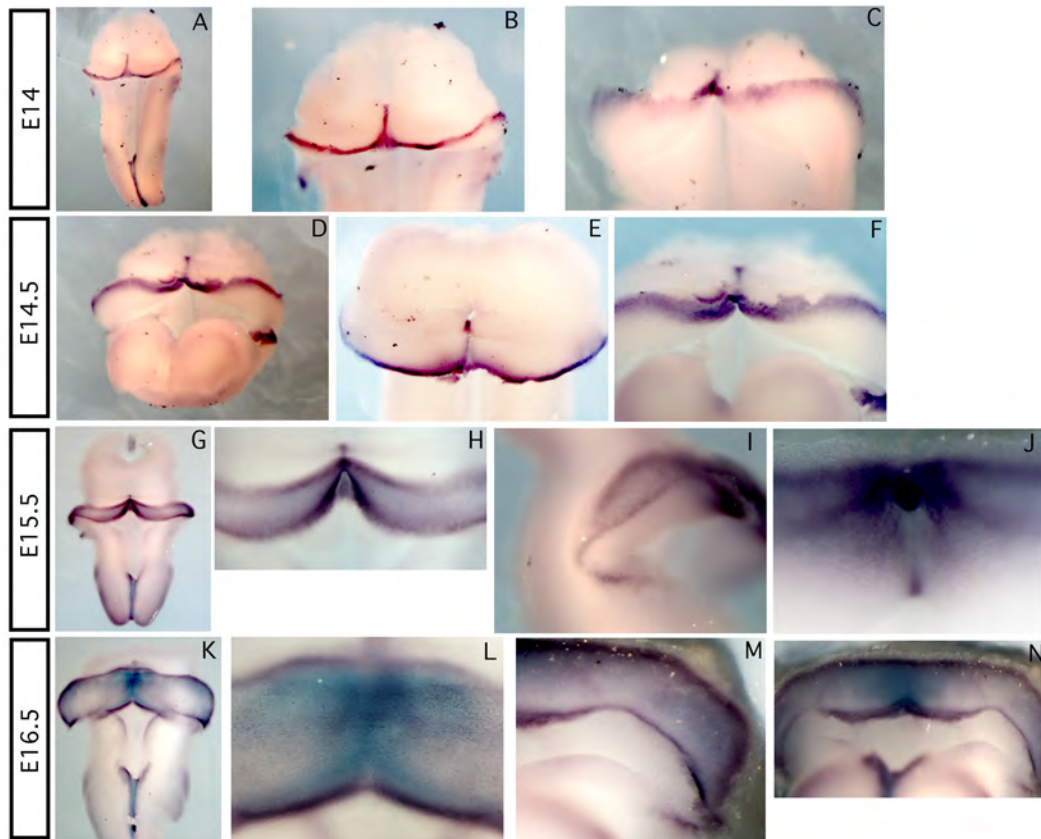
Figure 37: Expression pattern of *Gdf10* at embryonic stages. Whole mount *in situ* hybridizations of E14 (A- C), E14.5 (D- F), E15.5 (G- J) and E16.5 (K- L) mouse embryos. The telencephalon as well as the alar mesencephalon has been removed prior to the hybridization.

In order to gain more detailed information about the expression pattern of *Gdf10,* its expression was analyzed in cryostat sections from E14.5 until adulthood (Figure 38).

This analysis revealed that at embryonic stages, *Gdf10* was expressed not only in the VZ of the cerebellar roof plate and the rhombic lip but also in the VZ adjacent to the rhombic lip (Figure 38 A- D). The expression pattern varied along the antero- posterior axis of the cerebellum. Anteriorly *Gdf10+* cells were lining the VZ of the developing vermis, along the cerebellar midline (Figure 38 B, F, H),

whereas in the cerebellar hemispheres *Gdf10* was expressed in the ventricular epithelium adjacent to the rhombic lip and the rhombic lip itself, as illustrated at E14.5 (Figure 38 A, C) and E16.5 (Figure 38 F, G); which laterally continue the roof plate expression.
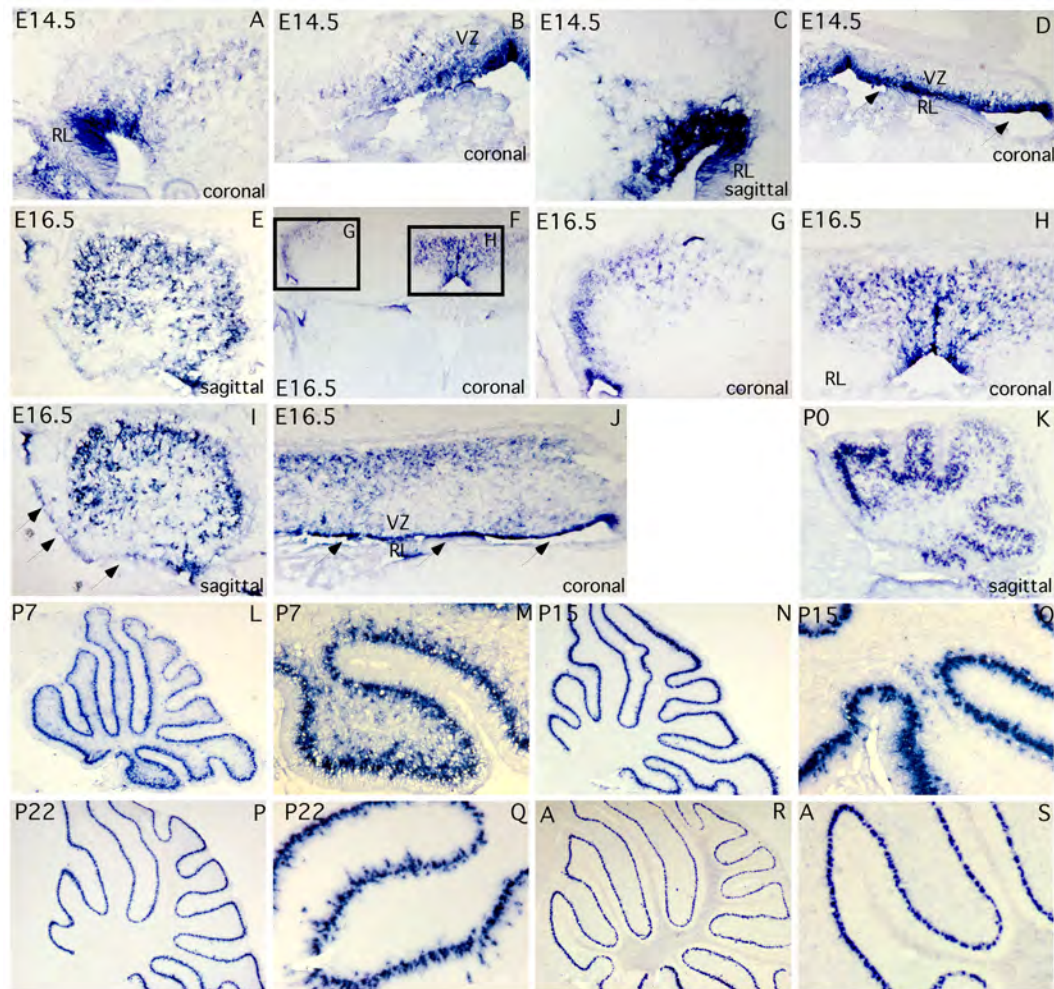
Figure 38: Expression pattern of Gdf10 mRNA in the cerebellum during development. The expression pattern of *Gdf10* was analyzed by *in situ* hybridization from E14.5 until adulthood (P28). At embryonic stages *Gdf10* expression was detected in the ventricular zone of the 4th ventricle and the rhombic lip (A- J). From P0 *Gdf10* expression began to localize in the Purkinje cell layer (K). Until P7 *Gdf10+* cells were detected in the white matter tracts and the granule cell layer as well as the Purkinje cell layer, (L, M). At P15 most of the expression within the white matter and the granule cell layer disappeared and *Gdf10* mRNA was predominantly detected in the Purkinje cell layer (N, O). This expression pattern was maintained until adulthood (P- S).

Posteriorly, *Gdf10* expression was detected along the entire cerebellar rhombic lip and the ventricular zone of the 4th ventricle (Figure 38 D, J). In contrast to anterior cerebellar sections, posteriorly, *Gdf10* was also detected in the

intermediate zone of the cerebellar plate, between the VZ and the pial surface (Figure 38 D, J).

The expression at the medial ventricular epithelium expanded radially (Figure 38 B, F, H), whereas the expression at the rhombic lip appeared to expand tangentially underlining the EGL (Figure 38 A, G). From P0 *Gdf10* expression began to localize in the Purkinje cell layer (Figure 38 K). Until P7 *Gdf10*+ cells were detected in the white matter tracts and the granule cell layer as well as the Purkinje cell layer (Figure 38 L, M). At P15 most of the expression within the white matter and the granule cell layer disappeared and *Gdf10* mRNA was predominantly detected in the Purkinje cell layer (Figure 38 N, O). This expression pattern was maintained until adulthood (Figure 38 P- S).

To confirm the obtained results, the expression of the Gdf10 protein was investigated with a human Gdf10 antibody revealed with DAB. The protein expression pattern coincided with the expression of the mRNA labeling *Gdf10*+ cells at embryonic stages in the ventricular epithelium of the 4th ventricle (Figure 39 A, C, D) and the rhombic lip (Figure 39 B). In addition to that the EGL also appeared to be Gdf10 positive (Figure 39 upper arrows). At postnatal stages Gdf10 was detected in the white matter, the granule cell layer and the Purkinje cell layer (Figure 39 E- H). The changes in expression pattern, ending in a focal expression of Gdf10 exclusively in the Purkinje cell layer at adult stages, coincides with the results obtained by *in situ* hybridization.
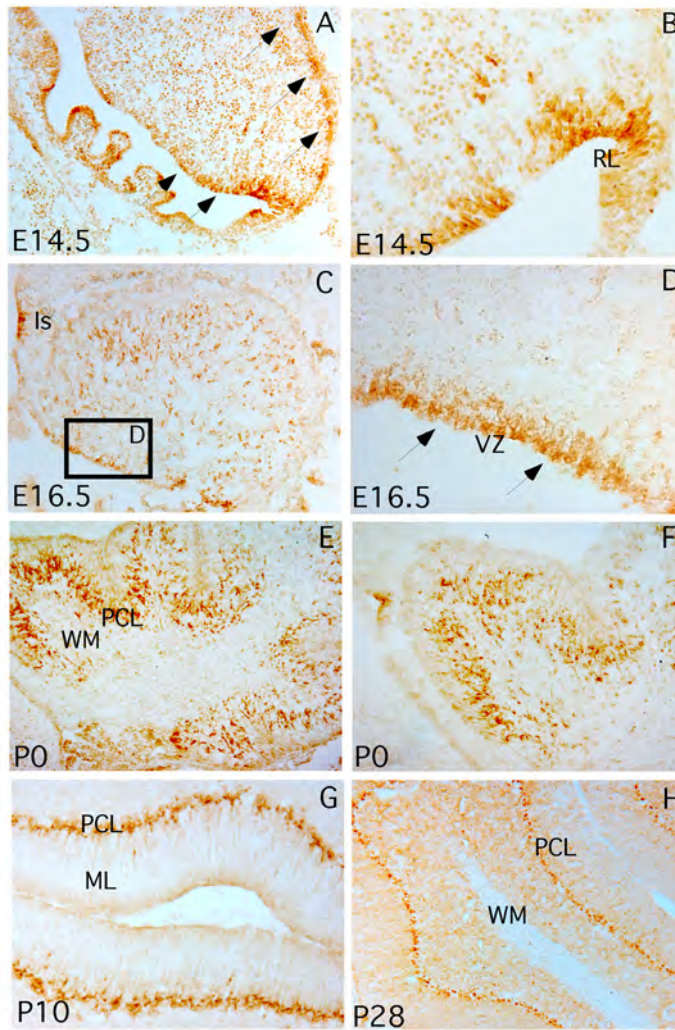
Figure 39: Expression of Gdf10 protein during cerebellar development. The expression pattern of Gdf10 visualized by a Gdf10 antibody parallels the pattern found by *in situ* hybridization.

Especially in posterior coronal sections of the cerebellum at E16.5 *Gdf10* appeared to be partially expressed in the upper rhombic lip. In order to proof this localization, a triple immunohistological staining was performed with Calbindin (brown) labeling Purkinje cells, Pax6 (black) labeling granule neurons and *Gdf10* (blue); (Figure 40). Due to the strong expression of *Gdf10* and Pax6 in the rhombic lip it was not possible to clearly identify double positive cells in this area. Nevertheless, this analysis revealed that *Gdf10* is also expressed in the rhombic lip (Figure 40 A- C). Furthermore it illustrates very well, that *Gdf10* in the lateral cerebellum was expressed beneath the EGL (Figure 40 D- F). Coexpression analysis of Calbindin and *Gdf10* did not show colocalization (Figure 40 G- I).
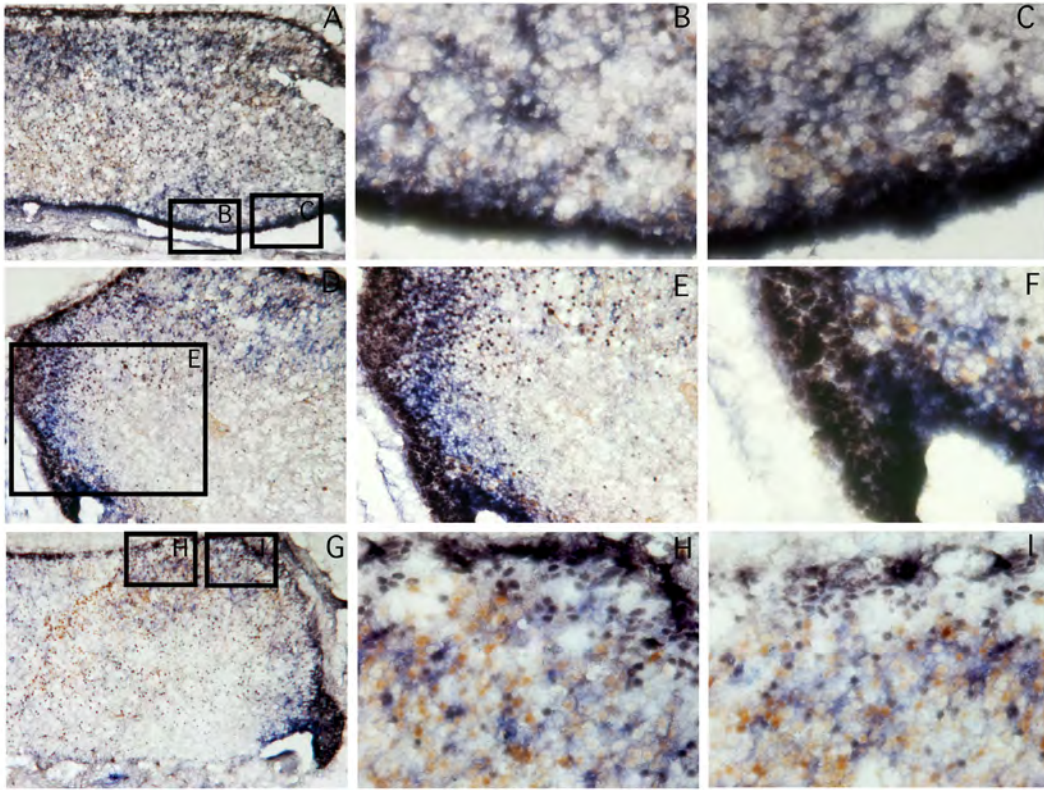
Figure 40: Characterization of sagittal E16.5 mouse embryo sections with *Gdf10* (blue), Pax6 (black) and Calbindin (brown).

3.2.2 Characterization of Gdf10 expressing cells in the cerebellum

Analysis with glial markers revealed a strong co-expression with all tested markers, namely GFAP, Nestin, GLAST and Vimentin.

From E14.5 until P0 *Gdf10* expression did not coincide with the expression of GFAP (Figure 41 A- D), but at P0 some *Gdf10*+ cells migrating towards the pial surface of the cerebellar cortex started expressing GFAP (Figure 41 E). The developing Purkinje layer at this time point was predominantly devoid of double-positive cells (Figure 41 F). From P5 onwards GFAP strongly colocalized with *Gdf10* in the Purkinje cell layer as well as in the white matter and the granule cell layer (Figure 41 G- I). The coexpression in the Purkinje cell layer was maintained until P28. Afterwards GFAP expression decreased and therefore not further analyzed.
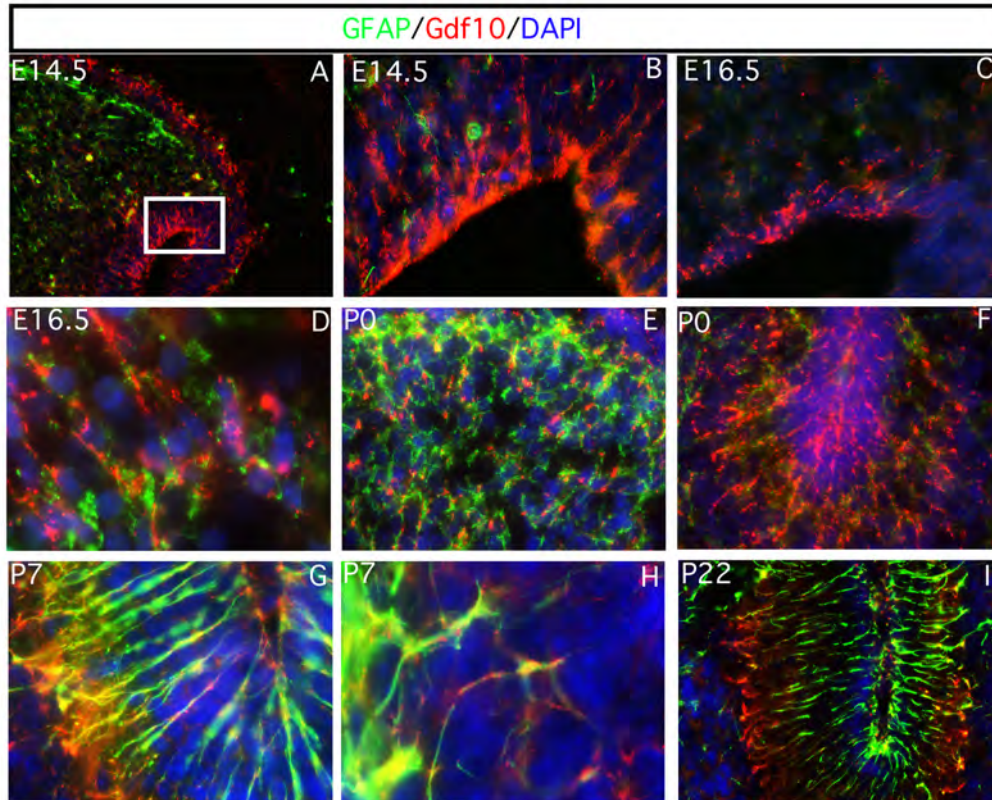
Figure 41: Characterization of *Gdf10* positive cells in the cerebellum with the astroglial marker GFAP. GFAP was expressed relatively late during development in *Gdf10*- positive cells (A-D). Until P0 there was hardly any colocalization with the astroglial marker (E). But from P0 onwards until adulthood GFAP was strongly expressed in *Gdf10+* cells, which at this stage of development were located mainly in the Purkinje cell layer (G- I).

Nestin expression was observed in *Gdf10+* cells from E14.5 onwards (Figure 42). The coexpression increased during development. At E14.5 there was a weak expression of Nestin in *Gdf10+* cells of the mantle layer (Figure 42 A, B). This expression increased at E16.5, where double-labeled cells were present not only in the ventricular epithelium but also in cells that migrated towards the pial surface (Figure 42 C, D). From P0, *Gdf10+*/ Nestin+ cells were present in the Purkinje cell layer (Figure 42 E, F)
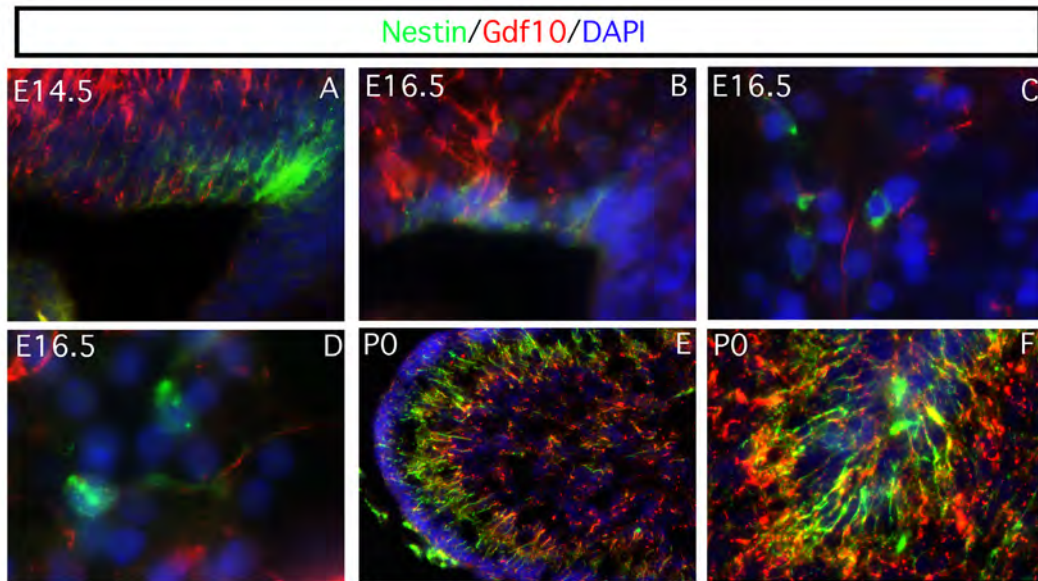
Figure 42: Characterization of *Gdf10* positive cells in the cerebellum with the radial glia marker Nestin. Nestin expression was found in *Gdf10*+ cells from E14.5 onwards. The coexpression increased during development. At E14.5 a weak expression of Nestin in *Gdf10*+ cells was present in the mantle layer (A, B). This expression increased at E16.5 (C, D), where double-labeled cells located not only in the ventricular epithelium but also in cells that migrated towards the developing Purkinje cell layer (E, F).

Additional analysis of GLAST expression in *Gdf10*+ cells revealed coexpression from E14.5 until adult stages (Figure 43). GLAST, in fact, was very similarly expressed to *Gdf10* with an early expression in the ventricular epithelium at E14.5 (Figure 43 A) and a strong colocalization in the white matter tracks and the Purkinje cell layer from P0 onwards (Figure 43 E, F), which later in development located in the Purkinje cell layer exclusively.
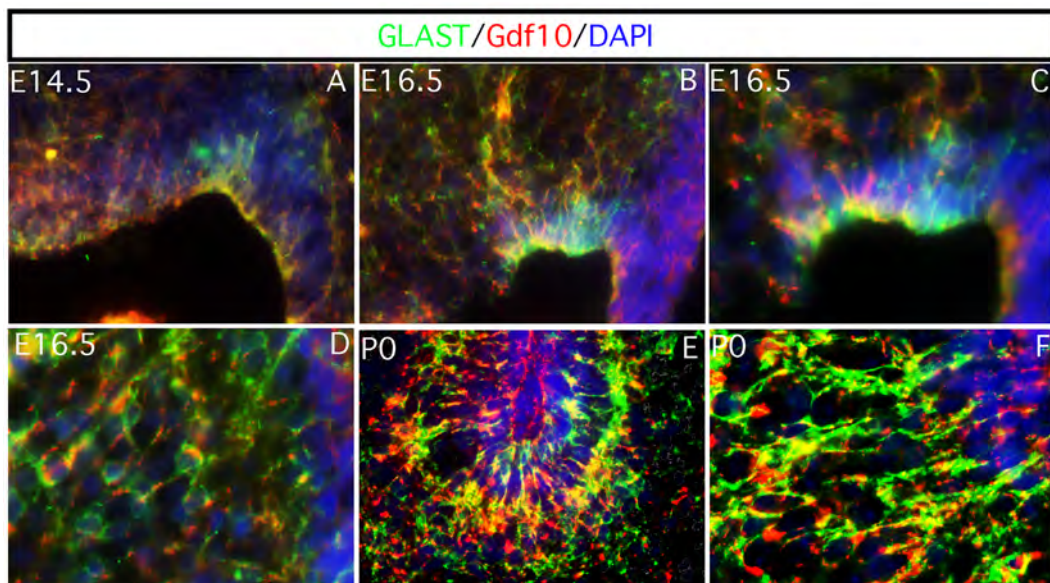
Figure 43: Strong similarities between the expression pattern of *Gdf10* and GLAST during cerebellar development. GLAST was expressed in *Gdf10+* cells from E14.5 until adult stages. GLAST was very similarly expressed to *Gdf10* with an early expression in the ventricular epithelium at E14.5 (A) and a strong colocalization in the white matter tracks and the Purkinje cell layer from P0 onwards (E, F), which later in development centralized in the Purkinje cell layer exclusively.

Finally, colabeling analysis of Vimentin revealed a coexpression in *Gdf10+* cells early at E16.5 (Figure 44 B). This coexpression was maintained until adulthood in *Gdf10+* cells migrating towards the pial surface through the white matter and granule cell layer. From P22 onwards *Gdf10+*/Vimentin+ cells were detected exclusively in the Purkinje cell layer (Figure 44 F).
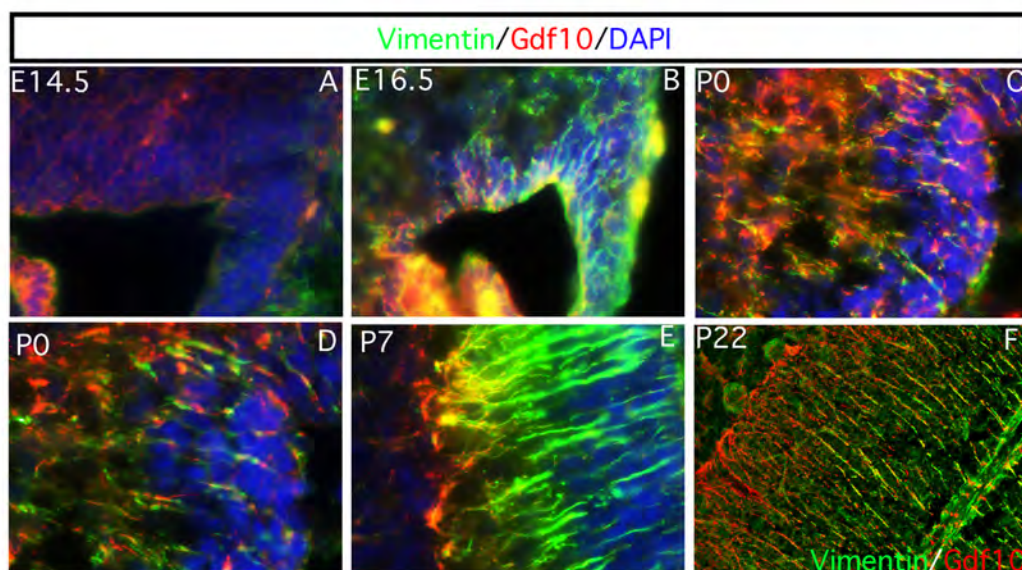
Figure 44: Vimentin expression in *Gdf10* positive Bergmann glial cells. *Gdf10+*/Vimentin+ cells were detected in the ventricular epithelium from E16.5 onwards (B). This co-expression expands similar to the expression of *Gdf10* (C, D) and was maintained until adulthood, where *Gdf10+*/Vimentin+ cells were detected exclusively in the Purkinje cell layer (E, F).

At early postnatal stages *Gdf10+* cells did not colocalize with any of the neuronal markers such as Calbindin (Figure 45 A, B), neuronal- nulcei (NeuN); (Figure 45 C, D) or Gad65/67 (Figure 45 E, F). Since calbindin was not expressed in *Gdf10+* cells, Purkinje cells as potential cell type were excluded. Likewise, interneurons labeled with Gad65/67, did not express *Gdf10.* NeuN, labeling newborn neurons, neither showed colocalization. Therefore a neuronal phenotype of *Gdf10* expressing cells can generally be excluded.
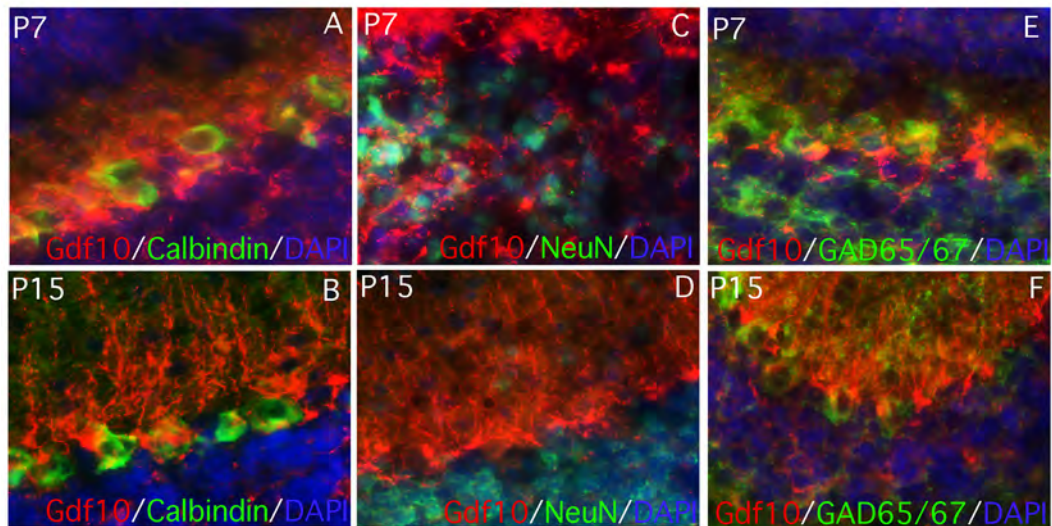
Figure 45: Characterization of *Gdf10* with neuronal markers. *Gdf10* did not colocalize with neuronal markers Calbindin (A, B), NeuN (C, D) and Gad65/67 (E. F).

3.2.3 Tangential vs. radial migration

Analyzing the expression pattern of *Gdf10* it often appeared, that *Gdf10* might expand tangentially from the rhombic lip and roof plate into the whole cerebellum. After proving that *Gdf10* is expressed in Bergmann glial cells, Nestin was used as a marker to follow the migration of this cell type on 150 µm coronal and sagittal sections as well as on whole mount preparations (Figures 46, 47).

After whole mount immunohistochemistry with Nestin at E14.5 it seemed that Bergmann glial cells migrated tangentially similar to what can be observed with granule cells (Figure 46 A – C). Nevertheless, when analyzing sagittal sections, this migration was not observed in any of the sections (Figure 46 F- L), but a possible tangential movement could be attributed to superficial cells that did not have a radial but rather round morphology with short prolongations (Figure 46 J, K). This cell type was found in whole mount embryo preparations (Figure 46 C-E) and coronal sections as well (Figure 46 M- O).

In addition to that, sagittal sections of the most lateral part of the cerebellum showed prolongations reaching the surface of the cerebellum, which appeared as small dark dots (Figure 46 F). These are glial endfeet, which together with the basal lamina, maintain the integrity of the cerebellum (Sudarov and Joyner 2007). Moving slightly medial to sections still containing lateral cerebellum, Bergmann

fibers appeared to extend radially from the ventricular zone towards the pial surface (Figure 46 G, H). These sections also contained the roundly shaped cells with short prolongations, which were *per se* bigger than the Bergmann glial cell bodies (Figure 46 H). Medial sections seemed to have two layers especially labeled with Nestin, the EGL and the ventricular zone (Figure 46 I). This layering disappeared from E15.5 onwards (Figure 47 F).
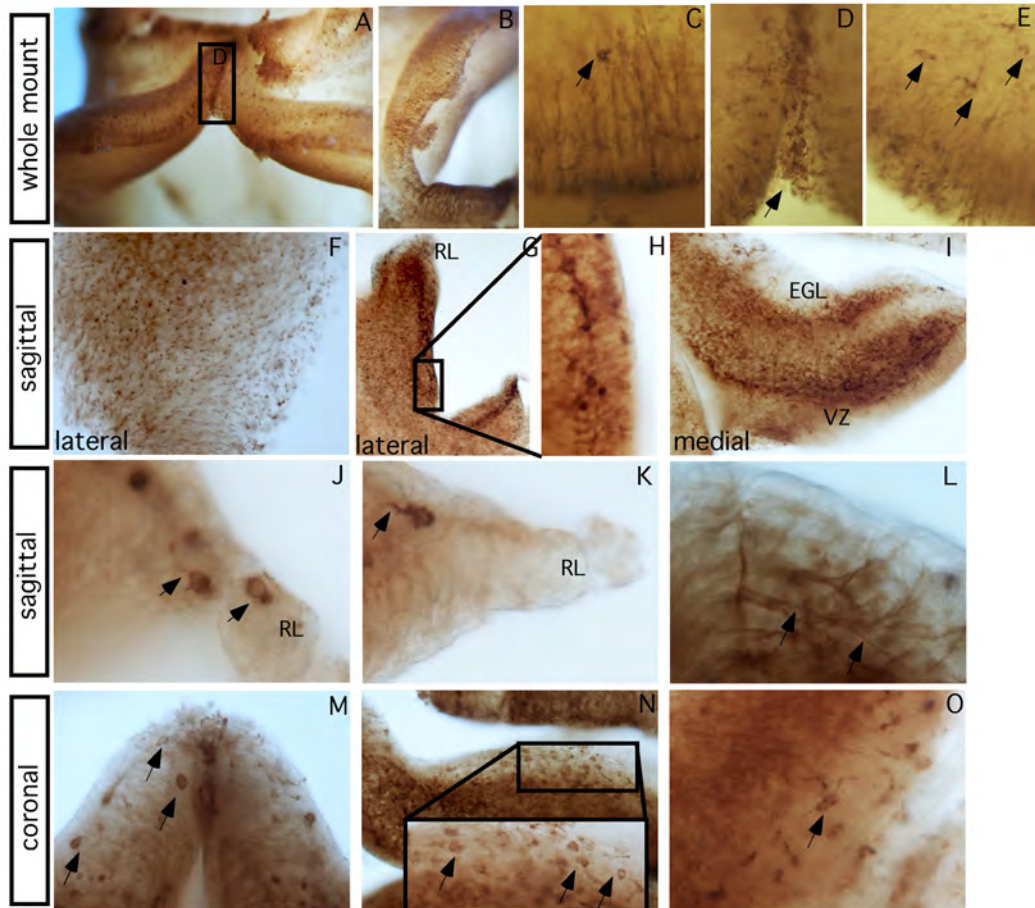
Figure 46: Nestin expression at E14.5 analyzed in whole mount cerebellum (A- E), sagittal sections (F- L) and coronal section (M- O) of 150 µm.

At E15.5 and E16.5 Bergmann fibers reaching the pial surface of the cerebellum appeared at the surface of the whole cerebellum (Figure 47 A- C, I- L). Radial fibers, as observed at E14.5, were no longer visible. But some roundly shaped cells with short prolongations were still present although to a lower amount (Figure 47 D).

More surprisingly was the finding that Bergmann fibers, located in the posterior part of the cerebellum close to the rhombic lip, extended radially following a

progressively more tangential direction to cover anterior cerebellar regions underneath the external granule layer. At different distances from their ventricular origin they made a 90°C (perpendicular) turn to extend through the EGL up to the pial surface (Figure 47 G, H). Due to the size of the sections we were able to follow various cases, which showed this type of migration in the posterior cerebellum. In contrast, Bergmann fibers of the vermis ventricular zone showed the typical radial migration and did not turn in this angle into the EGL.
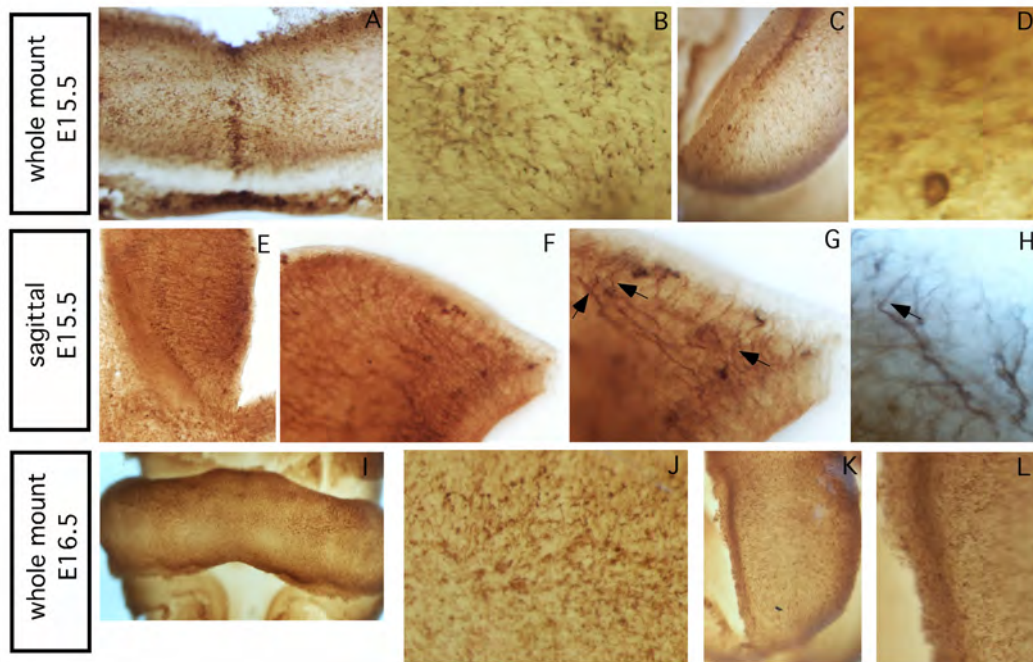
Figure 47: Nestin expression at E15.5 and E16.5 analyzed in whole mount cerebellum (A- D and I- L) and on sagittal sections (E- H) of 150 μm.

3.2.4 Treatment of brain slice cultures with Gdf10 recombinant protein

To investigate the function of *Gdf10* in the development of the cerebellum, E18.5/P0 brain slice cultures were treated with Gdf10 recombinant protein, either by placing Gdf10 soaked beats on top of the cerebellum or by directly applying Gdf10 recombinant protein to cerebellum by pipetting it on top of the slices.

Treatment with Gdf10 soaked beads

After incubating cerebellar brain slices with Gdf10 and PBS (control) soaked beads for 48 hours, the sections were fixed and immunostained with different

antibodies. As illustrated in figure 48 there were no differences between the Gdf10 treated slices and the controls- neither with neuronal markers such as NeuN (Figure 48 A, B) and Calbindin (Figure 48 E, F) nor with the astroglial marker GFAP (Figure 48 C, D). Therefore the experimental design was modified by applying Gdf10 protein to the brain slices directly.
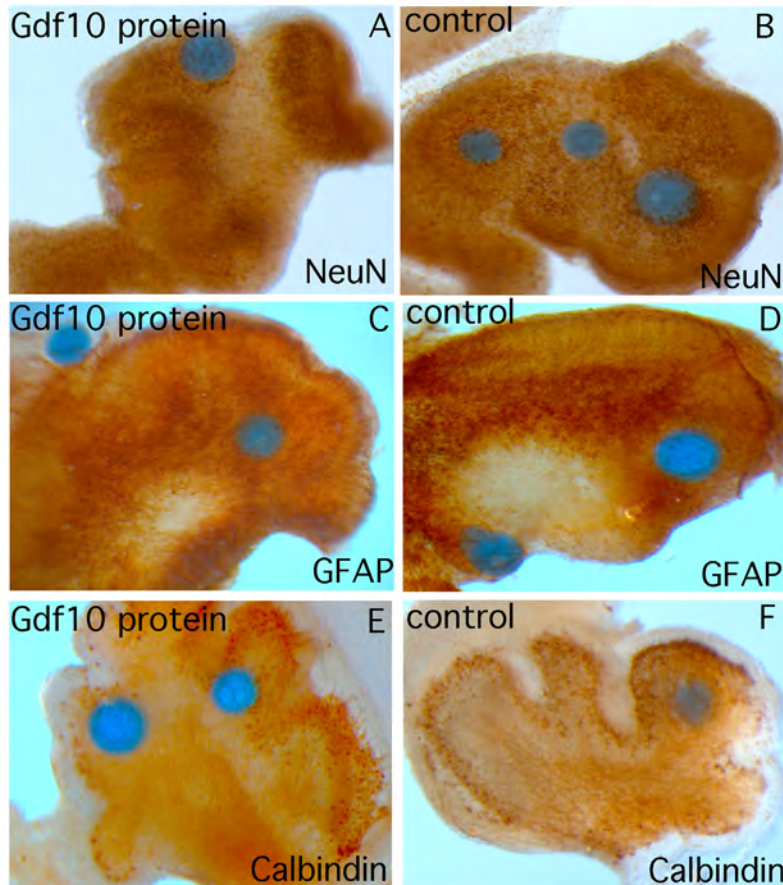
Figure 48: Treatment of brain slice cultures with Gdf10 protein. The treatment of cerebellar cultures with Gdf10 soaked beads did not change the expression of neuronal markers such as NeuN (A, B) and Calbindin (E, F) or the glial marker GFAP (C, D) in comparison to PBS soaked control beads.

Direct application of Gdf10 recombinant protein

After direct application of the recombinant protein, brain slices were incubated for 48 hours. Afterwards they were included in paraffin and cut into 7 µm sections for further immunohistological analysis. No morphological differences, visualized by cresyl violet staining, were observed (Figure 49 A, B). In addition, the treatment with Gdf10 recombinant protein did not appear to influence granule cell migration as analyzed with Pax6 (Figure 49 C, D) nor did it influence cell proliferation as analyzed with Ki67 (Figure 49 E, F).
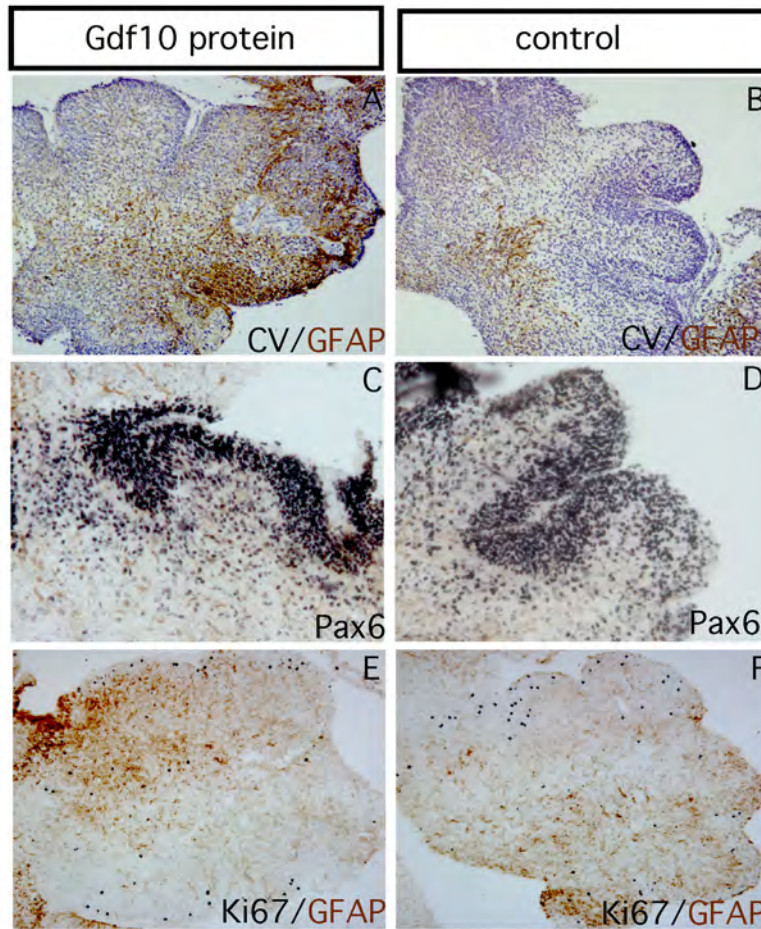
Figure 49: Brain slice cultures with recombinant Gdf10 protein treatment (48h). We did not observe structural differences, as shown by cresyl violet (CV) staining (A, B). In addition the treatment with Gdf10 recombinant protein did not appear to influence granule cell migration as analyzed with Pax6 (C, D) nor did it influence proliferation analyzed with Ki67 (E, F).

3.2.5 Characterization of Gdf10 in Shh mutants

Since recent publications have shown that Gdf10 is reduced in Purkinje cell degeneration mice, the expression in *En1^{cre+}/Shh^{flox/flox}* mice was analyzed. Shh is highly expressed in Purkinje cells and has a significant function in granule cell proliferation (Lewis et al. 2004) and Bergmann glia differentiation (Dahmane and Ruiz i Altaba 1999). The amount of *Gdf10* expressing cells was lower than in wildtype mice and additionally dislocated (Figure 50 B, E). In comparison to the wildtype, where *Gdf10* expressing cells migrate towards the pial surface of the cerebellum (Figure 50 A, D), in the mutants *Gdf10+* cells located in the ventricular epithelium. *Gdf10* expression in the isthmus was maintained in the mutants as observed in wildtype mice of the same age (Figure 50 squares in B and D).
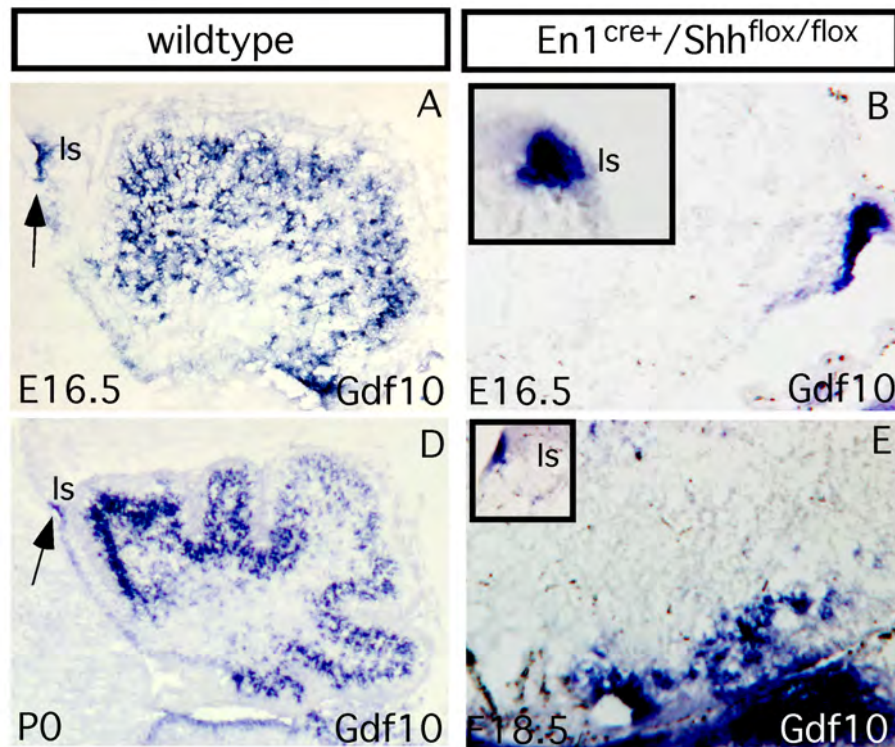
Figure 50: *Gdf10* expression in *En1^cre+^/Shh^flox/flox^* mice. Gdf10 in mutant embryos at E16.5 and E18.5 is expressed in the ventricular zone of the cerebellum as well as in the isthmus. The amount of *Gdf10* expressing cells is lower than in wildtype mice and dislocated (B, E). In comparison to the wildtype, where Gdf0 expressing cells migrate towards the pial surface of the cerebellum (A, D), in the mutants *Gdf10* expressing cells appeared to locate in the ventricular epithelium.

3.2.6 Transcription factor binding sites of Gdf10

Transcription factor binding sites were analyzed with the jasper core vertebra database (http://jaspar.genereg.net/ (Stormo 2000; Wasserman and Sandelin 2004) using the entire gene sequence. The threshold was set to 100%. This search revealed a number of transcription factors with binding sites in the *Gdf10* genome. The most prominent ones are listed in table 7. The order of listing reflects the frequency of occurrence. Databases were additionally searched for more detailed information on each of the transcription factors, which was briefly summarized in table 7. Transcription factors, which are expressed in the cerebellum, are highlighted in grey. For the other transcription factors no information about their expression pattern in the cerebellum was found.

Many of these TFs have been claimed to be involved in proliferation and/ or differentiation such as myeloid zink finger 1 (Mzf1), paired related homebox 2 (Prx2), zink finger E- box binding homebox 1 (Zeb1), Yin- Yang 1 (YY1),

pancreatic and duodendal homebox1 (Pdx1) and breast cancer 1 (BRCA1) (Gaboli et al. 2001; He et al. 2007; Korhonen et al. 2003; ten Berge et al. 2001; Wang et al. 2001; Wilsker et al. 2002; Yen et al. 2001). Two of these transcription factors have been shown to be involved in the regulation of tumorigenesis. Mzf1, which has 19 TFBs in the *Gdf10* genome, has been shown to control proliferation and tumorigenesis (Hromas et al. 1996). The overexpression of Mzf1 inhibits apoptosis and promotes oncogenesis (Gaboli et al. 2001). BRCA1 is a tumor suppressor gene involved in cell proliferation (Eccles et al. 2005; Eccles et al. 2003; Korhonen et al. 2003). It is highly associated with breast cancer, as the name of this TF is already indicating (Southey et al. 2011). This TF is expressed until P10 in the Purkinje cell layer (Korhonen et al. 2003).

Prx2 and Zeb1 play a role in the cellular response to ischemia/ stroke (Bui et al. 2009; Rashidian et al. 2009). Prx2 seems to play an essential role in multiple ischemic injury models (Rashidian et al. 2009), whereas Zeb1 induction is part of the protective response by neurons to ischemia/ stroke (Bui et al. 2009). The expression of Zeb1 is lost during the transition from proliferating precursors to differentiated neural cells (Yen et al. 2001) and might therefore be involved in the initial steps of differentiation of neural cells.

Some of the analyzed TFs, such as AT- rich interactive domain 3A (Arid3a), SPI-B, nuclear receptor erythroid derived 2, like 1 (NRF1), Pdx1 and nuclear receptor subfamily 2, group E, member3 (Nr2e3), are poorly studied in the context of brain development, which makes it difficult to assume parallels to *Gdf10*. But the TF NRF1 stands out of this group due to its expression pattern during development (http://mouse.brain-map.org), which is very similar to the one observed for *Gdf10*. NRF1 is supposed to mediate the apoptotic function of cMyc (Morrish et al. 2003).

The most interesting TF considering glial development is Yin- Yang 1 (YY1). It is expressed in the molecular layer of the cerebellar cortex (Rylski et al. 2008) where it regulates GLAST activity in glial cells and initiates oligodendrocyte differentiation (He et al. 2007).

Table 7: Analysis of transcription factor binding sites (TFBS) located within Gdf10 DNA sequence.

Name	Description	predicted site/ strand	Nr. of TF BS	Function
Mzf1	myeloid zink finger 1	TGGGGA/ -1	19	- increases Fgf2 protein expression in HeLa cells and primary astrocytes (Luo et al. 2009) - overexpression inhibts apoptosis and promotes oncogenesis (Hromas et al. 1996) - controls cell proliferation and tumorigenesis (Gaboli et al. 2001)
Prx2 (Prrx2)	paired related homeobox 2	AATTA / -1	17	- regulates morphogenesis of medial region of the mandibular process - upstream regulator of Shh and controls cell proliferation (ten Berge et al. 2001) - role of Cdk5- mediated phosphorylation of Prx2 in Parkinson´s disease (Qu et al. 2007) - essential role of cytoplasmic cdk5 and Prx2 in multiple ischemic injury models, in vivo (Rashidian et al. 2009)
Zeb1 (delta EF1; Zfhx1a, Tcf8, Areb6, Bzp, Nil2A, Zfhep	zinc finger E- box binding homeobox 1	CACCTG/ -1	12	- Zeb1 induction is part of protective response by neurons to ischemia/ stroke (Bui et al. 2009) - regulated by p53 family member (Bui et al. 2009) - = transcriptional repressor - expressed in the progenitor cells of the ventricular zone around the lateral ventricles (Yen et al. 2001) - loss of Zfhep expression during the transition from proliferating precursors to differentiated neural cells (Yen et al. 2001) - repressed proliferation of either U-138 or U-343 glioblastoma cells (Yen et al. 2001) - may play a role in proliferation or differentiation of neural cells (Yen et al. 2001)
Arid3a	AT- rich interactive domain 3A (Bright like)	ATTAAA/ -1	9	- Arid proteins implicated in control of cell growth, differentiation and development (Wilsker et al. 2002) - required for hematopoetic stem cells and B cell lineage development (Webb et al. 2011) - loss of Bright promotes developmental plasticity (An et al. 2010)
YY1, NF-E1	Yin- Yang 1	GCCATC/ -1	6	- YY1 overexpression in human gliomas and meningiomas correlates with Tgfß1, Igf1 and Fgf2 mRNA levels (Baritaki et al. 2009) - HDACs and YY1 initiate differentiation of oligodendrocytes (He et al. 2007) - expressed in oligodendrocytes and microglia (Rylski et al. 2008) - expression in the cerebellar cortex (in ML in adults) (Rylski et al. 2008) - in the hippocampus expressed in oligodendrocytes (Rylski et al. 2008) - regulates GLAST activity in glial cells (Bergmann glia) (Rosas et al. 2007)
SPIB	Spi-B transcription factor	AGAGGAA / -1	6	- required for human plasmacytoid dendritic development (Schotte et al. 2004) - Epstein barr virus - immune system - not expressed at embryonic stages but from P28

				in PCL (http://mouse.brain-map.org)
GATA3	GATA bindingprotein	AGATAG/ -1	5	- required for survival of embryonic and adult sympathetic neurons but not for their differentiation (Tsarovina et al. 2010) - expression in neurons but no coexpression with GFAP (Zhao et al. 2008) - intergeniculate leaf, ventral lateral – expression in the geniculate nucleus, pretectal nucleus, nucleus of the posterior commissure, superior colliculus, inferior colliculus, periaqueductal grey, substantia nigra and raphe nuclei (Zhao et al. 2008) - plays a major role in the development of the serotonergic neurons (Hikke van Doorninck et al. 1999) - acts downstream of Hedgehog in the development of serotonergic raphe neurons (probably conserved mechanism) (Teraoka et al. 2004) - downstream effector of Hoxb1 specification in rhombomere 4 (Pata et al. 1999) - weak expression in the PCL, possibly in Purkinje cells (http://mouse.brain-map.org)
NRF1, Lcrf1, TcF11 Nfe2ll	nuclear receptor, erythroid derived 2, -like1	CATGAC/ -1	5	- cMyc apoptopic function is mediated by NRF1 target genes (Morrish et al. 2003) - similar expression pattern to Gdf10 in the developing cerebellum (http://mouse.brain-map.org)
Pdx1	pancreatic and duodendal homeobox1	CTAATT/ -1	4	- expressed in climbing fibers (Song et al. 2010) - regulates Pax6b in zebrafish (Delporte et al. 2008) - defines pancreatic gene expression pattern and cell lineage differentiation (Wang et al. 2001)
Nr2e3	nuclear receptor subfamily 2, group E, member 3	CAAGCTT/ -1	3	- photoreceptor, regulates axonal guidance and cell identity in Drosophila (Lin et al. 2009) - weak expression in the PCL, possibly in Purkinje cells (http://mouse.brain-map.org)
BRCA1	breast cancer 1	ACAACAC/ -1	2	- required for embryonic development of the mouse cerebral cortex to normal size by preventing apoptosis of early neural progenitors (Pulvers and Huttner 2009) - might modulate neuronal cell cycle re-entry in Alzheimer´s disease (Evans et al. 2007) - BRCA1 mutation causes neuronal migration defects (Eccles et al. 2005; Eccles et al. 2003) - tumor suppressor gene expressed in embryonic and neural stem cells and involved in cell proliferation (Korhonen et al. 2003) - at embryonic stages, expressed in the EGL (www.eurexpress.org) - expressed in Purkinje cell layer until P10 (Korhonen et al. 2003)

4 Discussion

4.1 The Origin of cerebellar oligodenroglia

Previous works of this and other laboratories (Cobos et al. 2001; García-Lopez and Martínez 2010; Leber and Sanes 1995; Olivier et al. 2001; Pérez-Villegas et al. 1999) have shown that oligodendrocyte precursor cells (OPCs) arise from multiple restricted regions of the ventricular neuroepithelium from the spinal cord to the telencephalon. In the spinal cord, they originate close to the ventral midline, during a brief time-window around E14 in rat embryos (Noll and Miller 1993; Pringle and Richardson 1993). Although during the early stages of their migration they migrate radially, retroviral tagging experiments have demonstrated in chick embryos that, once hatched, these precursor cells can be encountered in the white matter several segments rostrally to their proliferation site, clearly showing that they also migrate tangentially along the antero- posterior axis of the spinal cord (Leber and Sanes 1995; Leber et al. 1996). In contrast, in the rhombencephalon the rostro-caudal distribution of the oligodendrocytes seems to be restricted to the rhombomere of origin (Pérez-Villegas et al. 1999). The situation is quite different in the diencephalon and telencephalon. In the former, quail/chick chimeras have shown that diencephalic oligodendrocytes emerge from a common neuroepithelial domain in the basal plate of prosomere 1 (the

parabasal band) and migrate tangentially, invading the dorsal regions of the diencephalic prosomeres (García-Lopez and Martínez 2010). In the telencephalon, also using chimeras, it has been demonstrated that oligodendrocyte precursors emerge from the medial subpallium and entopeduncular areas, and migrate tangentially to colonize the entire telencephalon (Olivier et al. 2001). These data allows us to conclude that oligodendrocyte precursors have their origin in restricted foci of the ventral region of the ventricular neuroepithelium (parabasal band), at a distance from their ultimate terminal domains, and that these precursor cells frequently follow a tangential migration across metameric borders to reach their final destinations.

Nevertheless, the picture of the origin of oligodendrocytes and their migration is not complete since a large CNS territory still remains partially unexplored, namely the cerebellum and its metencephalic vesicle of origin. Indeed, the use of the monoclonal antibodies O1 and O4, markers of early oligodendrocytic lineage, left the impression that cerebellar OPCs had their origin in the medial ventricular zone of E5 chick ventral metencephalon (Ono et al. 1997). However, more recent data obtained from transgenic mouse embryos with *Ascl1* inactivation indicates that this transcription factor is required for OPC maturation, since in the mutant cerebellum the number of OPCs is greatly reduced (Grimaldi et al. 2009). More importantly, transplantation and electroporation experiments in these mutant mice have provided indirect data indicating that while all GABAergic interneurons, which also require *Ascl*1 for their maturation, originate from the primitive cerebellar neuroepithelium, most, if not all, of the cerebellar OPCs were produced in extracerebellar locations. These latter OPCs reached the cerebellar anlage during embryonic life, and by E14.5 they were already present in the cerebellum (Grimaldi et al. 2009). However, the precise site of origin of these oligodendrocytes, their pathways to enter the cerebellum and their mode of migration are not known. The results reported in this work are aimed to fill this gap.

4.1.1 The mesencephalic parabasal band, major site of origin of cerebellar oligodendrocytes

The use of quail/chick chimeras demonstrated that cerebellar oligodendrocytes originate from the parabasal band of the mesencephalic neuroepithelium. This data, therefore, supports the following generalizations; first, the parabasal band

of the neural tube is the major locus of proliferation and differentiation of OPCs. Second, OPCs, with the exception of those emerging from the rhombencephalon, migrate for long distances, mostly by tangential migration, to populate their final domains.

The relatively recent discovery that Nkx2.2 was expressed in oligodendrocytes of the spinal cord in a biphasic pattern, each one associated with a distinct function in the development of these macroglial cells (Fu et al. 2002; Qi et al. 2001) favors the idea that this transcription factor is important for the acquisition of the oligodendrocytic phenotype. This hypothesis has been verified with a study using Nkx2.2-null mutants. In the latter, the differentiation of MBP-positive and PLP-DM20- positive oligodendrocytes is dramatically retarded along the entire rostro-caudal axis of the spinal cord, whereas the loss of Nkx2.2 has no effect on astrocytic differentiation (Qi et al. 2001). Thus, Nkx2.2 appears to be an excellent marker to identify cells fated to become oligodendrocytes. With this marker, Fu et al. have shown that oligodendrogenesis in the chicken midbrain commenced at approximately E6 (Fu et al. 2003), when Olig2+ OPCs begin to emerge from the Nkx2.2+ neuroepithelial cells in the ventro-lateral positions of the midbrain, similarly to what happens in the spinal cord and hindbrain. At this stage of development, the authors did not detect Olig2+ OPCs in the lateral or dorsal midbrain. Furthermore, the authors claimed that at later stages (E11), OPCs could also be generated from the ventricular and subventricular zones of the dorsal mesencephalon, where the emerging Olig2 positive OPCs start their Nkx2.2 expression as soon as they leave the ventricular neuroepithelium (Fu et al. 2003). Although these authors did not further investigate the final location of OPCs expressing Nkx2.2, neither those arising from the dorsal nor from the ventral neuroepithelium, their results provide additional support for the data obtained here with the quail/chick chimeras, and corroborate the possibility of a ventral mesencephalic origin of cerebellar OPCs.

Finally, the possibility that cerebellar oligodendroglia had not only a ventral but a dorsal origin too, as it is the case in the spinal cord (Kessaris et al. 2006) and forebrain (Olivier et al. 2001; Pérez-Villegas et al. 1999) remains opened, and the results discussed above on the late (E11) generation of dorsal mesencephalic OPCs (Fu et al. 2003) are very much in favor of this possibility. The advantage of this multiplicity of sources is that dorsally and ventrally derived OPCs could compensate for each other in the case of brain damage and/or disease, as

already shown for the telencephalon and the spinal cord (Kessaris et al. 2006; Vallstedt et al. 2005). The frequent specification of oligodendroglial precursors in the basal or parabasal domains has been closely related to the inductive activity of Shh signaling (Oh et al. 2005). The molecular mechanisms underlying this focal specification of cerebellar oligodendroglial progenitors in the parabasal mesencephalic neuroepithelium also remains to be elucidated, although the hindbrain choroid plexus could palliate the notochord for the production of Shh (Huang et al. 2009).

4.1.2 Cell fate analysis

In rodents, it is well known that progenitor cells migrating through the white matter of the cerebellum give rise to cortical interneurons, astroglia, and oligodendroglia (Milosevic and Goldman 2002; Milosevic and Goldman 2004). Since the GABAergic interneuronal progenitors proliferate in the white matter while migrating and express the transcription factor Pax2 as well as GAD67 (Maricich and Herrup 1999), we also analyzed to discard the possibility that part of the donor cells could be GABAergic interneurons. However, neither Pax2 positive nor GAD positive cells co-localized with the quail nuclear marker. Therefore, all identified donor cells in the host cerebellum were exclusively macroglial cells, regardless of the cortical layer in which they were located. Both types of macroglial cells (astrocytes and oligodendrocytes) were identified among the donor cells entering the cerebellum, although the vast majority were of oligodendrocytic nature, while several donor cells co-localized with the astrocytic marker S100, or the radial glia marker Vimentin, expressed by Bergmann fibers and immature astrocytes (Bovolenta et al. 1984). Both were detected in the white matter tracts as well as in the granule cell layer, the Purkinje cell layer and the molecular layer. There is also evidence that S100 is expressed in a subpopulation of oligodendrocytes in rats (Richter-Landsberg and Heinrich 1995; Rickmann and Wolff 1995) and in three month-old Japanese quail's CNS (Castagna et al. 2003). This includes the possibility that some of the S100 expressing donor cells in the white matter could actually also be of oligodendrocytic nature. More importantly, quail cells in the molecular layer, granule cell layer and white matter expressed Olig2 or PLP, corroborating that they are OPCs or oligodendrocytes. The fact that they belong to the oligodendrocytic lineage also explains the high amount of donor cells (up to 51%) present in the white matter, both at the folial axes and the central white matter.

The identification of the two types of macroglial cells (oligodendrocytes and astrocytes) together with radial glial cells and Bergmann fibers among the grafted quail cells seems to indicate that multipotent neural stem cells might have been originated in the grafted quail neuroepithelium, and that since they are pluripotent cells, are capable of giving rise to oligodendrocytes and astrocytes. Indeed, in 2005 Lee and collaborators have shown that the murine postnatal cerebellum contains multipotent neural stem cells, expressing prominin-1 (CD133). However, an important difference seems to exist between the prominin-1 positive stem cells and the bipotent cells found in our chimeras: the former are at the origin of neurons (GABAergic interneurons), astrocytes and oligodendrocytes; whereas the latter only generate macroglial cells (astrocytes and oligodendrocytes) since we haven´t seen neither Pax2+ nor GAD65+ interneurons. Recent findings claim that Bergmann glial cells might be the stem cells of the cerebellum generating at least 30% of basket and stellate GABAergic interneurons in the molecular layer up to P12, and thereafter give rise only to macroglial cells (Silbereis et al. 2009). Since the populations of cells that were detected within the group of donor cells were oligodendrocytes and astrocytes, the extracerebellar-generated Bergmann glial cells do not have the pluripotency required to be considered as stem cells. Nevertheless, our results do not exclude the possibility that Bergmann glial cells of cerebellar origin, or some specific categories of these cells, might have stem cell-like properties and give rise to neurons. The significant structural and functional differences between OPCs and Bergmann glia suggest that different progenitors are originated in the mesencephalic epithelium, but specific experiments are necessary to address this question.

4.1.3 The velum medullare, the route of entry of oligodendrocyte precursors into the cerebellum

The possibility that the velum medullare could be the route of passage for OPCs from the mesencephalon to the cerebellum has already been proposed more than 20 years ago (Reynolds and Wilkin 1988). These authors only reported some indirect evidence based upon the fact of a high density of G_{D3} positive cells (a marker of immature oligodendrocytes) in the subependymal layers of the 4th ventricle: the inferior colliculus as well as in the superior velum medullare and the cerebellar peduncles; previously to the occurrence of OPCs in the deeper regions of the cerebellum of the rat at birth. The direct evidence reported in the present study in favor of the velum medullare being the door for the cerebellar entry of

extracerebellar oligodendrocytes can be reinforced by the study of the expression pattern of Nkx2.2, which is strongly expressed in the mesencephalic parabasal band, here identified as the site of origin of cerebellar oligodendrocytes. The distribution of Nkx2.2 expressing cells parallels the migratory route of QCPN+ donor cells in their entry to the cerebellum via the velum medullare and folium I. Furthermore, the time point at which donor cells were detected for the first time in the cerebellum (E9) coincides with the expansion of Nkx2.2+ pre-isthmic band to the velum medullare and subsequently to the cerebellum (HH38/12 days), suggesting that the pre-isthmic band may be a permissive substrate to guide parabasal mesencephalic OPCs towards the cerebellum. Figure 51 summarizes the migratory behavior of donor cells at developmental stage E5, when OPCs start their migration towards the cerebellum and E12 when a great number of oligodendrocytes have already reached and entered the cerebellum.

4.1.4 Migratory routes

There are some indirect evidences that oligodendrocyte precursors might migrate towards their final destinations along pre-existing axonal tracts, mainly due to the tight temporal correlation between the migration of OPCs and the formation of fiber pathways in the cerebellum. Using anterograde axonal markers, it has been shown that spinocerebellar fibers originated in the lumbar spinal cord enter the prospective white matter of the anterior lobe by E10; by E12, the number of these fibers increases significantly in the inner granular layer (Okado et al. 1987). Somewhat earlier, climbing fibers should also reach the cerebellum, since they are present in the Purkinje cell plate by E10, and by E14 they already form their characteristic pericellular nests around the Purkinje bodies (Chédotal et al. 1996). In quail- chick transplants it became clear that the majority of donor cells migrates towards the cerebellum but does not enter it until developmental stage HH35 (9 embryonic days), when the climbing and mossy fibers have already spread within the cerebellar parenchyma. Thus, the first QCPN+ cells reach the cerebellum at E9. The DiI labeling experiments show that OPC migration through the velum medullare does happen at E9 (HH35), simultaneously with the spread of extracerebellar afferent fibers throughout the presumptive white matter, suggesting that oligodendroglial mesencephalic precursors could reach the central white matter of the cerebellum through folium I, and migrate to the cortex along climbing and mossy fibers.
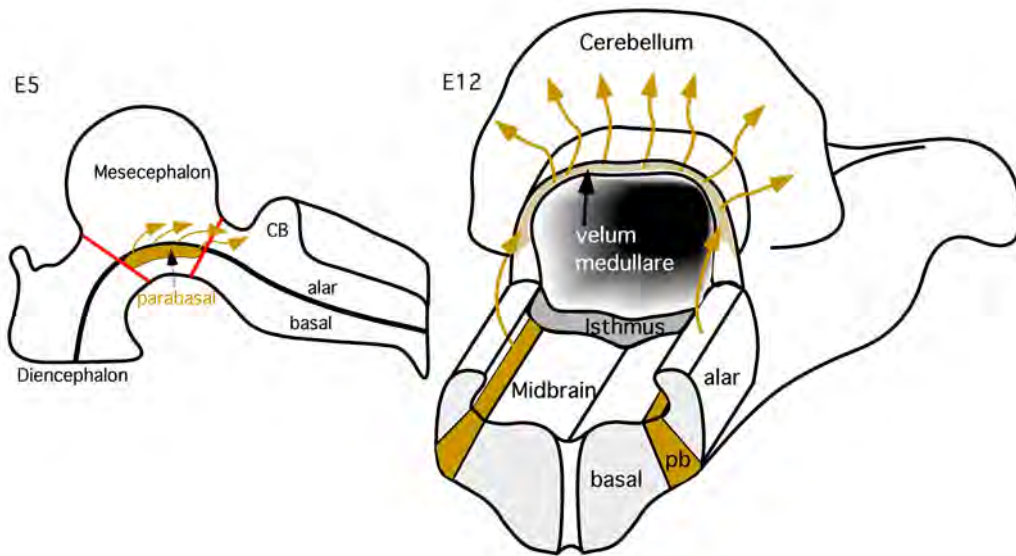
Figure 51: Rostro- caudal migration of oligodendrocytes from the mesencephalic parabasal plate into the cerebellum. Schematic representation defining the origin of cerebellar oligodendroglia in the parabasal plate of the mesencephalic vesicle. Transplanting this area results in a strong migration towards the cerebellum, which becomes apparent at around E5 of the chicken embryonic developmental. The first oligodendrocytes reach the cerebellum at E9. At about E12 a large number of donor cells are present in the velum medullare and, particularly in the cerebellum, entering via folium I (CB = cerebellum, pb = parabasal); (Mecklenburg et al. 2011)

4.2 *Gdf10* in the development of Bergmann glial cells

In the second part of this work it was demonstrated that *Gdf10* is highly expressed in the mouse cerebellum. The expression pattern in this region was characterized in detail by *in situ* hybridization and by cell fate analysis during embryonic and postnatal stages. The results of co-labeling analysis with glial markers from E14.5 onwards demonstrated that *Gdf10* labeled Bergmann glial cells from the moment they appear, around E14 (Sudarov et al. 2011), until adulthood.

4.2.1 The expression pattern of Gdf10 in the cerebellum indicates different routes of glial migration

Anteriorly, *Gdf10* expression was restricted to the developing vermis, the rhombic lip and the nearby VZ. Posteriorly, *Gdf10* labeled the entire cerebellum including the ventricular zone, the intermediate zone and superficial layers. Apart from the radial expansion of the expression from the VZ, *Gdf10* positive cells were observed beneath the EGL, which appeared to migrate tangentially from the rhombic lip and neighboring territories.

This type of migration, which typically is observed in granule cells originating from the rhombic lip (Englund et al. 2006; Gilthorpe et al. 2002; Wingate 2001), was recently observed in Purkinje cells as well (Miyata et al. 2010). The authors claim that Purkinje cells initiating the Purkinje plate formation at E14.5 are born in the posterior VZ at E10.5 and migrate tangentially in the lateral cerebellar primordium. Furthermore they suggest a potential role for glial cells in this type of migration due to the observed orientation of Nestin+ fibers and the movement of cells belonging to the glial cell lineage between E15.5 and E18.5 (Miyata et al. 2010).

In this study two different migratory pathways were observed, a simple radial migration as has been described for many years (Yamada and Watanabe 2002); (Figure 53 illustrated in blue) and a slightly different migration, which is divided in relation to the cellular orientation and the pial surface into a primary radial migration and a secondary perpendicular migration, of *Gdf10+* cells originating from the ventricular zone adjacent to the rhombic lip (Figure 53 illustrated in red).

Initially, in whole mount preparations of E14.5 embryos stained with Nestin, a putative tangential oriented extension of Bergmann fibers seemed to originate from the VZ adjacent to the rhombic lip. Analyzing the expression pattern of *Gdf10* after whole mount *in situ* hybridization also supported this idea. *Gdf10* at E15.5 and E16.5 was detected in Math1-expressing cells, a transcription factor that specifically labels granule neurons (Louvi et al. 2003); (Figure 52 A, B). In contrast, *Gdf10* at the same developmental stage did not share the same expression pattern as ROR alpha, expressed in Purkinje cells, illustrating the expansion of cells originating from the VZ of the 4th ventricle (Figure 52 C, D).

Nevertheless, the tangential migration of Bergmann glial cells was not observed in sagittal sections of E14.5 embryos. Furthermore, from E15.5, the pial surface of the cerebellum was covered with glial end-feet, whose origin was not observed in directly related underneath cellular strata, suggesting that the glial fibers, observed at E14.5, were located more profoundly under the developing EGL and extended to the EGL from E15.5.
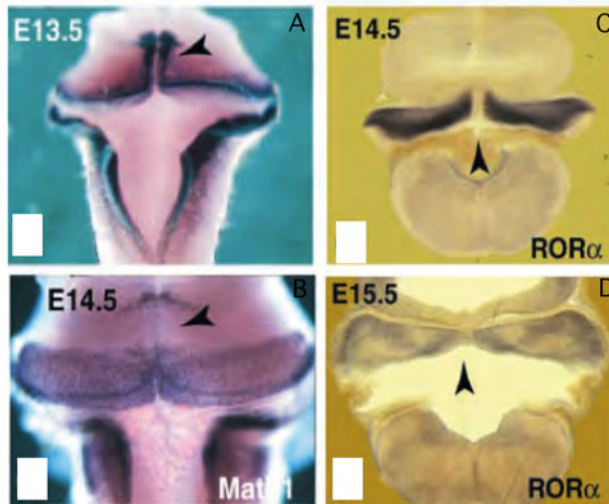
Figure 52: Expression of Math1 (A, B) and ROR alpha (C, D) between developmental stages E13.5 and E15.5 in the cerebellum. Adopted from Louvi et al 2003.

These findings suggest a new type of radial glia orientation and subsequent migration of Bergmann glia precursors. The careful analysis of 150 μm sagittal sections of E15.5 embryos revealed that pial extensions of caudal radial glia first followed a tangential direction turning progressively 90º to reach the pial surface after a transversal superficial segment. Then, the migration guided by these radial axes can be divided into a primarily radial migration followed by a turn in perpendicular direction towards the EGL. Both modes of migration are summarized in figure 53. The rhombic lip is highlighted in green, the medial ventricular zone, labeled by *Gdf10,* is shown in blue, whereas the *Gdf10+* ventricular zone adjacent to rhombic lip is highlighted in red.
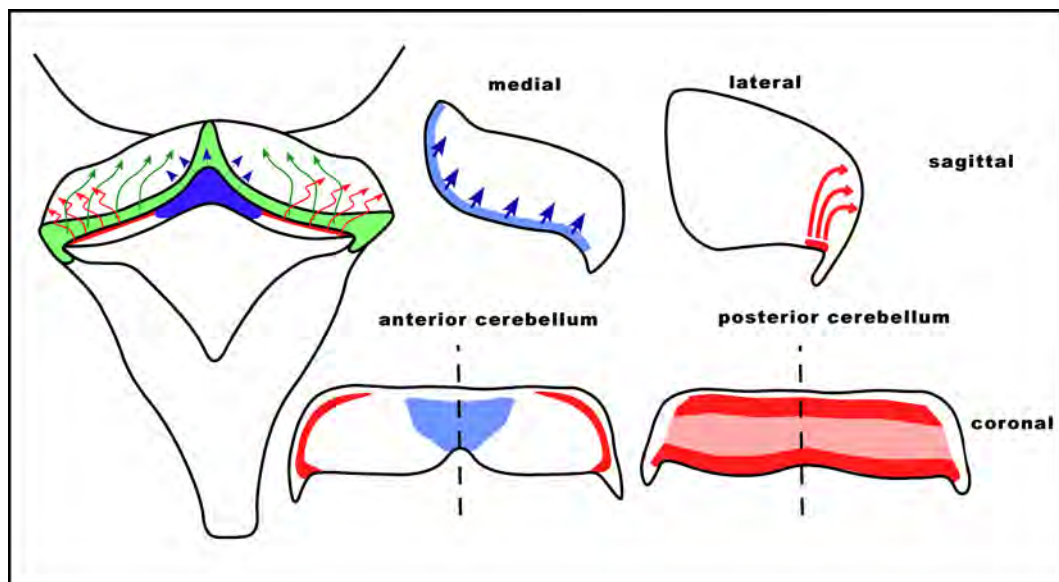
Figure 53: Summary of the observed expression pattern of *Gdf10* during embryonic development in a whole mount embryo at E16.5 as well as on sagittal sections of medial and lateral cerebellum and anterior and posterior coronal sections of the cerebellum.

Bergmann glial cells move their cell body along their fibers until they reach their final destination (Yamada and Watanabe 2002). The Bergmann fibers in the posterior region of the cerebellum have a shorter distance to travel to reach the pial surface than for example fibers originating from the medio- lateral ventricular zone of the cerebellum. Therefore their cell bodies are the first to reach the posterior region of the Purkinje cell plate.

This was observed in Purkinje cells as well. Miyata and colleagues claimed that Purkinje cells, which initiate the Purkinje plate formation at E14.5, are born in the posterior VZ at E10.5 and migrate tangentially in the lateral cerebellar primordium. Furthermore, they suggest a potential role for glial cells in this type of migration between E15.5 and E18.5, which are possibly migrating tangentially as well (Miyata et al. 2010).

Even though Purkinje cells appeared to migrate tangentially, they most likely migrate radially along the Bergmann fibers, which topologically represent the radial direction independently of secondary morphogenetic curvatures, and finally make the same perpendicular turn as Bergmann glial cells. Due to the structure of the posterior cerebellum, influenced by a strong wave of granule neurons originating from the rhombic lip, this migration may appear tangential.

4.2.2 The external granule cell layer- a possible migratory route for intermediate progenitors

The analysis of the extension of Bergmann fibers also revealed a tangentially oriented migration of cells, with a round morphology and short prolongations expressing Nestin. Nestin is a very prominent marker for stem cells, and is responsible for their self- renewal (Mignone et al. 2004; Park et al. 2010). Apart from Nestin positive radial/ Bergmann glial cells another subtype of Nestin positive cells was present in the rhombic lip and appeared to migrate tangentially in the EGL. In whole mount cerebellar preparations as well as in sagittal and coronal sections they were visible at the pial surface at E14.5, E15.5 and E16.5. This cellular population, although disperse could represent superficially migrating progenitors moving tangentially towards lateral and anterior cerebellum inside the EGL.

Until today, little is known about stem cells and glial precursors in the cerebellum. Investigations about the stem cell potential of astroglia started recently and focused mainly on postnatal development (Sievers et al. 1994; Silbereis et al. 2009; Silbereis et al. 2010). A recent publication demonstrated that astroglial cells in the EGL generate a subset of granule cells (Silbereis et al. 2010). The authors conclude that glial cells function as neuronal precursor cells. In an earlier publication they additionally demonstrated that GFAP+ cells transiently generate GABAergic interneurons in the postnatal cerebellum (Silbereis et al. 2009) indicating a multipotency of these astroglia. Whether or not this type of pluripotent astroglia can be characterized by the expression of specific proteins, distinguishing them from other astroglia, has not yet been analyzed. Even though these results were obtained from studies at postnatal stages and do not explore the origin of these progenitor cells along cerebellar development, they support the idea of the presence of progenitor cells in the EGL.

Similar results have been described in hamster by Sievers and collegues in 1994 (Sievers et al. 1994). In this study they first detected a Vimentin positive, but S100 and GFAP negative primordial glial scaffold in the cerebellum. With the formation of the EGL, a few GFAP positive cells appeared among the unstained EGL of the caudalmost part of the EGL, proliferating adjacent to the basement membrane. This expression expanded to the rostral EGL. At later stages the EGL cells also expressed S100. Subsequently, GFAP and S100+ cells were detected in the Purkinje cell layer, considered to be Bergmann glia (Sievers et al. 1994). These results are in favor of the idea that potential stem cells originate from the rhombic lip migrating among granule cells of the EGL to their final destination and that these cells may actually be astroglia.

The earliest study investigating this issue is the analysis of S100B expression in E13.5 mouse embryos. S100B is expressed in the rhombic lip as well as the EGL from E13.5 onwards (Figure 54), coinciding with the time Bergmann glia appear (Sudarov et al. 2011; Yamada and Watanabe 2002). Some of the S100B+ cells expressed Pax6. The authors concluded that the transient activation of the S100B gene distinguishes granule neuron precursors from all other types of precursors that have been identified so far in the rhombic lip (Hachem et al. 2007).
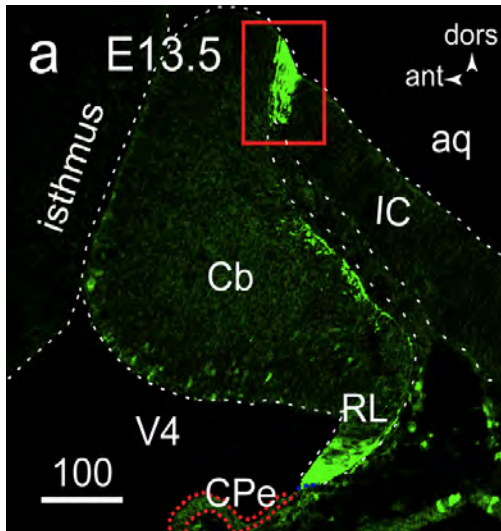
Figure 54: Pattern of *S100B* gene expression in the cerebellum and inferior colliculus before midline fusion of the cerebellar plates (E13.5). Adopted from Sudarov et al. 2011)

Nevertheless the authors do not discuss the presence of S100B+/ Pax6- cells in a territory predominantly occupied by granule precursors and granule neurons.

From the glial cell specification in the forebrain we know that during gliogenesis the radial glia produce intermediate progenitor cells and oligodendrocyte precursors, which in turn give rise to neurons and oligodendrocytes (Figure 55). In addition, radial glia can also differentiate to astrocytes and produce ependymal cells (Rowitch and Kriegstein 2010).
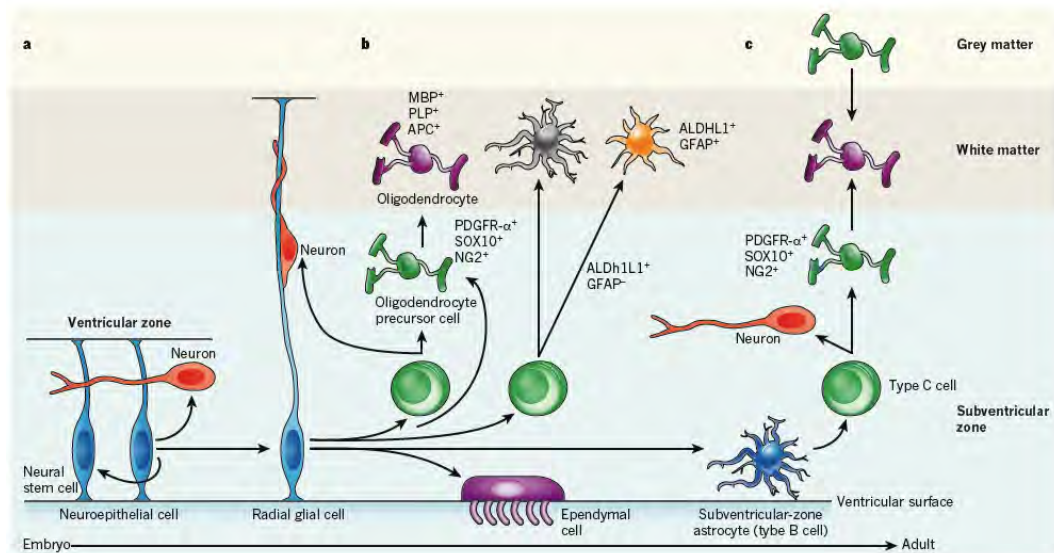
Figure 55: Patterns of gliogenesis in embryonic and adult progenitor zones. The progression from the embryo to the adult is shown from left to right (**a** to **c**). Black arrows indicate self-renewal or differentiation from one cell type to another. Mature and progenitor markers are listed. **a**, Self-renewing neuroepithelial cells line the ventricles throughout the neuraxis at the stages of neural tube closure. These cells are capable of generating neurons. Neuroepithelial cells are transformed into radial glial cells as neurogenesis begins. **b**, Radial glia produce intermediate progenitor cells and oligodendrocyte precursor cells (OPCs), which in turn produce neurons and oligodendrocytes, respectively. Radial glia can also become astrocytes, as well as intermediate progenitors that expand in number before producing astrocytes. Protoplasmic astrocytes and fibrous astrocytes might arise from common or independent progenitors. Radial glia also produce ependymal cells. **c**, In adults, oligodendrocytes are produced by two independent pathways: type B cells in the cortical subventricular zone produce transit-amplifying cells (known as type C cells), which in turn produce OPCs as well as neurons. The OPCs subsequently generate oligodendrocytes, and OPCs that are already resident in the grey matter also produce oligodendrocytes. ALDH1L1, aldehyde dehydrogenase 1 family, member L1; APC, adenomatous polyposis coli; GFAP, glial fibrillary acidic protein; MBP, myelin basic protein; PDGFR-α, platelet-derived growthfactor receptor-α; PLP, proteolipid protein 1. All green cells are intermediate progenitors, with type C cells being a subset of these, and all blue cells are neural stem cells (even though each blue cell is a different type). Adopted from **(Rowitch and Kriegstein 2010)**

The hypothesis for the Nestin-positive, roundly shaped cells observed in the rhombic lip and the EGL is that these cells are probably intermediate progenitors, originating from radial glia located in the rhombic lip. These progenitors would subsequently migrate in the EGL and later differentiate into neurons and astrocytes. This hypothesis raises two questions. First of all, are radial glial cells located in the rhombic lip? And second, do they follow a similar differentiation mechanism as radial glia located in the pallium/ cortex of the telencephalon?

In the literature there are numerous references concerning astroglial progenitor cells in the EGL, which has been discussed above. However, apart from the expression of the Bergmann glial marker Gdf10, the astroglial marker S100B (Sudarov and Joyner 2007) and the radial glial markers Sox2 and Blbp are also expressed in the rhombic lip (Huang et al. 2010); (Figure 56), strongly implying the presence of radial glia in the rhombic lip.

This has never been commented or discussed in any of articles reviewed for this work, but answers the question about the presence of radial glia in the cerebellar rhombic lip. From the Richard Wingate's point of view, who highly contributed to the characterization of the cerebellar rhombic lip and its derivatives, the rhombic lip territory is not specified early in embryonic development. The induction of the rhombic lip is rather a result of an ongoing interaction between neural tube and non-neural roof plate ectoderm (Wingate 2001). He proved that only precursors that are in contact with the roof plate could generate migratory derivatives (Wingate 2001; Wingate and Hatten 1999). Moreover, he concludes that the

rhombic lip, although being a spatially discrete epithelium, never constitutes a developmentally defined compartment (Wingate 2001).
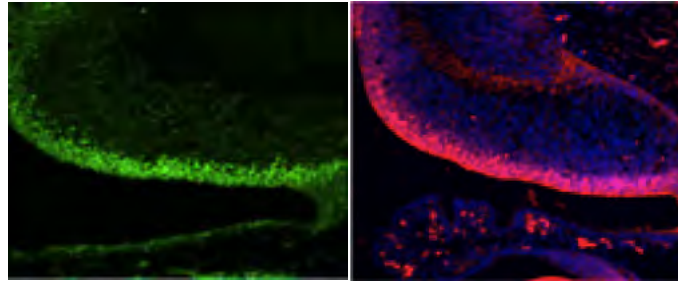
Figure 56: Sox2 (Green) and Blbp (red) expression in the cerebellum of E13.5 mouse embryos. (Huang et al. 2010)

Addressing the second question, whether or not the radial glial in the rhombic lip follow similar differentiation mechanisms as that observed in the telencephalon, can only be answered hypothetically for now. However, assuming that gliogenesis in the cerebellum is similar to the gliogenesis observed in the forebrain, Gdf10 in the rhombic lip might be a key regulator promoting the production of intermediate progenitor cells, which later differentiate into different astroglial and neuronal cell types. *Gdf10* expression starts at the time radial glia are converting into Bergmann glia (Yamada and Watanabe 2002) and might at the same time also induce the production of intermediate progenitors mediated by the radial glia in the rhombic lip. Even though extensive studies are necessary to address this issue, the obtained results of this work might be one possible starting point for further investigations.

Alcaraz and colleagues studied the 30-zinc finger transcription factor Zfp423 in cerebellar development and found that the loss of this transcription factor decreased proliferation by granule cell precursors in the EGL especially near the midline and leads to an abnormal differentiation and migration of Bergmann glia, which is accompanied by a reduction of *Gdf10* expression at the lateral edges of the cerebellum (Alcaraz et al. 2006). The authors identified precursors in the EGL by labeling them with BrdU, Ki67 and DAPI, which doesn't necessarily mean that all of them are granule cell precursors as discussed above. Hence, the observed precursor reduction may include astroglial precursor cells as well. The authors detected midline defects and abnormal migration in the lateral edges of the cerebellum. The observed regional defects coincide with the expression of *Gdf10* along the midline and in the lateral cerebellum. The reduction of Gdf10

due to the loss of Zfp423 leads to abnormal glial differentiation and migration. This supports the idea that Gdf10 is initiating the transition from radial glia to Bergmann glia cells in the ventricular epithelium of the cerebellum, which would lead to an abnormal differentiation and migration of these cells. Furthermore, the diminished proliferation of precursors in the EGL is also in favor of the hypothesis that Gdf10 might be involved in the production of intermediate precursors in the rhombic lip.

4.2.3 Functional studies with Gdf10 recombinant protein

To investigate the functional mechanisms of Gdf10, E18.5/ P0 brain slice cultures were treated with recombinant Gdf10 protein and analyzed by immunohistochemistry with a variety of neuronal and glial markers.

Bergmann glial cells are thought to produce a factor that antagonizes the proliferation of the external granular layer (EGL) cells induced by Shh, causing them to exit the cell cycle, migrate inwards along glial fibers and differentiate as granule neurons (Dahmane and Ruiz i Altaba 1999; Hatten 1999). In brain slice cultures of P0 cerebellum that have been treated for 48 hours with Gdf10 recombinant protein, no significant changes in the composition of the EGL, nor changes in the expression of Pax6, were observed. Also, proliferation analysis in these cultures with Ki67 did not reveal any significant changes. Conclusively, this would mean that Gdf10 is not involved in the differentiation of granule cells of the EGL. However, another possibility is that either the concentration of the protein was inadequate, or that the chosen developmental stage was too late in development. Despite the absence of any significant modification in these parameters we can't rule out these alternatives and this experiment needs to be modified in order to prove the validity of these results.

A possible mechanism underlying Bergmann glial development could be Shh signaling. Purkinje cells constantly secrete Shh and therefore induce Bergmann glia differentiation (Dahmane and Ruiz i Altaba 1999). The exact mechanism behind this differentiation still needs to be elucidated. To investigate a possible regulation of *Gdf10* by *Shh*, *En1*$^{cre+}$ */Shh*$^{flox/flox}$ mice were analyzed for the expression of *Gdf10* mRNA. Even though *Shh* was completely deleted from the cerebellum, the expression of *Gdf10* was still present, albeit dislocated. This is most likely due to the fact that the loss of *Shh* in the hindbrain generally causes

severe defects in the cerebellum (Lewis et al. 2004).   At E18.5 the gross cerebellar morphology of the mutant embryos is abnormal, with immature fissures and a reduction in the EGL, however there is no significant difference in cerebellar volumes between the mutant and control embryos (Lewis et al. 2004). Thus, the abnormal expression of *Gdf10* is most likely due to the astroglia loss in general.   Apparently, since Shh induces the differentiation of Bergmann glia in the cerebellum (Dahmane and Ruiz i Altaba 1999), glial precursors do not migrate out of the highly proliferative ventricular epithelium of the 4th ventricle towards the pial surface. Furthermore *Gdf10* was still detected in the isthmus, as in wildtype mice. *Shh* in these mutants is deleted in the regions where *En1* is expressed, which also includes the isthmic region (Vieira et al. 2009). Therefore, due to the loss of *Shh* in this region, a loss or gain of *Gdf10* expression in the isthmus should be observed, if *Gdf10* was directly regulated by *Shh*, which is not the case. This excludes a direct regulation of *Gdf10* by *Shh*.

4.4.4 Analysis of Transcription factor binding sites (TFBs)

In addition to these functional studies, the gene sequence of *Gdf10* was analyzed for possible TFBs. The focus was pointed to the 11 most prominent candidates and on their possible role in cerebellar glia development. Recently, *Gdf10* was described as a tumor suppressor gene acting through Tgfß signaling and being controlled by *stem cell antigen 1 (Sca1);* (Upadhyay et al. 2011). Upadhyay and colleagues found that *Sca1* promotes tumor growth through the suppression of *Gdf10*- dependent TGF-ß signaling in mammary tumor cells. They concluded that this mechanism may be particularly relevant to breast cancer (Upadhyay et al. 2011). Due to the fact that two additional TFs (*Mzf1* and *BRCA1*) were found to be involved in tumorigenesis (Gaboli et al. 2001; Hromas et al. 1996; Korhonen et al. 2003), of which Mzf1 has a notably high number of TFBs in the *Gdf10* gene, and BRCA1 being highly involved in breast cancer, suggest a strong role of *Gdf10* in tumorigenesis.

Within the group of transcription factors, some are expressed in neural progenitor cells and play a role in proliferation or differentiation. Zeb1 for example, is expressed in progenitor cells of the ventricular zone of the lateral ventricles and is downregulated during the transition from proliferating precursor to differentiated neural cells (Yen et al. 2001). Arid proteins are involved in cell

growth, differentiation and development (Wilsker et al. 2002) and Arid3a has 9 TFBs in the Gdf10 gene.

BRCA1 is expressed in embryonic and adult neural stem cells of the cerebral cortex and is involved in proliferation (Korhonen et al. 2003). In the cerebellum, BRCA1 is expressed in the EGL at embryonic stages (Eurexpress- http://www.eurexpress.org) and in the Purkinje cell layer at postnatal stages (Korhonen et al. 2003). Thus, there are further indications directing towards a role in precursor specification in general and in terms of cerebellar development in the specification of EGL precursors as described in 4.2.2.

Nevertheless, the most interesting TF considering glial development in the cerebellum is *Yin-Yang 1* (*YY1*). It is expressed in the molecular layer of the cerebellar cortex (Rylski et al. 2008) where it regulates GLAST activity in glial cells. It has been shown to initiate oligodendrocyte differentiation (He et al. 2007). Furthermore there is a positive correlation between the autocrine expression of *YY1* and *TGF-beta 1*, *IGF-1 and FGF-2*, known to be involved in the progression of gliomas and meningiomas (Baritaki et al. 2009), again emphasizing a possible involvement in turmorigenesis. Therefore, *YY1* is probably the most promising transcription factor for further studies on Bergmann glial cell development.

5 Conclusions

The first part of this study focused on the origin of cerebellar oligodendroglia in chick embryos. This work demonstrated that:

1. Cerebellar oligodendroglial cells originate from the parabasal band of the mesencephalic vesicle, which can be labelled with *Nkx2.2* and *Sulf1* at early embryonic developmental stages.

2. The majority of oligodendroglial cells, which migrated from the mesencephalic parabasal plate into the cerebellum, were oligodendrocytes expressing PLP (54%). Approximately 27 % were Bergmann glia and 10% were astrocytes.

3. The velum medullare was the entry of oligodendrocyte precursors into folium 1 of the cerebellum.

4. Oligodendrocytes originating from the mesencephalic vesicle started entering the cerebellum at chicken developmental stage E9/ HH35 and migrated through the white matter tracks to their final location.

Further investigations are necessary to explore why oligodendroglia migrate such a long distance, crossing the isthmic constriction to finally populate the cerebellum and which molecules are attracting/ guiding them.

In the second part of this work, *Gdf10* expression was analysed in the context of Bergmann glial development.

5. *Gdf10* is highly expressed in the cerebellum from E14.5 until adult stages.

6. At embryonic stages, the expression pattern varies along the antero-posterior axis of the cerebellum. The results showed that anteriorly *Gdf10+* cells were detected along the VZ of the developing vermis, through the dorsal cerebellar midline, whereas in the cerebellar hemispheres *Gdf10* was expressed both in the ventricular epithelium adjacent to the rhombic lip as well as in the rhombic lip itself. Posteriorly, *Gdf10* expression was detected throughout the entire cerebellar rhombic lip and ventricular zone of the 4th ventricle. Furthermore, *Gdf10*

expression was detected in the intermediate zone and close to the developing EGL.

7. A new mode of Bergmann glia migration was observed in the posterior cerebellum. This migration was divided into a primarily radial migration, which finally underwent a perpendicular turn towards the EGL.

8. Expression analysis in *Shh* mutants showed that *Gdf10* was not regulated by Shh in the cerebellum.

9. The analysis of the transcription factor binding sites provided many insights for further studies of Gdf10, for example:

   - indications for Gdf10 being involved in breast cancer as a tumor suppressor are very interesting from the medical point of view;
   - there are further clues directing towards a role of Gdf10 in precursor specification;
   - and YY1 was pointed out as a possible regulator of Gdf10 in Bergmann glia differentiation in the cerebellum.

A *Gdf10* reporter mouse line would be a useful tool to further investigate if cerebellar intermediate precursors express *Gdf10* and whether or not they give rise to both neurons and astrocytes.

In utero electroporation of the VZ of the 4th ventricle at E12.5 in mouse embryos would clarify if *Gdf10* can pre-induce radial glia differentiation, and thus reveal if it is essential for the transition from radial glia to Bergmann glia.

However, this work provides a basis for further studies on this very promising candidate gene for Bergmann glia maturation and differentiation, which is becoming of increased interest in terms of brain development.

6 References

Alcaraz WA, Gold DA, Raponi E, Gent PM, Concepcion D, Hamilton BA. 2006. Zfp423 controls proliferation and differentiation of neural precursors in cerebellar vermis formation. Proceedings of the National Academy of Sciences of the United States of America 103(51):19424-9.

Alexandre P, Bachy I, Marcou M, Wassef M. 2006. Positive and negative regulations by FGF8 contribute to midbrain roof plate developmental plasticity. Development 133(15):2905-2913.

Altman J. 1972a. Postnatal development of the cerebellar cortex in the rat. 3. Maturation of the components of the granular layer. J Comp Neurol 145(4):465-513.

Altman J. 1972b. Postnatal development of the cerebellar cortex in the rat. I. The external germinal layer and the transitional molecular layer. J Comp Neurol 145(3):353-97.

Altman J. 1972c. Postnatal development of the cerebellar cortex in the rat. II. Phases in the maturation of Purkinje cells and of the molecular layer. J Comp Neurol 145(4):399-463.

Altman J. 1975. Postnatal development of the cerebellar cortex in the rat. IV. Spatial organization of bipolar cells, parallel fibers and glial palisades. J Comp Neurol 163(4):427-47.

Altman J, Bayer SA. 1997. Development of the Cerebellar System. CRC Press.

Alvarado-Mallart RM. 2000. The chick/quail transplantation model to study central nervous system development. Prog Brain Res 127:67-98.

Alvarez Otero R, Sotelo C, Alvarado-Mallart RM. 1993. Chick/quail chimeras with partial cerebellar grafts: an analysis of the origin and migration of cerebellar cells. J Comp Neurol 333(4):597-615.

An G, Miner CA, Nixon JC, Kincade PW, Bryant J, Tucker PW, Webb CF. 2010. Loss of Bright/ARID3a function promotes developmental plasticity. Stem Cells 28(9):1560-7.

Andrae J, Hansson I, Afink GB, Nister M. 2001. Platelet-derived growth factor receptor-alpha in ventricular zone cells and in developing neurons. Mol Cell Neurosci 17(6):1001-13.

Aroca P, Lorente-Cánovas B, Mateos FR, Puelles L. 2006. Locus coeruleus neurons originate in alar rhombomere 1 and migrate into the basal plate: Studies in chick and mouse embryos. The Journal of Comparative Neurology 496(6):802-818.

Bansal R, Warrington AE, Gard AL, Ranscht B, Pfeiffer SE. 1989. Multiple and novel specificities of monoclonal antibodies O1, O4, and R-mAb used in the analysis of oligodendrocyte development. J Neurosci Res 24(4):548-57.

Baritaki S, Chatzinikola AM, Vakis AF, Soulitzis N, Karabetsos DA, Neonakis I, Bonavida B, Spandidos DA. 2009. YY1 Over-expression in human brain gliomas and meningiomas correlates with TGF-beta1, IGF-1 and FGF-2 mRNA levels. Cancer Invest 27(2):184-92.

Baumann N, Pham-Dinh D. 2001. Biology of oligodendrocyte and myelin in the mammalian central nervous system. Physiol Rev 81(2):871-927.

Boggs JM. 2006. Myelin basic protein: a multifunctional protein. Cell Mol Life Sci 63(17):1945-61.

Bovolenta P, Liem RKH, Mason CA. 1984. Development of cerebellar astroglia: Transitions in form and cytoskeletal content. Developmental Biology 102(1):248-259.

Bui T, Sequeira J, Wen TC, Sola A, Higashi Y, Kondoh H, Genetta T. 2009. ZEB1 links p63 and p73 in a novel neuronal survival pathway rapidly induced in response to cortical ischemia. PLoS One 4(2):e4373.

Carletti B, Rossi F. 2008. Neurogenesis in the cerebellum. Neuroscientist 14(1):91-100.

Cai J, Qi Y, Hu X, Tan M, Liu Z, Zhang J, Li Q, Sander M, Qiu M. 2005. Generation of oligodendrocyte precursor cells from mouse dorsal spinal cord independent of Nkx6 regulation and Shh signaling. Neuron 45(1):41-53.

Castagna C, Viglietti-Panzica C, Carlo Panzica G. 2003. Protein S100 immunoreactivity in glial cells and neurons of the Japanese quail brain. J Chem Neuroanat 25(3):195-212.

Chédotal A, Pourquié O, Ezan F, San Clemente H, Sotelo C. 1996. BEN as a presumptive target recognition molecule during the development of the olivocerebellar system. J Neurosci 16(10):3296-310.

Cobos I, Shimamura K, Rubenstein JL, Martinez S, Puelles L. 2001. Fate map of the avian anterior forebrain at the four-somite stage, based on the analysis of quail-chick chimeras. Dev Biol 239(1):46-67.

Colas JF, Schoenwolf GC. 2001. Towards a cellular and molecular understanding of neurulation. Dev Dyn 221(2):117-45.

Colucci-Guyon E, Gimenez YRM, Maurice T, Babinet C, Privat A. 1999. Cerebellar defect and impaired motor coordination in mice lacking vimentin. Glia 25(1):33-43.

Corrales JD, Rocco GL, Blaess S, Guo Q, Joyner AL. 2004. Spatial pattern of sonic hedgehog signaling through Gli genes during cerebellum development. Development 131(22):5581-90.

Cunningham NS, Jenkins NA, Gilbert DJ, Copeland NG, Reddi AH, Lee SJ. 1995. Growth/differentiation factor-10: a new member of the transforming growth factor-beta superfamily related to bone morphogenetic protein-3. Growth Factors 12(2):99-109.

Dahmane N, Ruiz i Altaba A. 1999. Sonic hedgehog regulates the growth and patterning of the cerebellum. Development 126(14):3089-100.

Dehart DB, Lanoue L, Tint GS, Sulik KK. 1997. Pathogenesis of malformations in a rodent model for Smith-Lemli-Opitz syndrome. American journal of medical genetics 68(3):328-37.

Delaunay D, Heydon K, Miguez A, Schwab M, Nave KA, Thomas JL, Spassky N, Martinez S, Zalc B. 2009. Genetic tracing of subpopulation neurons in the prethalamus of mice (Mus musculus). J Comp Neurol 512(1):74-83.

Delporte FM, Pasque V, Devos N, Manfroid I, Voz ML, Motte P, Biemar F, Martial JA, Peers B. 2008. Expression of zebrafish pax6b in pancreas is regulated by two enhancers containing highly conserved cis-elements bound by PDX1, PBX and PREP factors. BMC Dev Biol 8:53.

Dessaud E, McMahon AP, Briscoe J. 2008. Pattern formation in the vertebrate neural tube: a sonic hedgehog morphogen-regulated transcriptional network. Development 135(15):2489-503.

Diamandis EP, Christopoulos TK. 1991. The biotin-(strept)avidin system: principles and applications in biotechnology. Clin Chem 37(5):625-36.

Eccles D, Bunyan D, Barker S, Castle B. 2005. BRCA1 mutation and neuronal migration defect: implications for chemoprevention. Journal of Medical Genetics 42(5):e24.

Eccles DM, Barker S, Pilz DT, Kennedy C. 2003. Neuronal migration defect in a BRCA1 gene carrier: possible focal nullisomy? J Med Genet 40(3):e24.

Englund C, Kowalczyk T, Daza RA, Dagan A, Lau C, Rose MF, Hevner RF. 2006. Unipolar brush cells of the cerebellum are produced in the rhombic lip and migrate through developing white matter. J Neurosci 26(36):9184-95.

Ericson J, Rashbass P, Schedl A, Brenner-Morton S, Kawakami A, van Heyningen V, Jessell TM, Briscoe J. 1997. Pax6 controls progenitor cell identity and neuronal fate in response to graded Shh signaling. Cell 90(1):169-80.

Evans TA, Raina AK, Delacourte A, Aprelikova O, Lee HG, Zhu X, Perry G, Smith MA. 2007. BRCA1 may modulate neuronal cell cycle re-entry in Alzheimer disease. Int J Med Sci 4(3):140-5.

Fink AJ, Englund C, Daza RAM, Pham D, Lau C, Nivison M, Kowalczyk T, Hevner RF. 2006. Development of the Deep Cerebellar Nuclei: Transcription Factors and Cell Migration from the Rhombic Lip. J Neurosci 26(11):3066-3076.

Finzsch M, Stolt CC, Lommes P, Wegner M. 2008. Sox9 and Sox10 influence survival and migration of oligodendrocyte precursors in the spinal cord by regulating PDGF receptor alpha expression. Development 135(4):637-46.

Fogarty M, Richardson WD, Kessaris N. 2005. A subset of oligodendrocytes generated from radial glia in the dorsal spinal cord. Development 132(8):1951-9.

Fu H, Cai J, Rutledge M, Hu X, Qiu M. 2003. Oligodendrocytes can be generated from the local ventricular and subventricular zones of embryonic chicken midbrain. Developmental Brain Research 143(2):161-165.

Fu H, Qi Y, Tan M, Cai J, Takebayashi H, Nakafuku M, Richardson W, Qiu M. 2002. Dual origin of spinal oligodendrocyte progenitors and evidence for the cooperative role of Olig2 and Nkx2.2 in the control of oligodendrocyte differentiation. Development 129(3):681-93.

Fuccillo M, Joyner AL, Fishell G. 2006. Morphogen to mitogen: the multiple roles of hedgehog signalling in vertebrate neural development. Nature reviews Neuroscience 7(10):772-83.

Fuchs E, Weber K. 1994. Intermediate filaments: structure, dynamics, function, and disease. Annu Rev Biochem 63:345-82.

Fukuda S, Kato F, Tozuka Y, Yamaguchi M, Miyamoto Y, Hisatsune T. 2003. Two distinct subpopulations of nestin-positive cells in adult mouse dentate gyrus. J Neurosci 23(28):9357-66.

Furuta A, Rothstein JD, Martin LJ. 1997. Glutamate transporter protein subtypes are expressed differentially during rat CNS development. J Neurosci 17(21):8363-75.

Gaboli M, Kotsi PA, Gurrieri C, Cattoretti G, Ronchetti S, Cordon-Cardo C, Broxmeyer HE, Hromas R, Pandolfi PP. 2001. Mzf1 controls cell proliferation and tumorigenesis. Genes Dev 15(13):1625-30.

García-Lopez R, Martínez S. 2010. Oligodendrocyte precursors originate in the parabasal band of the basal plate in prosomere 1 and migrate into the alar prosencephalon during chick development. Glia 58(12):1437-50.

García-Lopez R, Pombero A, Martínez S. 2009a. Fate map of the chick embryo neural tube. Dev Growth Differ 51(3):145-65.

García-Lopez R, Soula C, Martinez S. 2009b. Expression analysis of Sulf1 in the chick forebrain at early and late stages of development. Dev Dyn 238(9):2418-29.

Gilthorpe JD, Papantoniou EK, Chedotal A, Lumsden A, Wingate RJ. 2002. The migration of cerebellar rhombic lip derivatives. Development 129(20):4719-28.

Gilyarov AV. 2008. Nestin in central nervous system cells. Neurosci Behav Physiol 38(2):165-9.

Gimenez YRM, Langa F, Menet V, Privat A. 2000. Comparative anatomy of the cerebellar cortex in mice lacking vimentin, GFAP, and both vimentin and GFAP. Glia 31(1):69-83.

Gimeno L, Martinez S. 2007. Expression of chick Fgf19 and mouse Fgf15 orthologs is regulated in the developing brain by Fgf8 and Shh. Dev Dyn 236(8):2285-97.

Gold DA, Baek SH, Schork NJ, Rose DW, Larsen DD, Sachs BD, Rosenfeld MG, Hamilton BA. 2003. ROR[alpha] Coordinates Reciprocal Signaling in Cerebellar Development through Sonic hedgehog and Calcium-Dependent Pathways. Neuron 40(6):1119-1131.

Grimaldi P, Parras C, Guillemot F, Rossi F, Wassef M. 2009. Origins and control of the differentiation of inhibitory interneurons and glia in the cerebellum. Developmental Biology 328(2):422-433.

Hachem S, Laurenson AS, Hugnot JP, Legraverend C. 2007. Expression of S100B during embryonic development of the mouse cerebellum. BMC Dev Biol 7:17.

Hack MA, Sugimori M, Lundberg C, Nakafuku M, Gotz M. 2004. Regionalization and fate specification in neurospheres: the role of Olig2 and Pax6. Mol Cell Neurosci 25(4):664-78.

Hallonet ME, Alvarado-Mallart RM. 1997. The chick/quail chimeric system: a model for early cerebellar development. Perspect Dev Neurobiol 5(1):17-31.

Hallonet ME, Teillet MA, Le Douarin NM. 1990. A new approach to the development of the cerebellum provided by the quail-chick marker system. Development 108(1):19-31.

Hamburger V, Hamilton HL. 1992. A series of normal stages in the development of the chick embryo. Developmental Dynamics 195(4):231-272.

Hatten ME. 1999. Central nervous system neuronal migration. Annu Rev Neurosci 22:511-39.

Haubst N, Berger J, Radjendirane V, Graw J, Favor J, Saunders GF, Stoykova A, Gotz M. 2004. Molecular dissection of Pax6 function: the specific roles of the paired domain and homeodomain in brain development. Development 131(24):6131-40.

He Y, Sandoval J, Casaccia-Bonnefil P. 2007. Events at the transition between cell cycle exit and oligodendrocyte progenitor differentiation: the role of HDAC and YY1. Neuron Glia Biol 3(3):221-31.

Hendelmann WJ. 2000. Atlas of functional neuroanatomy. CRC Press.

Hidalgo-Sánchez M, Millet S, Bloch-Gallego E, Alvarado-Mallart R-M. 2005. Specification of the meso-isthmo-cerebellar region: The Otx2/Gbx2 boundary. Brain Research Reviews 49(2):134-149.

Hikke van Doorninck J, van der Wees J, Karis A, Goedknegt E, Coesmans M, Rutteman M, Grosveld F, De Zeeuw CI. 1999. GATA-3 Is Involved in the Development of Serotonergic Neurons in the Caudal Raphe Nuclei. The Journal of Neuroscience 19(12):RC12.

Hino J, Nishimatsu S-i, Nagai T, Matsuo H, Kangawa K, Nohno T. 2003. Coordination of BMP-3b and cerberus is required for head formation of Xenopus embryos. Developmental Biology 260(1):138-157.

Hino J, Takao M, Takeshita N, Konno Y, Nishizawa T, Matsuo H, Kangawa K. 1996. cDNA Cloning and Genomic Structure of Human Bone Morphogenetic Protein-3b (BMP-3b). Biochemical and Biophysical Research Communications 223(2):304-310.

Hockfield S, McKay RD. 1985. Identification of major cell classes in the developing mammalian nervous system. J Neurosci 5(12):3310-28.

Holm PC, Mader MT, Haubst N, Wizenmann A, Sigvardsson M, Gˆtz M. 2007. Loss- and gain-of-function analyses reveal targets of Pax6 in the

developing mouse telencephalon. Molecular and Cellular Neuroscience 34(1):99-119.

Hromas R, Boswell S, Shen RN, Burgess G, Davidson A, Cornetta K, Sutton J, Robertson K. 1996. Forced over-expression of the myeloid zinc finger gene MZF-1 inhibits apoptosis and promotes oncogenesis in interleukin-3-dependent FDCP.1 cells. Leukemia 10(6):1049-50.

Hsu SM, Raine L, Fanger H. 1981a. A comparative study of the peroxidase-antiperoxidase method and an avidin-biotin complex method for studying polypeptide hormones with radioimmunoassay antibodies. Am J Clin Pathol 75(5):734-8.

Hsu SM, Raine L, Fanger H. 1981b. Use of avidin-biotin-peroxidase complex (ABC) in immunoperoxidase techniques: a comparison between ABC and unlabeled antibody (PAP) procedures. Journal of Histochemistry & Cytochemistry 29(4):577-80.

Huang X, Ketova T, Fleming JT, Wang H, Dey SK, Litingtung Y, Chiang C. 2009. Sonic hedgehog signaling regulates a novel epithelial progenitor domain of the hindbrain choroid plexus. Development 136(15):2535-43.

Huang X, Liu J, Ketova T, Fleming JT, Grover VK, Cooper MK, Litingtung Y, Chiang C. 2010. Transventricular delivery of Sonic hedgehog is essential to cerebellar ventricular zone development. Proceedings of the National Academy of Sciences of the United States of America 107(18):8422-7.

Huangfu D, Anderson KV. 2006. Signaling from Smo to Ci/Gli: conservation and divergence of Hedgehog pathways from Drosophila to vertebrates. Development 133(1):3-14.

Kálmán M, Székely AD, Csillag A. 1998. Distribution of glial fibrillary acidic protein and vimentin-immunopositive elements in the developing chicken brain from hatch to adulthood. Anatomy and Embryology 198(3):213-235.

Katoh Y, Katoh M. 2006. Comparative integromics on BMP/GDF family. Int J Mol Med 17(5):951-5.

Kessaris N, Fogarty M, Iannarelli P, Grist M, Wegner M, Richardson WD. 2006. Competing waves of oligodendrocytes in the forebrain and postnatal elimination of an embryonic lineage. Nat Neurosci 9(2):173-179.

Kimmel RA, Turnbull DH, Blanquet V, Wurst W, Loomis CA, Joyner AL. 2000. Two lineage boundaries coordinate vertebrate apical ectodermal ridge formation. Genes Dev 14(11):1377-89.

Koirala S, Corfas G. 2010. Identification of Novel Glial Genes by Single-Cell Transcriptional Profiling of Bergmann Glial Cells from Mouse Cerebellum. PLoS ONE 5(2).

Kordes U, Cheng Y-C, Scotting PJ. 2005. Sox group E gene expression distinguishes different types and maturational stages of glial cells in developing chick and mouse. Developmental Brain Research 157(2):209-213.

Korhonen L, Brannvall K, Skoglosa Y, Lindholm D. 2003. Tumor suppressor gene BRCA-1 is expressed by embryonic and adult neural stem cells and involved in cell proliferation. J Neurosci Res 71(6):769-76.

Kuspert M, Hammer A, Bosl MR, Wegner M. 2010. Olig2 regulates Sox10 expression in oligodendrocyte precursors through an evolutionary conserved distal enhancer. Nucleic Acids Res 39(4):1280-93.

Lafont JrmE, Talma S, Hopfgarten C, Murphy CL. 2008. Hypoxia Promotes the Differentiated Human Articular Chondrocyte Phenotype through SOX9-dependent and -independent Pathways. Journal of Biological Chemistry 283(8):4778-4786.

Laine J, Axelrad H. 1994. The candelabrum cell: a new interneuron in the cerebellar cortex. J Comp Neurol 339(2):159-73.

Lanoue L, Dehart DB, Hinsdale ME, Maeda N, Tint GS, Sulik KK. 1997. Limb, genital, CNS, and facial malformations result from gene/environment-induced cholesterol deficiency: further evidence for a link to sonic hedgehog. American journal of medical genetics 73(1):24-31.

Le Bras B, Chatzopoulou E, Heydon K, Martínez S, Ikenaka K, Prestoz L, Spassky N, Zalc B, Thomas JL. 2005. Oligodendrocyte development in the embryonic brain: the contribution of the plp lineage. Int J Dev Biol 49(2-3):209-20.

Le Douarin N, Barg G. 1969. [Use of Japanese quail cells as "biological markers" in experimental embryology]. C R Acad Sci Hebd Seances Acad Sci D 269(16):1543-6.

Le Douarin N, Dieterlen-Lièvre F, Teillet MA. 1996. Quail-chick transplantations. Methods Cell Biol 51:23-59.

Le Douarin N, DieterlenLièvre F, Creuzet S, Teillet M, Bronner-Fraser M. 2008. Chapter 2 Quail-Chick Transplantations. Methods in Cell Biology: Academic Press. p 19-58.

Leber SM, Sanes JR. 1995. Migratory paths of neurons and glia in the embryonic chick spinal cord. J Neurosci 15(2):1236-48.

Leber SM, Yamagata M, Sanes JR. 1996. Gene transfer using replication-defective retroviral and adenoviral vectors. Methods Cell Biol 51:161-83.

Lewis PM, Dunn MP, McMahon JA, Logan M, Martin JF, St-Jacques B, McMahon AP. 2001. Cholesterol modification of sonic hedgehog is required for long-range signaling activity and effective modulation of signaling by Ptc1. Cell 105(5):599-612.

Lewis PM, Gritli-Linde A, Smeyne R, Kottmann A, McMahon AP. 2004. Sonic hedgehog signaling is required for expansion of granule neuron precursors and patterning of the mouse cerebellum. Developmental Biology 270(2):393-410.

Li H, Lu Y, Smith HK, Richardson WD. 2007. Olig1 and Sox10 interact synergistically to drive myelin basic protein transcription in oligodendrocytes. J Neurosci 27(52):14375-82.

Ligon KL, Fancy SP, Franklin RJ, Rowitch DH. 2006. Olig gene function in CNS development and disease. Glia 54(1):1-10.

Lin S, Huang Y, Lee T. 2009. Nuclear receptor unfulfilled regulates axonal guidance and cell identity of Drosophila mushroom body neurons. PLoS One 4(12):e8392.

Louvi A, Alexandre P, Métin C, Wurst W, Wassef M. 2003. The isthmic neuroepithelium is essential for cerebellar midline fusion. Development 130(22).

Lu QR, Sun T, Zhu Z, Ma N, Garcia M, Stiles CD, Rowitch DH. 2002. Common developmental requirement for Olig function indicates a motor neuron/oligodendrocyte connection. Cell 109(1):75-86.

Luo X, Zhang X, Shao W, Yin Y, Zhou J. 2009. Crucial roles of MZF-1 in the transcriptional regulation of apomorphine-induced modulation of FGF-2 expression in astrocytic cultures. J Neurochem 108(4):952-61.

Machold RP, Kittell DJ, Fishell GJ. 2007. Antagonism between Notch and bone morphogenetic protein receptor signaling regulates neurogenesis in the cerebellar rhombic lip. Neural Develop 2007; 2: 5

Maricich SM, Herrup K. 1999. Pax-2 expression defines a subset of GABAergic interneurons and their precursors in the developing murine cerebellum. J Neurobiol 41(2):281-94.

Martínez S, Alvarado-Mallart RM. 1989. Rostral Cerebellum Originates from the Caudal Portion of the So-Called 'Mesencephalic' Vesicle: A Study Using Chick/Quail Chimeras. Eur J Neurosci 1(6):549-560.

Massagué J. 1998. TGF-ß SIGNAL TRANSDUCTION. Annual Review of Biochemistry 67(1):753-791.

Matsumura S, Takagi K, Okuda-Ashitaka E, Lu J, Naritsuka H, Yamaguchi M, Ito S. 2010. Characterization of nestin expression in the spinal cord of GFP transgenic mice after peripheral nerve injury. Neuroscience 170(3):942-53.

Mecklenburg N, Garcia-Lopez R, Puelles E, Sotelo C, Martinez S. 2011. Cerebellar oligodendroglial cells have a mesencephalic origin. Glia.

Miale IL, Sidman RL. 1961. An autoradiographic analysis of histogenesis in the mouse cerebellum. Exp Neurol 4:277-96.

Mignone JL, Kukekov V, Chiang AS, Steindler D, Enikolopov G. 2004. Neural stem and progenitor cells in nestin-GFP transgenic mice. The Journal of Comparative Neurology 469(3):311-24.

Milosevic A, Goldman JE. 2002. Progenitors in the postnatal cerebellar white matter are antigenically heterogeneous. The Journal of Comparative Neurology 452(2):192-203.

Milosevic A, Goldman JE. 2004. Potential of progenitors from postnatal cerebellar neuroepithelium and white matter: lineage specified vs. multipotent fate. Molecular and Cellular Neuroscience 26(2):342-353.

Miyata T, Ono Y, Okamoto M, Masaoka M, Sakakibara A, Kawaguchi A, Hashimoto M, Ogawa M. 2010. Migration, early axonogenesis, and Reelin-dependent layer-forming behavior of early/posterior-born Purkinje cells in the developing mouse lateral cerebellum. Neural development 5:23.

Morrish F, Giedt C, Hockenbery D. 2003. c-MYC apoptotic function is mediated by NRF-1 target genes. Genes Dev 17(2):240-55.

Mugnaini E, Dino MR, Jaarsma D. 1997. The unipolar brush cells of the mammalian cerebellum and cochlear nucleus: cytology and microcircuitry. Prog Brain Res 114:131-50.

Nadkarini V, Lindhardt R. 1997. Enhancement of Diaminobenzidine Colorimetric Signal in Immunoblotting. BioTechniques 23:385-388.

Nishiyama A, Komitova M, Suzuki R, Zhu X. 2009. Polydendrocytes (NG2 cells): multifunctional cells with lineage plasticity. Nat Rev Neurosci 10(1):9-22.

Noble M, Murray K, Stroobant P, Waterfield MD, Riddle P. 1988. Platelet-derived growth factor promotes division and motility and inhibits premature differentiation of the oligodendrocyte/type-2 astrocyte progenitor cell. Nature 333(6173):560-2.

Noll E, Miller RH. 1993. Oligodendrocyte precursors originate at the ventral ventricular zone dorsal to the ventral midline region in the embryonic rat spinal cord. Development 118(2):563-573.

Oh S, Huang X, Chiang C. 2005. Specific requirements of sonic hedgehog signaling during oligodendrocyte development. Developmental Dynamics 234(3):489-496.

Okado N, Yoshimoto M, Furber SE. 1987. Pathway formation and the terminal distribution pattern of the spinocerebellar projection in the chick embryo. Anat Embryol (Berl) 176(2):165-74.

Olivier C, Cobos I, Perez Villegas EM, Spassky N, Zalc B, Martinez S, Thomas JL. 2001. Monofocal origin of telencephalic oligodendrocytes in the anterior entopeduncular area of the chick embryo. Development 128(10):1757-69.

Ono K, Fujisawa H, Hirano S, Norita M, Tsumori T, Yasui Y. 1997. Early development of the oligodendrocyte in the embryonic chick metencephalon. Journal of Neuroscience Research 48(3):212-225.

Ono K, Takebayashi H, Ikenaka K. 2009. Olig2 transcription factor in the developing and injured forebrain; cell lineage and glial development. Mol Cells 27(4):397-401.

Osumi N, Hirota A, Ohuchi H, Nakafuku M, Iimura T, Kuratani S, Fujiwara M, Noji S, Eto K. 1997. Pax-6 is involved in the specification of hindbrain motor neuron subtype. Development 124(15):2961-72.

Park D, Xiang AP, Mao FF, Zhang L, Di CG, Liu XM, Shao Y, Ma BF, Lee JH, Ha KS and others. 2010. Nestin is required for the proper self-renewal of neural stem cells. Stem Cells 28(12):2162-71.

Pata I, Studer M, van Doorninck JH, Briscoe J, Kuuse S, Engel JD, Grosveld F, Karis A. 1999. The transcription factor GATA3 is a downstream effector of Hoxb1 specification in rhombomere 4. Development 126(23):5523-5531.

Pérez Villegas EM, Olivier C, Spassky N, Poncet C, Cochard P, Zalc B, Thomas JL, Martínez S. 1999. Early specification of oligodendrocytes in the chick embryonic brain. Dev Biol 216(1):98-113.

Pérez-Villegas EM, Olivier C, Spassky N, Poncet C, Cochard P, Zalc B, Thomas JL, Martínez S. 1999. Early specification of oligodendrocytes in the chick embryonic brain. Dev Biol 216(1):98-113.

Pringle NP, Richardson WD. 1993. A singularity of PDGF alpha-receptor expression in the dorsoventral axis of the neural tube may define the origin of the oligodendrocyte lineage. Development 117(2):525-33.

Pringle NP, Yu WP, Guthrie S, Roelink H, Lumsden A, Peterson AC, Richardson WD. 1996. Determination of neuroepithelial cell fate: induction of the oligodendrocyte lineage by ventral midline cells and sonic hedgehog. Dev Biol 177(1):30-42.

Puelles L, Martínez S, Martínez-de-la-Torre M. 2008. Neuroanatomía. Editorial medica panamericana.

Pulvers JN, Huttner WB. 2009. Brca1 is required for embryonic development of the mouse cerebral cortex to normal size by preventing apoptosis of early neural progenitors. Development 136(11):1859-68.

Qi Y, Cai J, Wu Y, Wu R, Lee J, Fu H, Rao M, Sussel L, Rubenstein J, Qiu M. 2001. Control of oligodendrocyte differentiation by the Nkx2.2 homeodomain transcription factor. Development 128(14):2723-33.

Qu D, Rashidian J, Mount MP, Aleyasin H, Parsanejad M, Lira A, Haque E, Zhang Y, Callaghan S, Daigle M and others. 2007. Role of Cdk5-mediated phosphorylation of Prx2 in MPTP toxicity and Parkinson's disease. Neuron 55(1):37-52.

Rakic P. 1971. Neuron-glia relationship during granule cell migration in developing cerebellar cortex. A Golgi and electronmicroscopic study in Macacus Rhesus. J Comp Neurol 141(3):283-312.

Rashidian J, Rousseaux MW, Venderova K, Qu D, Callaghan SM, Phillips M, Bland RJ, During MJ, Mao Z, Slack RS and others. 2009. Essential role of cytoplasmic cdk5 and Prx2 in multiple ischemic injury models, in vivo. J Neurosci 29(40):12497-505.

Regan MR, Huang YH, Kim YS, Dykes-Hoberg MI, Jin L, Watkins AM, Bergles DE, Rothstein JD. 2007. Variations in promoter activity reveal a differential expression and physiology of glutamate transporters by glia in the developing and mature CNS. J Neurosci 27(25):6607-19.

Reichenbach A, Siegel A, Rickmann M, Wolff JR, Noone D, Robinson SR. 1995. Distribution of Bergmann glial somata and processes: implications for function. J Hirnforsch 36(4):509-17.

Repetto M, Maziere JC, Citadelle D, Dupuis R, Meier M, Biade S, Quiec D, Roux C. 1990. Teratogenic effect of the cholesterol synthesis inhibitor AY 9944 on rat embryos in vitro. Teratology 42(6):611-8.

Reynolds R, Wilkin GP. 1988. Development of macroglial cells in rat cerebellum. II. An in situ immunohistochemical study of oligodendroglial lineage from precursor to mature myelinating cell. Development 102(2):409-25.

Richardson WD, Pringle N, Mosley MJ, Westermark B, Dubois-Dalcq M. 1988. A role for platelet-derived growth factor in normal gliogenesis in the central nervous system. Cell 53(2):309-19.

Richter-Landsberg C, Heinrich M. 1995. S-100 immunoreactivity in rat brain glial cultures is associated with both astrocytes and oligodendrocytes. J Neurosci Res 42(5):657-65.

Rickmann M, Wolff JR. 1995. S100 immunoreactivity in a subpopulation of oligodendrocytes and Ranvier's nodes of adult rat brain. Neurosci Lett 186(1):13-6.

Rong Y, Wang T, Morgan JI. 2004. Identification of candidate Purkinje cell-specific markers by gene expression profiling in wild-type and pcd3J mice. Molecular Brain Research 132(2):128-145.

Rosas S, Vargas MA, López-Bayghen E, Ortega A. 2007. Glutamate-dependent transcriptional regulation of GLAST/EAAT1: a role for YY1. Journal of Neurochemistry 101(4):1134-1144.

Rowitch DH, Kriegstein AR. 2010. Developmental genetics of vertebrate glial-cell specification. Nature 468(7321):214-22.

Rylski M, Amborska R, Zybura K, Konopacki F, Wilczynski G, Kaczmarek L. 2008. Yin Yang 1 Expression in the Adult Rodent Brain. Neurochemical Research 33(12):2556-2564.

Sadler TW. 2005. Embryology of neural tube development. American Journal of Medical Genetics Part C: Seminars in Medical Genetics 135C(1):2-8.

Sanes DH, Reh TA, Harris WA. 2006. Development of the nervous system. Elsevier Academic Press.

Schmahl W, Knoedlseder M, Favor J, Davidson D. 1993. Defects of neuronal migration and the pathogenesis of cortical malformations are associated with Small eye (Sey) in the mouse, a point mutation at the Pax-6-locus. Acta Neuropathol 86(2):126-35.

Schotte R, Nagasawa M, Weijer K, Spits H, Blom B. 2004. The ETS Transcription Factor Spi-B Is Required for Human Plasmacytoid Dendritic Cell Development. The Journal of Experimental Medicine 200(11):1503-1509.

Shin DH, Lee KS, Lee E, Chang YP, Kim JW, Choi YS, Kwon BS, Lee HW, Cho SS. 2003. Pax-7 immunoreactivity in the post-natal chicken central nervous system. Anat Histol Embryol 32(6):378-83.

Sievers J, Pehlemann FW, Gude S, Hartmann D, Berry M. 1994. The development of the radial glial scaffold of the cerebellar cortex from

GFAP- positive cells in the external granular layer. Journal of Neurocytology 23(2):97-115.

Silbereis J, Cheng E, Ganat YM, Ment LR, Vaccarino FM. 2009. Precursors with glial fibrillary acidic protein promoter activity transiently generate GABA interneurons in the postnatal cerebellum. Stem Cells 27(5):1152-63.

Silbereis J, Heintz T, Taylor MM, Ganat Y, Ment LR, Bordey A, Vaccarino F. 2010. Astroglial cells in the external granular layer are precursors of cerebellar granule neurons in neonates. Molecular and cellular neurosciences 44(4):362-73.

Sillitoe RV, Joyner AL. 2007. Morphology, Molecular Codes, and Circuitry Produce the Three-Dimensional Complexity of the Cerebellum. Annual Review of Cell and Developmental Biology 23(1):549-577.

Simons M, Trotter J. 2007. Wrapping it up: the cell biology of myelination. Current Opinion in Neurobiology 17(5):533-540.

Song J, Xu Y, Hu X, Choi B, Tong Q. 2010. Brain expression of Cre recombinase driven by pancreas-specific promoters. Genesis 48(11):628-34.

Sotelo C. 2004. Cellular and genetic regulation of the development of the cerebellar system. Prog Neurobiol 72(5):295-339.

Sotelo C, Alvarado-Mallart RM, Frain M, Vernet M. 1994. Molecular plasticity of adult Bergmann fibers is associated with radial migration of grafted Purkinje cells. J Neurosci 14(1):124-33.

Southey MC, Ramus SJ, Dowty JG, Smith LD, Tesoriero AA, Wong EE, Dite GS, Jenkins MA, Byrnes GB, Winship I and others. 2011. Morphological predictors of BRCA1 germline mutations in young women with breast cancer. Br J Cancer 104(6):903-9.

Spassky N, Goujet-Zalc C, Parmantier E, Olivier C, Martinez S, Ivanova A, Ikenaka K, Macklin W, Cerruti I, Zalc B and others. 1998. Multiple restricted origin of oligodendrocytes. J Neurosci 18(20):8331-43.

Stolt CC, Lommes P, Sock E, Chaboissier MC, Schedl A, Wegner M. 2003. The Sox9 transcription factor determines glial fate choice in the developing spinal cord. Genes Dev 17(13):1677-89.

Stormo GD. 2000. DNA binding sites: representation and discovery. Bioinformatics 16(1):16-23.

Stoykova A, Gotz M, Gruss P, Price J. 1997. Pax6-dependent regulation of adhesive patterning, R-cadherin expression and boundary formation in developing forebrain. Development 124(19):3765-77.

Sudarov A, Joyner AL. 2007. Cerebellum morphogenesis: the foliation pattern is orchestrated by multi-cellular anchoring centers. Neural Develop 2:26.

Sudarov A, Turnbull RK, Kim EJ, Lebel-Potter M, Guillemot F, Joyner AL. 2011. Ascl1 genetics reveals insights into cerebellum local circuit assembly. The Journal of neuroscience : the official journal of the Society for Neuroscience 31(30):11055-69.

Sun T, Pringle NP, Hardy AP, Richardson WD, Smith HK. 1998. Pax6 influences the time and site of origin of glial precursors in the ventral neural tube. Mol Cell Neurosci 12(4-5):228-39.

Susumu I, Fumiko I, Marie-JosÈ G, Peter ten D. 2000. Signaling of transforming growth factor-ß family members through Smad proteins. European Journal of Biochemistry 267(24):6954-6967.

Takada N, Kucenas S, Appel B. 2010. Sox10 is necessary for oligodendrocyte survival following axon wrapping. Glia 58(8):996-1006.

Takahashi M, Osumi N. 2002. Pax6 regulates specification of ventral neurone subtypes in the hindbrain by establishing progenitor domains. Development 129(6):1327-38.

Takayasu Y, Iino M, Shimamoto K, Tanaka K, Ozawa S. 2006. Glial Glutamate Transporters Maintain One-to-One Relationship at the Climbing Fiber¬ñPurkinje Cell Synapse by Preventing Glutamate Spillover. The Journal of Neuroscience 26(24):6563-6572.

Takebayashi H, Nabeshima Y, Yoshida S, Chisaka O, Ikenaka K. 2002. The basic helix-loop-helix factor olig2 is essential for the development of motoneuron and oligodendrocyte lineages. Curr Biol 12(13):1157-63.

Tanabe Y, Jessell TM. 1996. Diversity and pattern in the developing spinal cord. Science 274(5290):1115-23.

ten Berge D, Brouwer A, Korving J, Reijnen MJ, van Raaij EJ, Verbeek F, Gaffield W, Meijlink F. 2001. Prx1 and Prx2 are upstream regulators of sonic hedgehog and control cell proliferation during mandibular arch morphogenesis. Development 128(15):2929-38.

Teraoka H, Russell C, Regan J, Chandrasekhar A, Concha ML, Yokoyama R, Higashi K, Take-Uchi M, Dong W, Hiraga T and others. 2004. Hedgehog and Fgf signaling pathways regulate the development of tphR-expressing serotonergic raphe neurons in zebrafish embryos. J Neurobiol 60(3):275-88.

Tsarovina K, Reiff T, Stubbusch J, Kurek D, Grosveld FG, Parlato R, Schütz G, Rohrer H. 2010. The Gata3 Transcription Factor Is Required for the

Survival of Embryonic and Adult Sympathetic Neurons. The Journal of Neuroscience 30(32):10833-10843.

Upadhyay G, Yin Y, Yuan H, Li X, Derynck R, Glazer RI. 2011. Stem cell antigen-1 enhances tumorigenicity by disruption of growth differentiation factor-10 (GDF10)-dependent TGF-{beta} signaling. Proc Natl Acad Sci U S A 108(19):7820-5.

Vaillant C, Monard D. 2009. SHH pathway and cerebellar development. Cerebellum 8(3):291-301.

Vallstedt A, Klos JM, Ericson J. 2005. Multiple dorsoventral origins of oligodendrocyte generation in the spinal cord and hindbrain. Neuron 45(1):55-67.

Vieira C, Pombero A, Garcia-Lopez R, Gimeno L, Echevarria D, Martinez S. 2009. Molecular mechanisms controlling brain development: an overview of neuroepithelial secondary organizers. Int J Dev Biol 54(1):7-20.

Voogd J, Glickstein M. 1998. The anatomy of the cerebellum. Trends Neurosci 21(9):370-5.

Wallace VA. 1999. Purkinje-cell-derived Sonic hedgehog regulates granule neuron precursor cell proliferation in the developing mouse cerebellum. Current biology : CB 9(8):445-8.

Wang H, Maechler P, Ritz-Laser B, Hagenfeldt KA, Ishihara H, Philippe J, Wollheim CB. 2001. Pdx1 level defines pancreatic gene expression pattern and cell lineage differentiation. J Biol Chem 276(27):25279-86.

Warren N, Price DJ. 1997. Roles of Pax-6 in murine diencephalic development. Development 124(8):1573-82.

Wasserman WW, Sandelin A. 2004. Applied bioinformatics for the identification of regulatory elements. Nat Rev Genet 5(4):276-87.

Watanabe Y, Nakamura H. 2000. Control of chick tectum territory along dorsoventral axis by Sonic hedgehog. Development 127(5):1131-40.

Webb CF, Bryant J, Popowski M, Allred L, Kim D, Harriss J, Schmidt C, Miner CA, Rose K, Cheng HL and others. 2011. The ARID family transcription factor bright is required for both hematopoietic stem cell and B lineage development. Mol Cell Biol 31(5):1041-53.

Wechsler-Reya RJ, Scott MP. 1999. Control of Neuronal Precursor Proliferation in the Cerebellum by Sonic Hedgehog. Neuron 22(1):103-114.

Wei LC, Shi M, Chen LW, Cao R, Zhang P, Chan YS. 2002. Nestin-containing cells express glial fibrillary acidic protein in the proliferative regions of

central nervous system of postnatal developing and adult mice. Brain Res Dev Brain Res 139(1):9-17.

Wilsker D, Patsialou A, Dallas PB, Moran E. 2002. ARID proteins: a diverse family of DNA binding proteins implicated in the control of cell growth, differentiation, and development. Cell Growth Differ 13(3):95-106.

Wingate RJ. 2001. The rhombic lip and early cerebellar development. Curr Opin Neurobiol 11(1):82-8.

Wingate RJ, Hatten ME. 1999. The role of the rhombic lip in avian cerebellum development. Development 126(20):4395-404.

Woodruff RH, Tekki-Kessaris N, Stiles CD, Rowitch DH, Richardson WD. 2001. Oligodendrocyte development in the spinal cord and telencephalon: common themes and new perspectives. International Journal of Developmental Neuroscience 19(4):379-385.

Yamada K, Watanabe M. 2002. Cytodifferentiation of Bergmann glia and its relationship with Purkinje cells. Anatomical Science International 77(2):94-108.

Yan Y, Lagenaur C, Narayanan V. 1993. Molecular cloning of M6: identification of a PLP/DM20 gene family. Neuron 11(3):423-31.

Yan Y, Narayanan V, Lagenaur C. 1996. Expression of members of the proteolipid protein gene family in the developing murine central nervous system. J Comp Neurol 370(4):465-78.

Yang Y, Lewis R, Miller RH. 2011. Interactions between oligodendrocyte precursors control the onset of CNS myelination. Developmental Biology 350(1):127-138.

Yen G, Croci A, Dowling A, Zhang S, Zoeller RT, Darling DS. 2001. Developmental and functional evidence of a role for Zfhep in neural cell development. Molecular Brain Research 96(1-2):59-67.

Yuasa S, Kawamura K, Kuwano R, Ono K. 1996. Neuron-glia interrelations during migration of Purkinje cells in the mouse embryonic cerebellum. Int J Dev Neurosci 14(4):429-38.

Yuasa S, Kawamura K, Ono K, Yamakuni T, Takahashi Y. 1991. Development and migration of Purkinje cells in the mouse cerebellar primordium. Anat Embryol (Berl) 184(3):195-212.

Zhao GY, Li ZY, Zou HL, Hu ZL, Song NN, Zheng MH, Su CJ, Ding YQ. 2008. Expression of the transcription factor GATA3 in the postnatal mouse central nervous system. Neurosci Res 61(4):420-8.

Zhao R, Lawler AM, Lee S-J. 1999. Characterization of GDF-10 Expression Patterns and Null Mice. Developmental Biology 212(1):68-79.

Zhou Q, Anderson DJ. 2002. The bHLH transcription factors OLIG2 and OLIG1 couple neuronal and glial subtype specification. Cell 109(1):61-73.

7 Publications

Mecklenburg N, Garcia-Lopez R, Puelles E, Sotelo C, Martinez S.
Cerebellar oligodendroglial cells have a mesencephalic origin.
GLIA 59:1946–1957 (2011)

GLIA

1988

Cerebellar Oligodendroglial Cells have a Mesencephalic Origin

NORA MECKLENBURG,[1] RAQUEL GARCIA-LÓPEZ,[1] EDUARDO PUELLES,[1]
CONSTANTINO SOTELO,[2,3] AND SALVADOR MARTINEZ[1]*
[1]Instituto de Neurociencias (UMH-CSIC), Universidad Miguel Hernandez, San Juan, Alicante, Spain
[2]Cátedra de Neurobiología del Desarrollo "Remedios Caro Almela" Instituto de Neurociencias de Alicante. (UMH-CSIC),
Universidad Miguel Hernandez, San Juan, Alicante, Spain
[3]INSERM, U968, Paris, F-75012, France, and UPMC Univ Paris 06, UMR_S 968, Institut de la Vision, Paris, F-75012, France,
CNRS, UMR_7210, Paris, F-75012, France